Climate Change in Queensland under Enhanced Greenhouse Conditions

Third Annual Report, 1999-2000

Report on research undertaken for Queensland Departments of State Development, Main Roads, Health, Transport, Mines and Energy, Treasury, Public Works, Primary Industries, and Natural Resources

Kevin Walsh, Kevin Hennessy, Roger Jones, Kathy McInnes, Cher Page, Barrie Pittock, Ramasamy Suppiah and Peter Whetton

CSIRO

Important Disclaimer

This report relates to climate change scenarios based on computer modelling. Models involve simplifications of the real physical processes that are not fully understood. Accordingly, no responsibility will be accepted by CSIRO or the QLD government for the accuracy of forecasts or predictions inferred from this report or for any person's interpretations, deductions, conclusions or actions in reliance on this report.

February 2001

Address for correspondence

Dr Kevin Walsh
CSIRO Atmospheric Research
PMB 1
Aspendale Victoria 3195
Telephone: (03) 9239 4532
Fax: (03) 9239 4444
E-mail: kevin.walsh@dar.csiro.au
World wide web: http://www.dar.csiro.au

For additional copies of this report, contact

Ken Brook
Queensland Department of Natural Resources,
80 Meiers Road,
Indooroopilly,
Queensland,
AUSTRALIA, 4068.
Telephone: (07) 3896 9379
Fax: (07) 3896 9606
World wide web: http://www.dpi.qld.gov.au/qcca/Welcome.html

Contents

ACKNOWLEDGMENTS

List of Abbreviations and Acronyms

AOGCM	[Coupled] Atmosphere-Ocean GCM
CAR	CSIRO Atmospheric Research
DARLAM	Division of Atmospheric Research Limited Area Model
ENSO	El Niño Southern Oscillation
GCM	General Circulation Model – also Global Climate Model
SOI	Southern Oscillation Index
SST	Sea Surface Temperature

Summary for Policy Makers

Almost all scientists agree that the enhanced greenhouse effect will cause changes in Earth's climate. It is clear that increases in the atmospheric concentration of greenhouse gases, such as carbon dioxide (CO_2), methane (CH_4), nitrous oxide (N_2O) and halons (CFCs), are increasing the greenhouse heat trapping capabilities of the atmosphere, thus enhancing the greenhouse effect. Several of these predicted climate changes will likely affect Queensland. Most confidently predicted are increases in temperatures, as these have already been observed in the 20th century in many locations, using a number of different techniques. Less confidently predicted are changes in rainfall. This is because rainfall amounts in Queensland depend to a large extent on the current state of the El Niño-Southern Oscillation phenomenon (ENSO). The causes of ENSO are complicated and not fully understood, which makes ENSO difficult to represent in climate models, the main tool used to make predictions about the effects of climate change on rainfall.

Progress has been made on this issue, and although there are differing opinions regarding the possible effect of climate change on ENSO, the balance of evidence from a number of different models suggests a trend towards more El Niño-like conditions. Since El Niño conditions are often associated with drought in Queensland, this suggests the possibility of more droughts in Queensland in a warmer world. One of the main outcomes from an increase in drought frequency is a predicted decrease in the average moisture of Queensland soils. This a consequence of the greater evaporation caused by higher temperatures combined with rainfall that is not predicted to increase substantially, and which may even decrease in some seasons.

Results from a substantially improved version of the CSIRO climate model suggest that this new model has a much better simulation of ENSO, with the size of the ENSO variations larger and therefore more realistic than previous versions of the CSIRO model. This gives optimism that this model can be used in the future to provide a better estimate of the effect of climate change on Queensland rainfall.

Even if changes in average rainfall are still relatively uncertain, a number of studies suggest increases in the intensity of the heaviest rainfall events. This may have a number of different policy implications, as listed below.

Tropical cyclones regularly affect the Queensland coast. One prediction of climate change research, both at CSIRO and elsewhere, is that tropical cyclone intensities are likely to increase somewhat in a warmer world. In research undertaken by CSIRO and summarized in this report, it is shown that high wind speeds caused by tropical cyclones may become more frequent along much of the Queensland coast. This may have implications for design standards of building construction in coastal cities and towns.

Climate model results provide the indispensable foundation for estimating the impacts of climate change. Researchers have used CSIRO results, as well as those of other institutions, to examine specific impacts of climate change on Queensland. These impacts are likely to include the following:

The impact of increases in temperature may include:

- sea-level rise and resulting effects on coastal infrastructure;
- temperature stresses on coral reefs, leading to more frequent episodes of reef mortality;
- decreasing suitability for growing fruit requiring 'chilling' to set fruit (e.g. stone fruit, apples);
- increase in risk of fruit-fly infestation in southern Queensland;
- increased vulnerability of cold climate adapted species to habitat loss;
- spread of warm climate adapted weeds;
- changes in electricity demand patterns associated with warmer summers;
- changes in cooling efficiencies associated with warmer ambient temperatures (e.g. in power stations using cooling towers/cooling water);
- public health issues e.g. less vulnerability to cold weather diseases, greater vulnerability to 'tropical' diseases;
- increased risk of fire; and
- increased heat stress on dairy cattle.

The impact of increases in the intensity of the heaviest rainfall events may include:
- sporadic increased runoff and/or soil saturation depending on surface conditions (but average runoff due to changes in average soil moisture may decrease);
- increased vulnerability to salinity, soil erosion and concomitant nutrient loss;
- impact on water supply infrastructure from increased siltation resulting from episodes of intense soil erosion;
- impacts on existing/future water storage design to account for changes in extreme events;
- crop damage from heavier rainfall events;
- impact on freshwater and marine ecosystems from any increase in soil erosion and associated nutrient and pollutant mobilization in near-coastal regions;
- increases in insurance costs associated with increase likelihood of storm damage to public and private infrastructure;
- implications for emergency planning and evacuation of low lying regions; and
- altering the design of roads and bridges to cope with enhanced runoff and flood events.

Not all of the impacts of climate change would necessarily be negative, however. There could be a number of positive effects, including the following:

- an initial increase in wheat yield
- little impact on heat-related mortality
- beneficial effects on native pastures, provided that rainfall does not decrease more than 10%
- increases in productivity in plantation forests located in fertile areas, for moderate warmings

Extended Abstract

New, finer resolution climate change simulations of Queensland

Climate model simulations provide the foundation for estimating the impacts of climate change. To make useful inferences regarding most impacts, the most accurate and detailed simulations available are required. Accordingly, a number of fine resolution climate model simulations of Queensland have been performed during the course of this work. In the previous year's report (Walsh et al., 2000), simulations of the regional climate model DARLAM at a horizontal resolution of 125 km were described. It was also noted that simulations at a finer resolution of 60 km were at an experimental stage, with some improvements still needed. Improvements have now been made to the 60-km simulation; these are now described and the simulation is referred to as DARLAM-60.

It is important to note that the understanding of the effects of climate change involves assessment of the predictions of a number of different climate models. Although the DARLAM simulation described here is the most detailed climate change simulation ever performed for the Queensland region, it is nevertheless one model amongst a number of models. A climate change scenario used for climate impact studies should be constructed from the consensus of predictions over several models.

Average Temperature

The DARLAM 60-km resolution model (DARLAM-60) has a good simulation of average temperature when compared with the observed current climate. The model slightly underestimates temperatures in the interior of the continent and overestimates temperatures along the coast. Predicted temperature changes in a warmer world are consistent with previous climate change scenarios released by CSIRO and others, and are summarized below.

Maximum and Minimum Temperatures

There is good agreement between observations and DARLAM-60 current climate simulations of maximum and minimum temperatures. The DARLAM-60 simulation underestimates maximum temperature in the far interior of the state in most seasons. DARLAM-60 also slightly underestimates minimum temperatures in the same region in summer and spring. Differences between observations and simulations are modest elsewhere.

Under enhanced greenhouse conditions, predicted increases in maximum and minimum temperatures are generally largest in the interior and smaller along the coast. Between the years 2000 and 2100, maximum temperatures increase by about 4°C in the interior and by about 3.5°C in the northern and south-eastern regions of Queensland. Increases in minimum temperatures are about 4°C in the interior and about 3°C in the northern and south-east regions.

Average rainfall

Current observed rainfall is well simulated by DARLAM-60 in summer and winter. Simulated autumn rainfall is generally less than observed in the interior, and simulated spring rainfall is too great, with greatest differences also in the far interior. Under enhanced greenhouse conditions, relatively small changes in rainfall are simulated in summer. Some increases are simulated in autumn, and decreases in spring and winter.

As mentioned above, in constructing a climate change scenario for Queensland rainfall, these predictions would be compared with those of other models. Many of these models predict rainfall decreases over Queensland, rather than the increases required to counteract the drying effect of increased temperature. DARLAM-60 itself does not simulate such increases in rainfall and thus does not provide strong evidence to counterbalance the consensus model prediction towards drier conditions.

Year-to-year variability of rainfall

In general, the year-to-year variability of rainfall is considerably underestimated in DARLAM-60. This is mostly because the variability of the El Niño-Southern Oscillation phenomenon (ENSO) is weaker than observed in the global model used to force DARLAM-60. By 2100, little change in year-to-year variability is predicted in summer by DARLAM-60, whereas rainfall variability rises slightly in winter. Because of the smaller than observed variability simulated by DARLAM-60, however, confidence in predictions of changes in year-to-year variability in the decades to come must be regarded as low.

Much of the year-to-year variability in DARLAM-60 is caused by the CSIRO Mark 2 global climate model, as the global model determines the sea surface temperatures used by DARLAM-60. Efforts to improve this aspect of model performance have been made with the development of the CSIRO Mark 3 global model, which simulates observed ENSO variability and strength better than its Mark 2 counterpart.

Extreme temperatures

Many of the important impacts of climate change rely on estimates of changes in the frequency of extreme temperature and rainfall rather than changes in averages or variability. DARLAM-60 simulates strong upward trends in the coming decades in extreme maximum temperatures in all regions of Queensland. Here, extreme maximum temperatures are defined as numbers of days over 40°C in the north and in the interior, and over 35°C in the south-east. Using moderate assumptions about increases in greenhouse gases (specifically, the IS92a scenario), by 2100 the numbers of days of extreme maximum temperatures in summer roughly double in the north and south-east and triple in the interior. In contrast, numbers of very cold days decrease sharply in all regions in winter. These are defined as minima less than 10°C in the north and less than 5°C in the interior and south-east.

There is a considerable range of predicted results for all of the above temperature variables depending on assumptions about the future emissions of greenhouse gases and depending upon which climate model is used. Taking both of those factors into

account, predictions for 2050 are summarized in the tables below, for the winter and summer halves of the year respectively. Increases in average maximum and minimum temperatures are predicted, as well as percentage increases in the number of hot days and decreases in the number of cold days.

April-September

	South-east	Central	North
Ave. max temp (°C)	↑ 0.4 to 1.9	↑ 0.6 to 2.1	↑ 0.7 to 2.2
Ave. min temp (°C)	↑ 0.7 to 2.1	↑ 0.8 to 2.3	↑ 0.7 to 2.3
No. of hot days (% change)	↑ 30% to 162%	↑ 92% to 411%	↑ 62% to 216%
No. of cold days (% change)	↓ 18% to 56%	↓ 20% to 58%	↓ 27% to 61%

October-March

	South-east	Central	North
Ave. max temp (°C)	↑ 0.7 to 2.2	↑ 1.0 to 2.5	↑ 0.8 to 2.2
Ave. min temp (°C)	↑ 0.7 to 2.2	↑ 0.9 to 2.4	↑ 0.7 to 2.1
No. of hot days (% change)	↑ 16% to 46%	↑ 49% to 128%	↑ 35% to 83%
No. of cold days (% change)	↓ 72% to 89%	↓ 75% to 93%	↓ 100%

Extreme Rainfall

Extreme rainfall events are likely to become more common in a warmer world, despite possible decreases in average rainfall. This is a result that has been simulated previously by a number of climate models, and DARLAM-60 is no exception, with increases in the size of heavy rainfall events predicted by 2050.

Intercomparison of climate models

The intercomparison of model predictions is an important process in the construction of climate change scenarios. Different climate models have different simulations of climate change. As climate models improve, a more discriminating evaluation can be performed of their strengths and weaknesses, even to the point of leaving out a model when constructing a climate change scenario. The quality of the simulation of several different climate models is compared here. From the analysis presented in this report, it is reasonable to conclude that some models are less reliable than others on the basis of their poorer simulation of the current climate. Most models predict similar temperature increases over Queensland, with increases larger in the interior than along the coast. Models differ in their prediction of precipitation changes, but the predominant tendency is for rainfall decreases, particularly if one model is excluded from consideration on the basis of its less than adequate simulation of the current climate. A final decision on this will be made in conjunction with the construction of new climate change scenarios by CSIRO, to be released in 2001.

Climate change and ENSO

In general, although the balance of evidence suggests a trend towards an average climate that is more El Niño-like (and thereby more likely to cause droughts in Queensland), it is still true to say that consensus has not yet been reached on this issue. Despite most climate model simulations suggesting such a trend, there are still

some differences between various models in their simulations of the effect of climate change on ENSO.

It remains controversial whether the more frequent El Niños of the 1990s are an early sign of global warming or whether they are due to slow, natural oscillations in the climate system.

The development of climate models with a substantially improved representation of ENSO is a high priority. Through the support of the Queensland Government, a new version of the CSIRO global model, Mark 3, has been developed. Although development of Mark 3 continues, preliminary results indicate that Mark 3 better captures the characteristics of observed ENSO variability than the previous Mark 2 model. Results of this research are discussed in Chapter 2, Section 2.5.

Tropical cyclones

Recent results continue to suggest that there are likely to be increases in tropical cyclone intensities in a warmer world. Increases in tropical cyclone wind speeds may have implications for building design standards. Based on plausible increases in tropical cyclone wind speeds, the change in the return periods (or time between events of the same magnitude) for wind gusts is calculated for five coastal locations in Queensland, for conditions after about 2050. The results suggests that there would be little impact on design standards in south-east Queensland. Further north, effects become more likely, with greatest impact in Cairns, where plausible increases in cyclone wind speeds exceed current building design standards. The same is true to a lesser extent in Mackay. However, whether this would require changes to building design standards still needs to be assessed.

Scenarios for new climate variables and the development of OZCLIM

Climate change scenarios are developed for new variables that are important inputs for climate impact models. It is also shown that changes in potential evaporation and precipitation simulated by climate models are not independent, but rather are related to each other. Since potential evaporation and precipitation must vary together rather than independently, this reduces the possible number of future climate conditions, as not all possible changes in potential evaporation would occur for a specified change in precipitation. Analysis of the change in precipitation minus evaporation suggests most climate models are predicting generally drier conditions for Queensland in a warmer world.

In addition, a new version (Version 2.0.1 Beta) of OZCLIM, the interactive climate change scenario generator, is described. This version includes three new variables important for climate impact studies: evaporation, vapour pressure and radiation. In addition, patterns of change for eight more models have been included. This has been done to more fully represent the possible range of model predictions. Version 2.0.1 of OZCLIM also has substantially increased functionality, which is described in more detail in the report. A CD containing this software is included with this report.

Climate impacts on Queensland

Tools such as climate models and OZCLIM are indispensable to enable the specific impacts of climate change on Queensland to be estimated. Researchers have employed a number of different techniques to estimate these impacts. These include the following, ranked in order of highest to lowest confidence:

Very high confidence (better than 9 out of 10 probability):
- Effects of sea-level rise on coastal infrastructure

- Potential for expansion of vector-borne diseases (in the absence of existing effective health measures)

- Higher energy costs for buildings as a result of higher temperatures and the increased need for air conditioning

- Increased heat stress on dairy cattle.

High confidence (about 9 out of 10)
- Temperature stresses on coral reefs, leading to more frequent episodes of reef mortality

- Loss of biodiversity in native forests

- Increase in risk of fruit-fly infestation in southern Queensland.

Medium to high confidence (2 out of 3 or better)
- Increases in storm surge heights in some locations by 2050

- Significant effects on transport infrastructure by 2070

- Increased risk of fire

- Little impact on heat-related mortality by 2030.

Moderate confidence (better than 1 in 2)
- Increased drought

- Reduction in river and stream flow

- Initial increase in wheat yield.

Low confidence (possible only)
- Beneficial effects on native pastures (provided rainfall does not fall too much).

1. Introduction

This is the third annual report under a four-year consultancy (1997-2001) between CSIRO and the Government of Queensland. The consultancy addresses the following aspects of climate change:

- changes in average climate (temperature, rainfall and other relevant variables) from the present until the year 2100 and beyond,

- possible changes to ENSO, notably in its variability and amplitude, and related changes in drought and flood frequencies,

- possible changes to tropical cyclone frequency, intensity and location,

- potential changes in climatic variability, including daily, within-season, interannual and multi-decadal variability and extremes,

- the development of methodologies to assess the risk of occurrence of critical climatic thresholds for relevant impacts and adaptation measures,

- the identification of potential impacts of climate change across relevant sectors in Queensland, in collaboration with interested parties, and the facilitation of studies thereof, where appropriate through separately funded collaborative impact studies.

1.1   Progress against Milestones

Here we detail the achievements of the third year of the consultancy and compare them to the agreed milestones of the contract.

Item 2.3.1 Provide scenarios of changes in average climate, and climatic variability, on daily, interannual and multi-decadal timescales (including the effects of changes in ENSO), up to year 2100. This will be based on regional model estimates at 60-km resolution, nested in the Mark 2 coupled AOGCM, and will take account of a range of CO_2 emission scenarios. Estimates of possible changes in the frequency and magnitude of extreme temperatures and rainfalls, and of droughts and floods, will be included.
        - these tasks have been performed and are summarized in Section 2.

Item 2.3.2 Provide the best possible estimates of changes in tropical cyclone frequency, location and intensity in the Queensland region. Results from multiple nesting will also be examined.
        - in addition, a study examining the effect of climate change on wind gust return periods in Queensland has been completed. These topics are discussed in Section 3.

Item 2.3.3 Provide estimates of changes in the risk of exceeding relevant climatic thresholds (as determined by Queensland stakeholders), based in part on the CSIRO Mark 2 coupled AOGCM and CSIRO regional model. Incorporate selected climate variables and types of variability into OZCLIM according to the needs of impact

researchers (to be chosen in collaboration with designated Queensland contacts). Structure OzClim for transient scenarios and risk assessment.

- a new version of OZCLIM has been released that addresses these issues, which are discussed in Section 4.

Extra work: a considerable amount of work has now been performed by researchers at CSIRO and elsewhere on the specific impacts of climate change on Queensland. These results have been summarized in Section 5.

2. DARLAM simulation of climate change at a horizontal resolution of 60 km (Item 2.3.1)

2.1   Introduction

Climate model simulations provide the foundation for estimating the impacts of climate change. For most impacts, to make useful inferences, the most accurate and detailed simulations available are required. Accordingly, a number of fine resolution climate model simulations of Queensland have been performed during the course of this work. In the previous year's report (Walsh et al. 2000), DARLAM simulations at a horizontal resolution of 125 km were described. It was also noted that simulations at a finer resolution of 60 km were at an experimental stage, with some improvements still needed. Improvements have now been made to the 60-km simulation; these are now detailed and the simulation is referred to as DARLAM-60.

It is important to note that understanding the effects of climate change involves assessment of the predictions of a number of different climate models. Although the DARLAM simulation described here is the most detailed climate change simulation ever performed for the Queensland region, it is nevertheless one model amongst a number of models. A climate change scenario used for climate impact studies should be constructed from the consensus of predictions over several models.

As in Walsh et al. (2000), for the purposes of data analysis, Queensland is divided into three regions: north, south-east and central (see Fig. 2.1). Temperature observations are taken from the data set described in Jones and Trewin (2000). These data are averaged over the period 1961-1990, and were derived from station data interpolated to a 1°x1° grid. The rainfall data set was taken over the same period, and is described in Jeffrey et al. (2001). These data were also derived from station data and then interpolated to a regular grid.
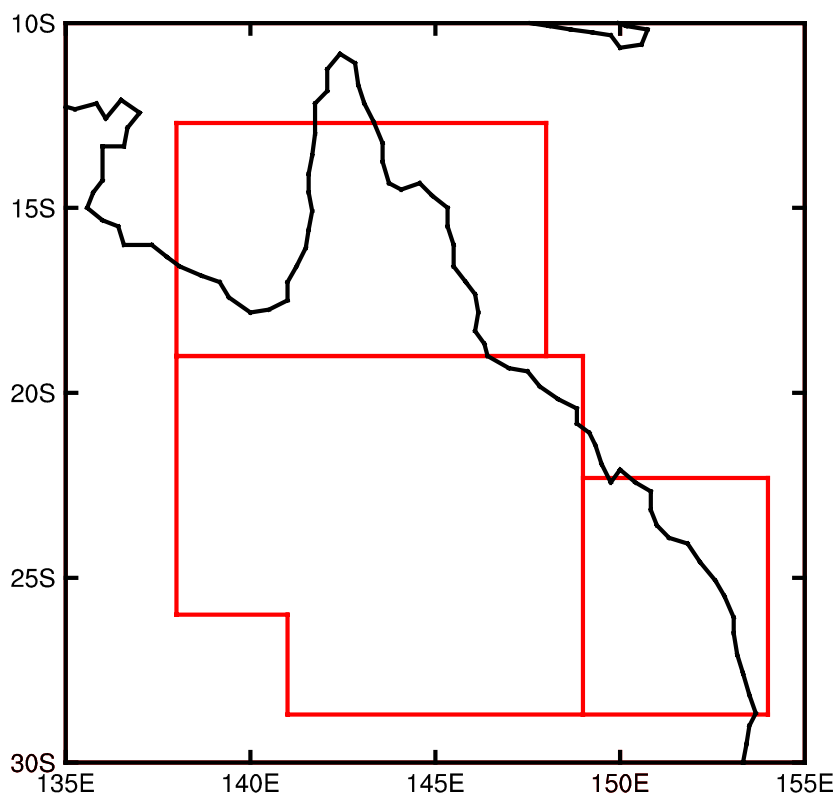
Figure 2.1. Regions of Queensland for data analysis: (top) northern Queensland; (lower left) central Queensland; (lower right) south-east Queensland. Latitudes and longitudes (in degrees) are indicated.

2.2   Climate simulated by DARLAM-60

2.2.1   *Mean climate*

Temperature

Figures 2.2 and 2.3 show the observed average temperatures over Queensland compared with the DARLAM-60 simulation. In general, the model simulation is very good: absolute values of temperature are well simulated (with the possible exception of summer) and the geographically-varying patterns of temperature are very well simulated. This is partly due to the better representation of topography in DARLAM-60 compared with other climate models. Figure 2.4 shows the differences between the model simulation and observed. There is a tendency for the model to simulate lower temperatures than observed in the interior of Queensland, although these differences are small, mostly less than 2°C. The model slightly overestimates temperature along the coast, but these differences are even smaller, mostly less than 1°C.

Some analysis has been performed to determine the reasons for these biases. The underestimate of temperature in the interior is likely associated with too much cloud simulated in DARLAM-60. The largest effect occurs in the interior of the continent, where the observed cloudiness is low, rather than along the coast, where observed

cloudiness is high. This explains the larger biases in the interior. There is also inherent cold bias in the temperature simulated by the forcing GCM, whose cause is currently unknown.

Changes in mean temperature under enhanced greenhouse conditions

Temperature changes under enhanced greenhouse conditions are shown in Figure 2.5. Here, the values presented are changes per degree of global warming. In other words, for a global warming of 1°C, the temperature changes over Queensland would be those shown in Fig. 2.5. For a global warming of 2°C, the changes would be twice those shown in Fig. 2.5, and so on. These numbers are calculated by a technique known as the "slope method". This is done by linearly regressing the modelled local seasonal mean temperatures (or rainfalls) against modelled global average temperatures (smoothed with an 11-year running mean) and taking the slope of the relationship at each grid point as the estimated response. This method has two advantages over simply displaying differences: the global warming signal is less likely to be obscured by natural variability, and the impact of differing scenarios of global warming on local temperatures can be easily estimated. The main disadvantage of the method is that it assumes a linear relationship between the local response and global temperature, and this may not always hold. For example, Figure 2.6 shows the time series of spring rainfall over the central Queensland area as simulated in the CSIRO GCM along with the fitted response using the slope method. Before 1960, there is evidence of an initial non-linear rainfall response in the CSIRO simulation (as discussed in last year's report), although the major response in the 21st century appears linear with global warming. It should also be noted that this method is still susceptible to noise or decadal variability, as the trend line in Fig. 2.6 is not a tight fit to the data and therefore a component of the response may be spurious. This could be reduced by using longer simulations or by making many simulations using the same model ("ensemble" simulations).

In the DARLAM-60 simulation (Fig. 2.5), as expected, temperature changes are highest inland and lowest along the coast. A coastal effect, caused by the slower warming of the adjacent ocean, is seen quite clearly at this high resolution, indicated by a narrow band of smaller increases running up the entire coastline into the tropics. Greatest increases are generally seen in the far west interior of the State.

Differences in warming between seasons do not appear to be pronounced, except that slightly smaller warmings are simulated in winter. For all seasons, warming along the coast is 0.8-0.9°C per degree of global warming, whereas in the interior, warming is 1.0-1.2°C per degree of global warming. These values are similar to, although slightly lower than, those given in the scenarios provided by CSIRO (1996).

In summary, the DARLAM 60-km resolution model has a very good simulation of mean temperature in the current climate. Predicted temperature changes in a warmer world are consistent with previous climate change scenarios.

tmean_obs
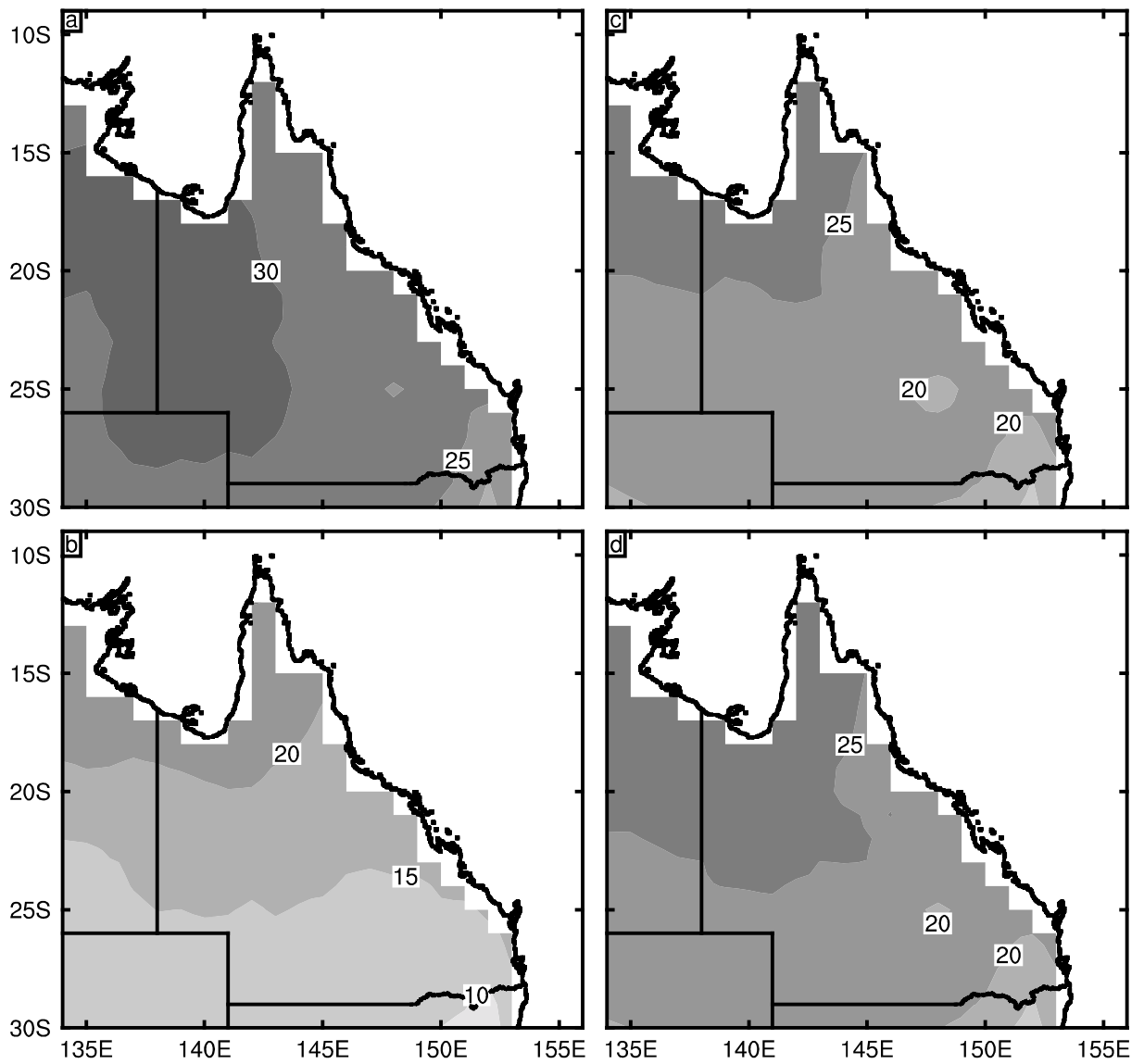
Figure 2.2. Observed mean temperature for (a) summer (Dec.-Jan.); (b) winter (June-Aug.); (c) autumn (Mar.-May); and (d) spring (Sep.-Nov.). Contour interval is 5°C.

tmean_qld60
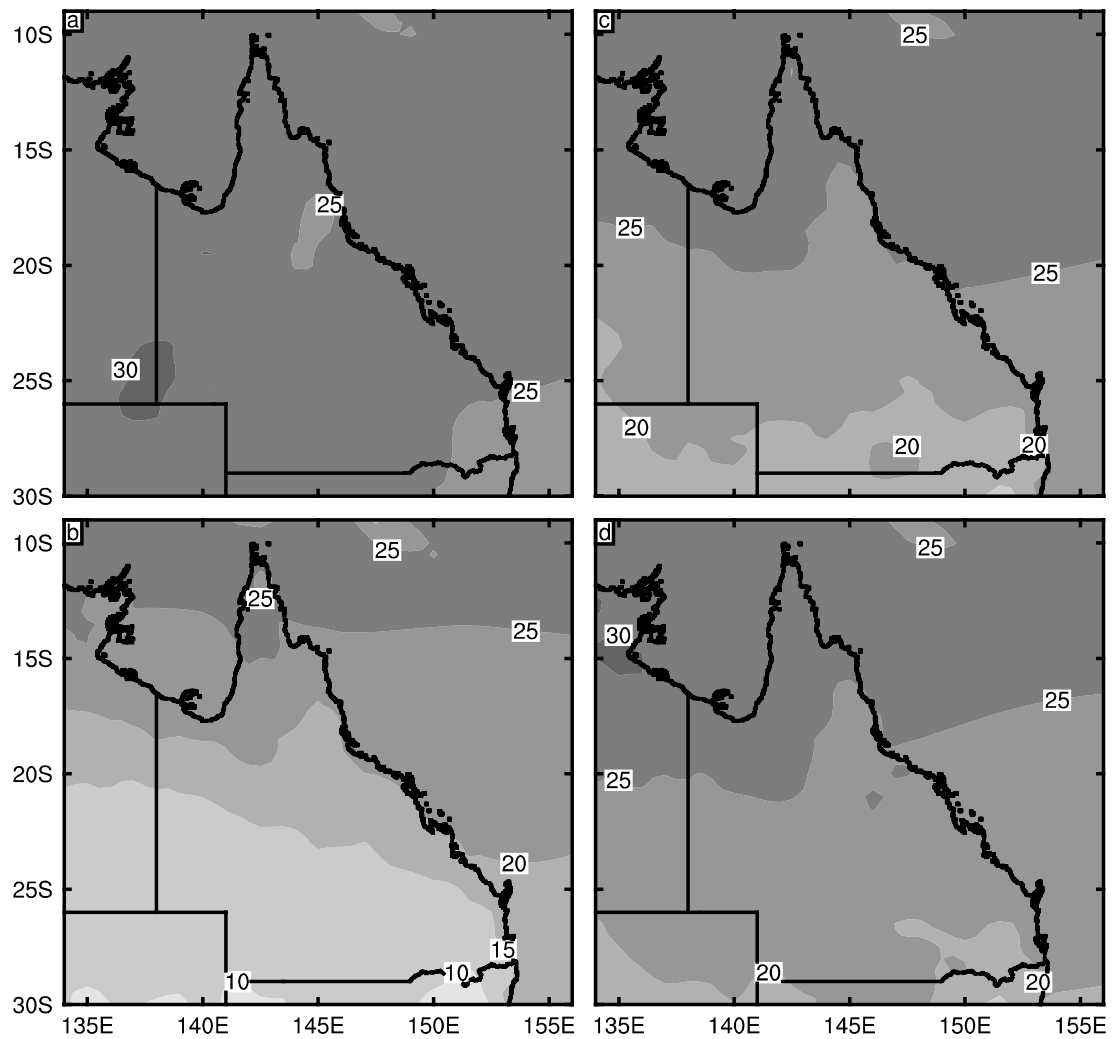
Figure 2.3. The same as Fig. 2.2 but for DARLAM-simulated mean temperature for the model equivalent of 1961-1990.
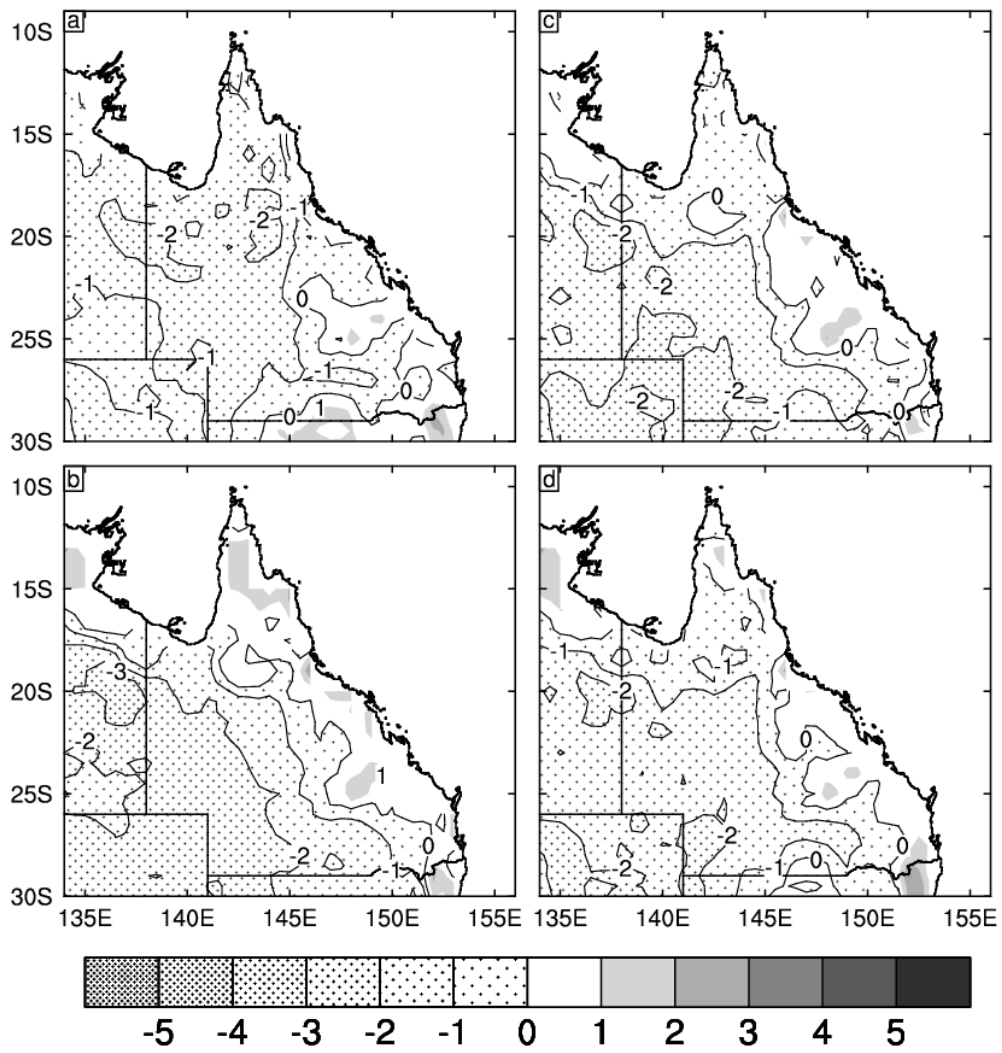
Figure 2.4. The same as Fig. 2.2 but for the differences, model simulated minus observed.

tmean_qld60
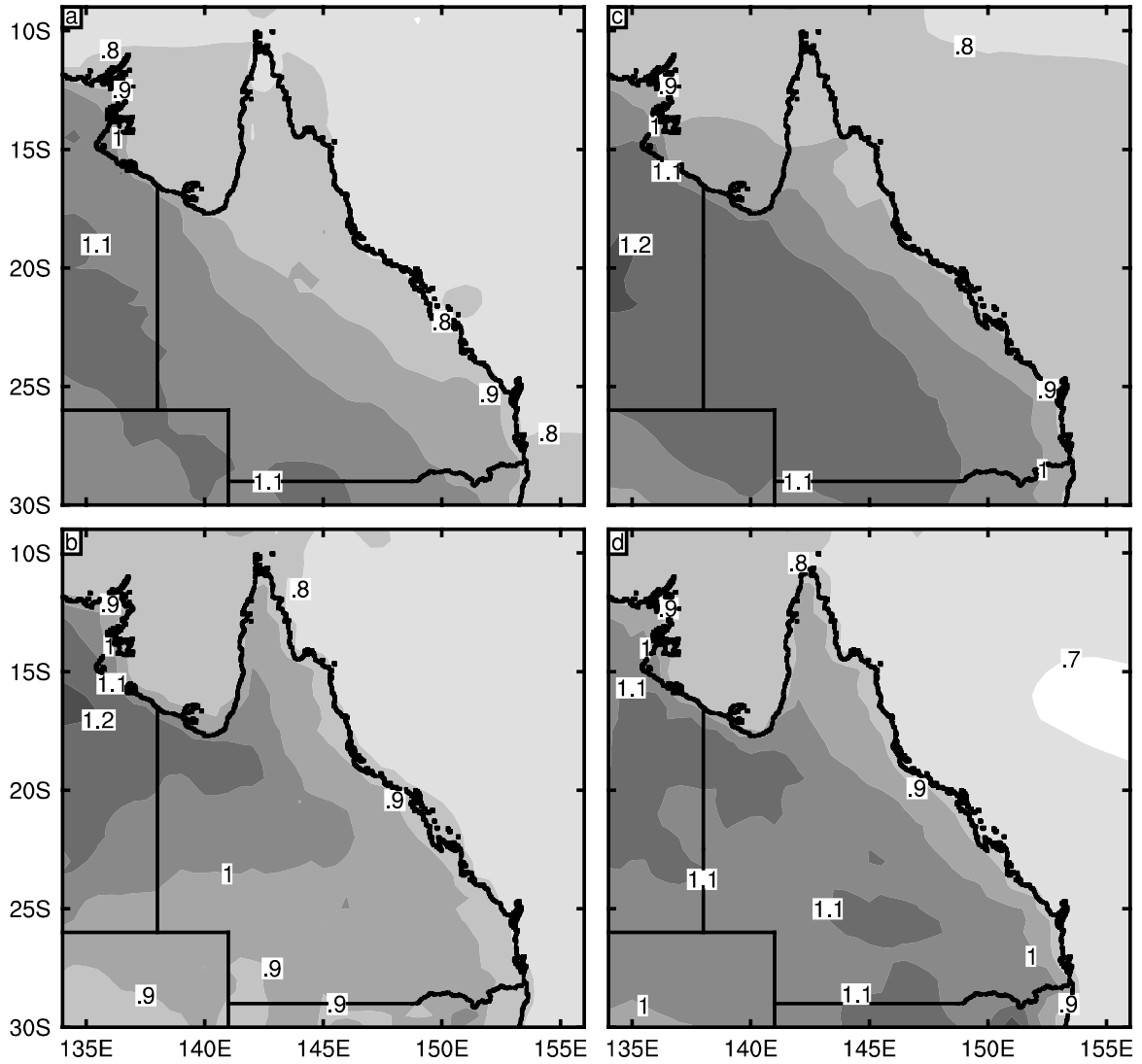
Figure 2.5. The change in temperature over Queensland per degree of global warming, for (a) summer; (b) winter; (c) autumn and (d) spring. Contour interval is 0.1 (°C).
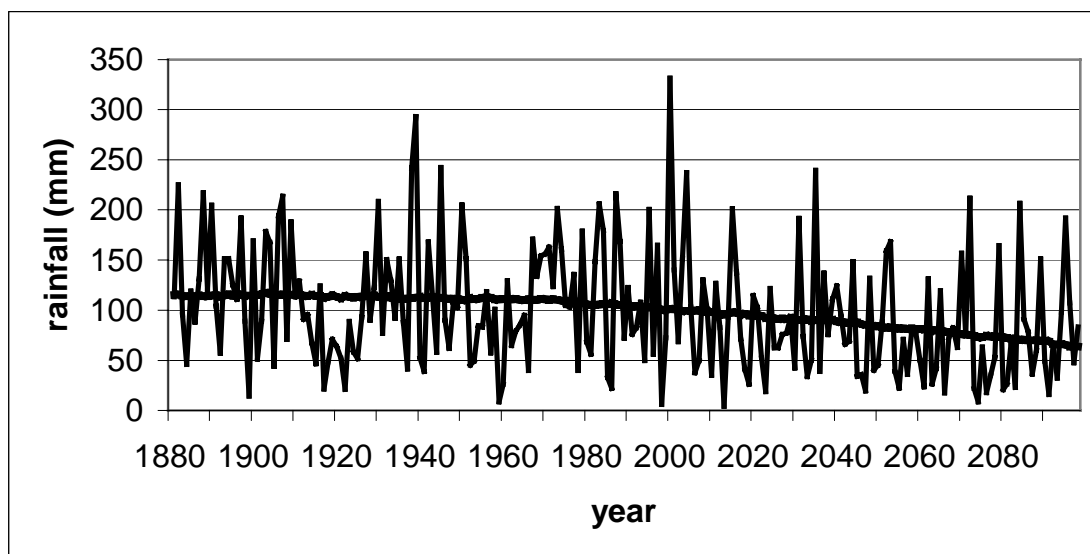
Figure 2.6. Rainfall from the CSIRO GCM for the central region of Queensland shown in Fig. 2.1, with the response estimated using the slope method superimposed.

Minimum and maximum temperature

Figure 2.7 compares maps of observed and simulated minimum temperatures over Queensland. The simulations are good: as for the mean temperatures, there is very good agreement between the patterns of simulated and observed minimum temperatures. Figure 2.8 shows the differences between simulated and observed minima. These are mostly small (less than 2°C) with the exception of far south-west Queensland in the summer and spring. Also shown in Fig. 2.8 is the predicted increase in minimum temperature per degree of global warming. As for mean temperatures, increases are largest in the interior and smaller along the coast.

Figure 2.9 shows the same pattern for maximum temperatures. The agreement is not as good as it is for minimum temperatures, but still a very reasonable pattern of temperatures is produced. Some biases are evident, as shown in Fig. 2.10. The DARLAM-60 simulation underestimates maximum temperature by more than 4°C in the far interior of the state in summer, spring and winter. Biases in most other regions are modest.

The predicted temperature change per degree of global warming is also shown in Fig. 2.10. As for the mean temperatures, temperature changes are highest in the interior and less along the coast, with the exception of winter, where largest changes are simulated in the northern interior.

tmin_obs

tmin_qld60
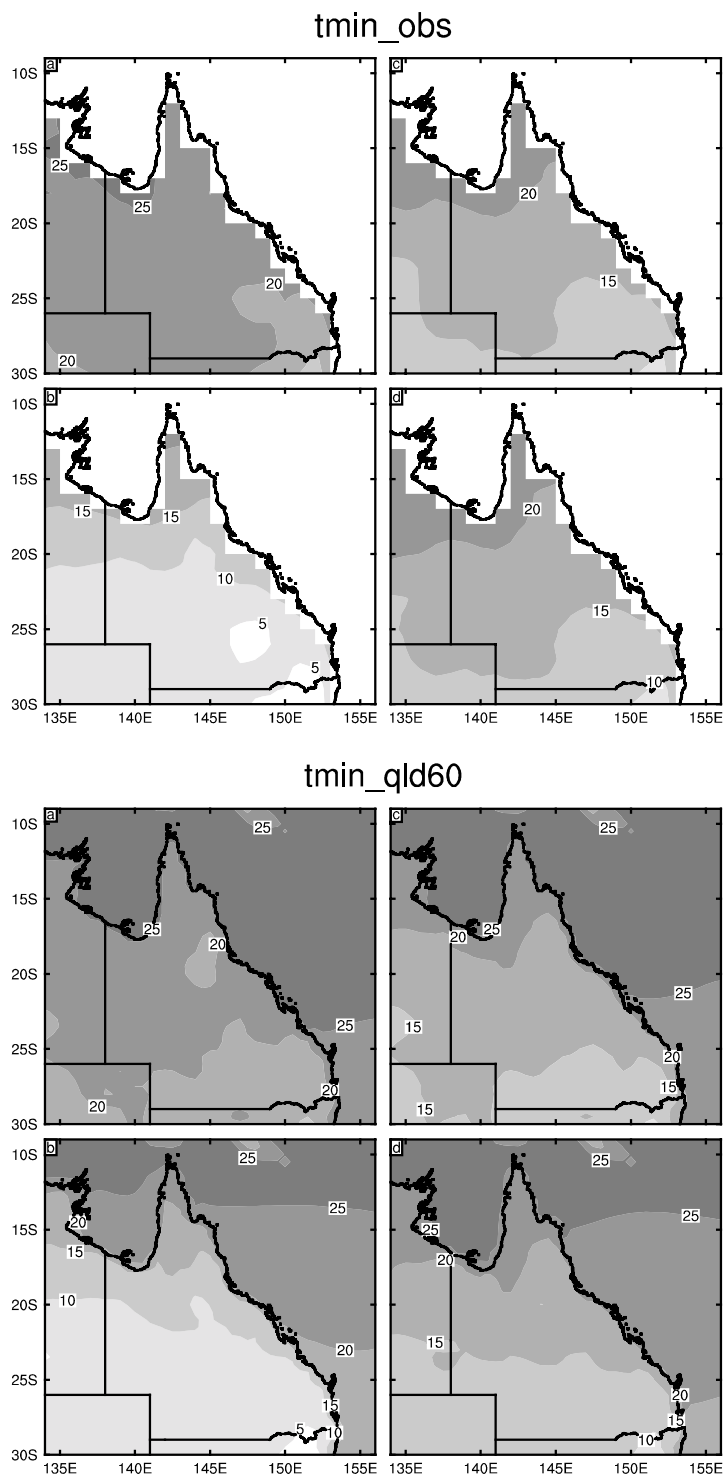

Figure 2.7. Minimum temperatures in the current climate (top) observed; and (bottom) simulated, for (a) summer (Dec.-Feb.); (b) winter (June-Aug.); (c) Autumn (Mar.-May); and (d) spring (Sep.-Nov.).

tminqld60-obs

tmin_qld60
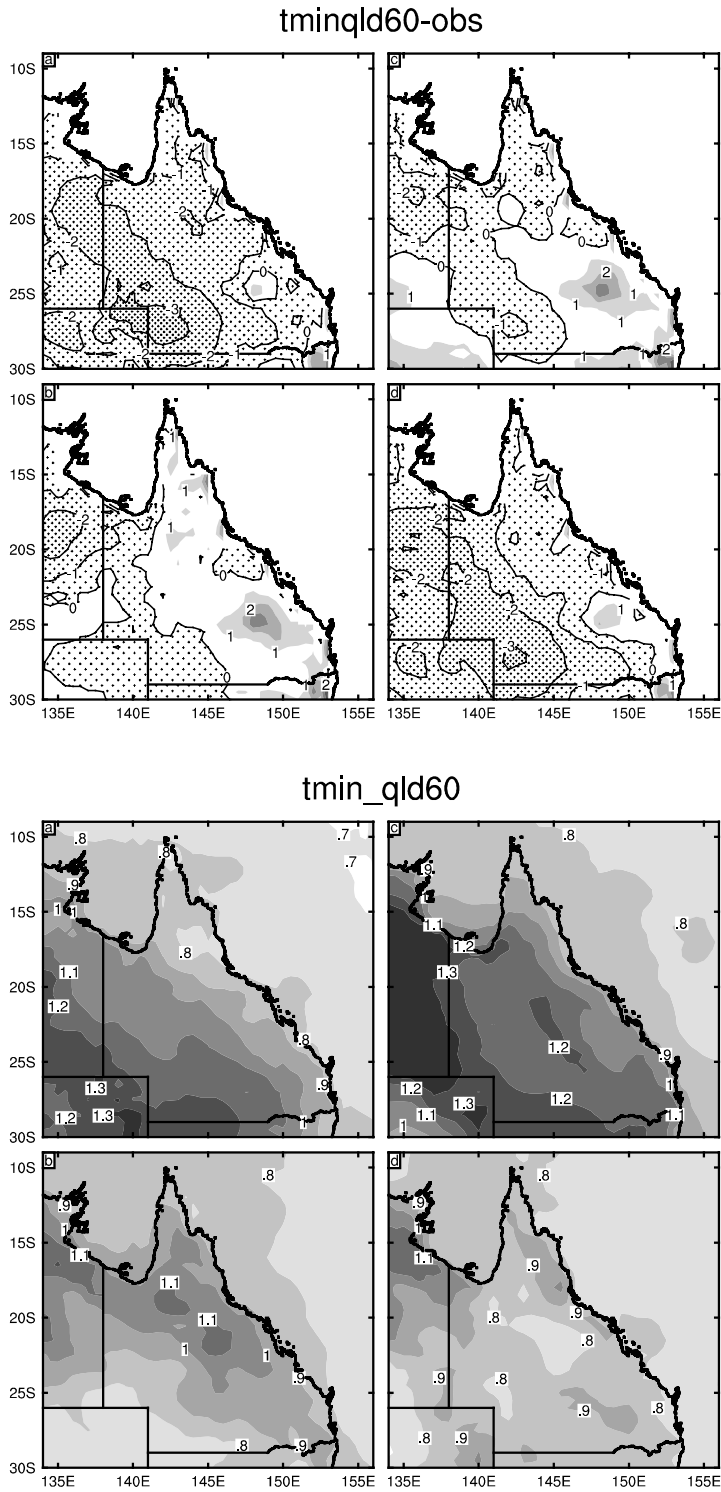
Figure 2.8. (top) 60-km simulation of minimum temperatures minus observations; and (bottom) the change in temperature per degree of global warming, for the same seasons as Fig. 2.7.

tmax_obs

tmax_qld60
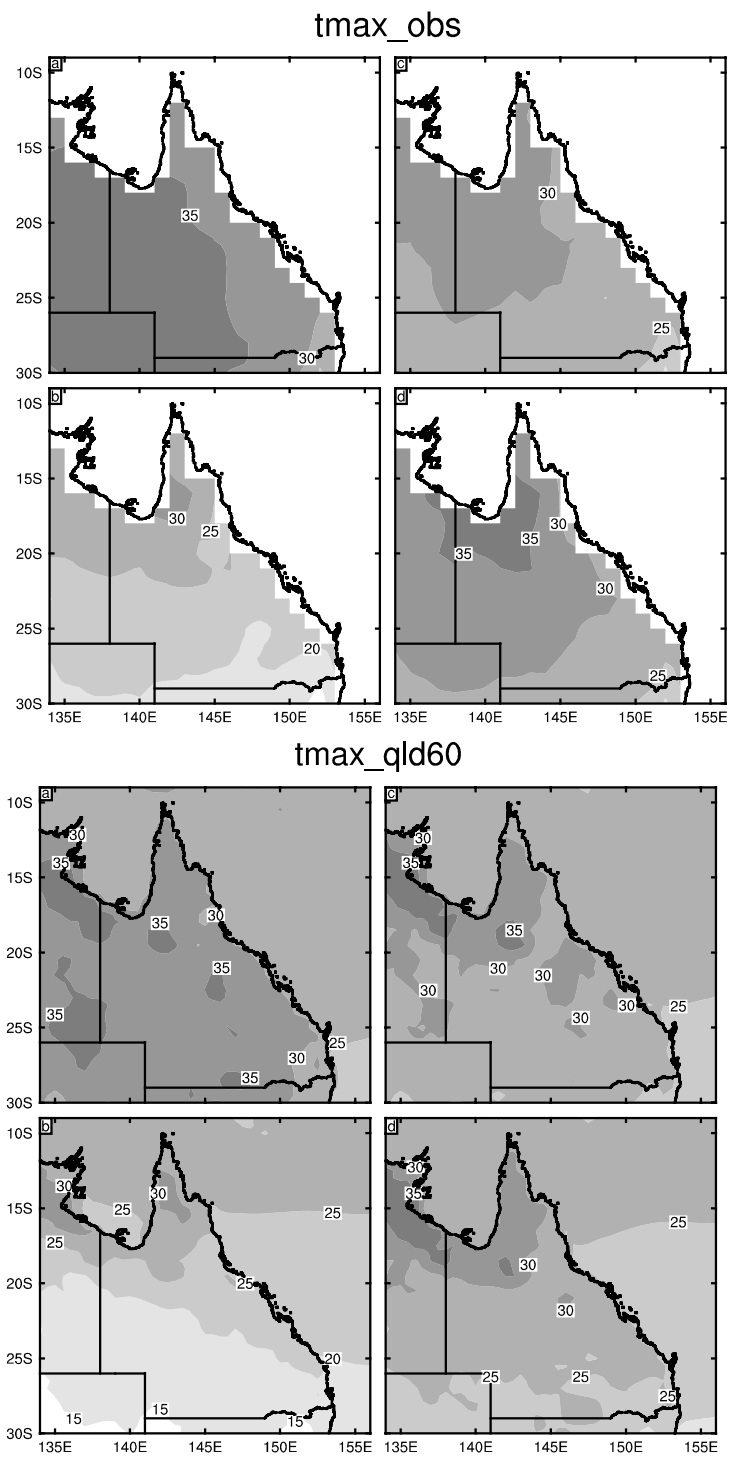
Figure 2.9. The same as Fig. 2.7 but for maximum temperature.

tmaxqld60-obs

tmax_qld60
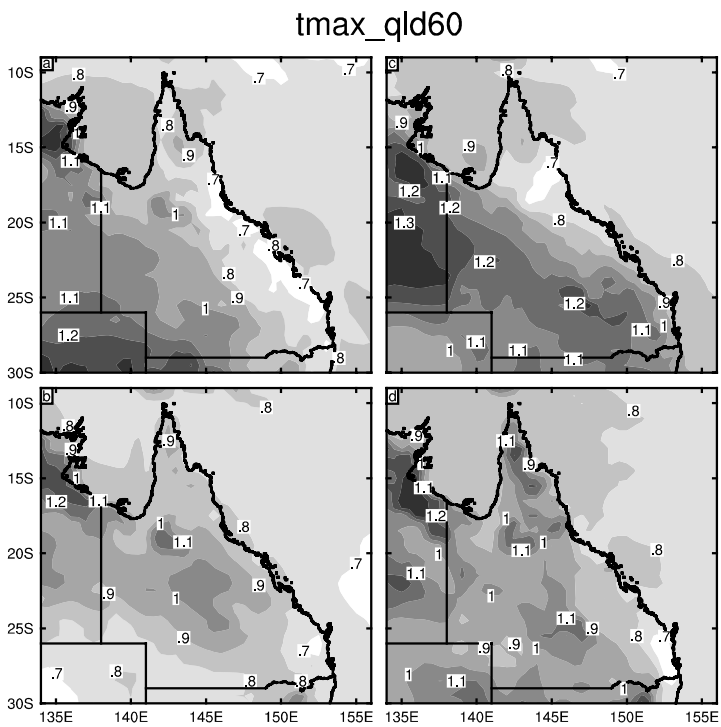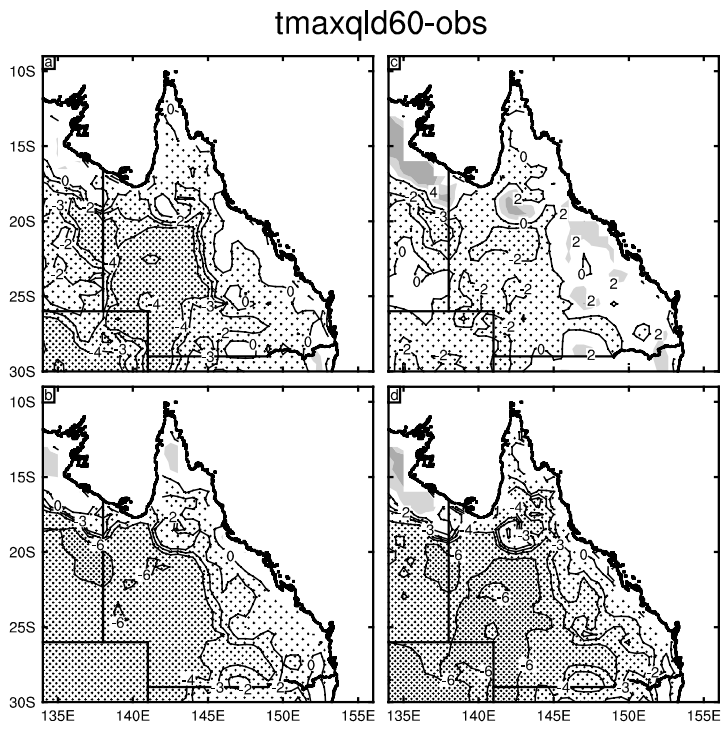
Figure 2.10. The same as Fig. 2.8 but for maximum temperatures.

Figures 2.11 and 2.12 show time series of annual mean minimum and maximum temperature compared with observations. When averaged over the three regions, there is very good agreement between the observed and simulated records. Minimum temperature (Fig. 2.11) increases between the years 2000 and 2100 are greatest in the central region, at around 4°C. Increases are slightly less in the northern region and about 3°C in the south-east. Maximum temperature (Fig. 2.12) increases by about 4°C between 2000 and 2100 in the central region, by about 3.5°C in the northern and south-east regions.

The dark line through the time series in these two figures is the eleven-year running mean. This indicates decadal-scale variability, which is mostly generated by the forcing GCM. These figures indicate that decadal variability continues to be simulated in the model into the later part of this century. One implication of the presence of decadal variability is that it is large enough to, at times, halt the simulated upward trend of temperature for periods of a decade or more.

In summary, there is good agreement between observations and DARLAM-60 simulations of maximum and minimum temperatures. The DARLAM-60 simulation underestimates maximum temperature in the far interior of the state in most seasons and also underestimates minimum temperatures in the same region in summer and spring. Differences between observations and simulations are modest elsewhere.

Rainfall

Figures 2.13 and 2.14 show observed and simulated rainfall for summer, winter, autumn and spring. The simulated rainfall is averaged over the first 30 years of the DARLAM-60 simulation, for the model equivalent of 1961-1990. In general, the summer (December-February) rainfall pattern is good. Particularly good is the position of the 500-mm contour, which simulates the observed higher rainfall over the mountainous regions near Mackay and in the south-east hinterland. Fig. 2.15 shows the precipitation simulation minus the observations, and shows that summer rainfall is overestimated in the interior of Queensland. Simulated summer rainfall is less than observed along certain portions of the coast.

In contrast to the summer rainfall pattern, autumn rainfall is largely underestimated in the simulation. The spatial pattern of rainfall shown in Fig. 2.14 remains reasonable, with a distinct gradient away from the coastline, as observed. The pattern of winter rainfall is also good, with the position of the 50-mm contour very close to that observed. Too much winter rainfall is simulated in the seasonally dry regions of the northern interior, and not enough in the south-east of the State. The observed and simulated spring rainfall patterns are poorly correlated, with rainfall overestimated throughout the state, and with a failure to capture the observed gradient from the south-east coast into the interior of the state.

Average Minimum Temperature
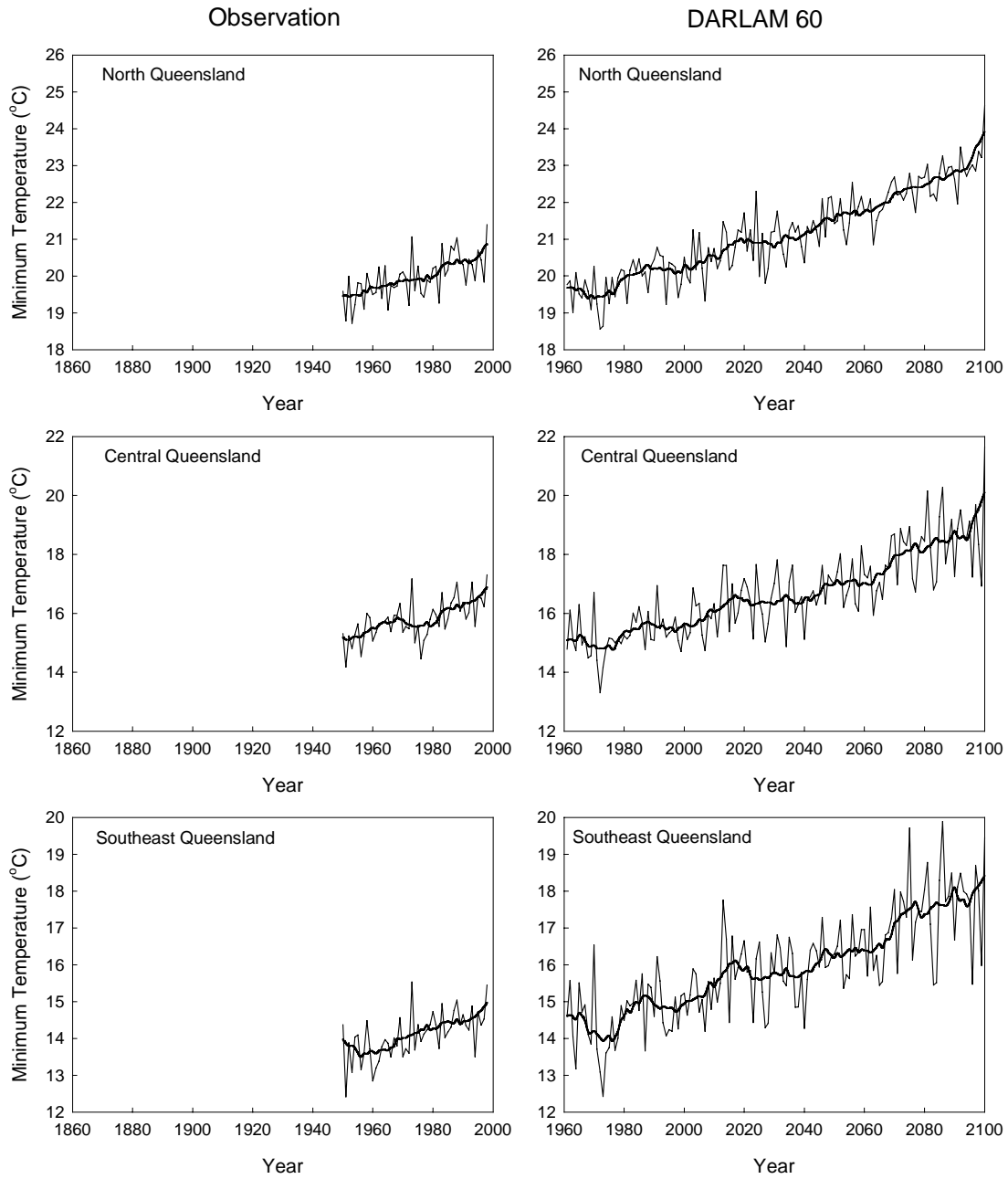
Figure 2.11. Annual mean minimum temperature, observed and simulated. The dark line is the eleven-year running mean.

Average Maximum Temperature

Observation   DARLAM 60
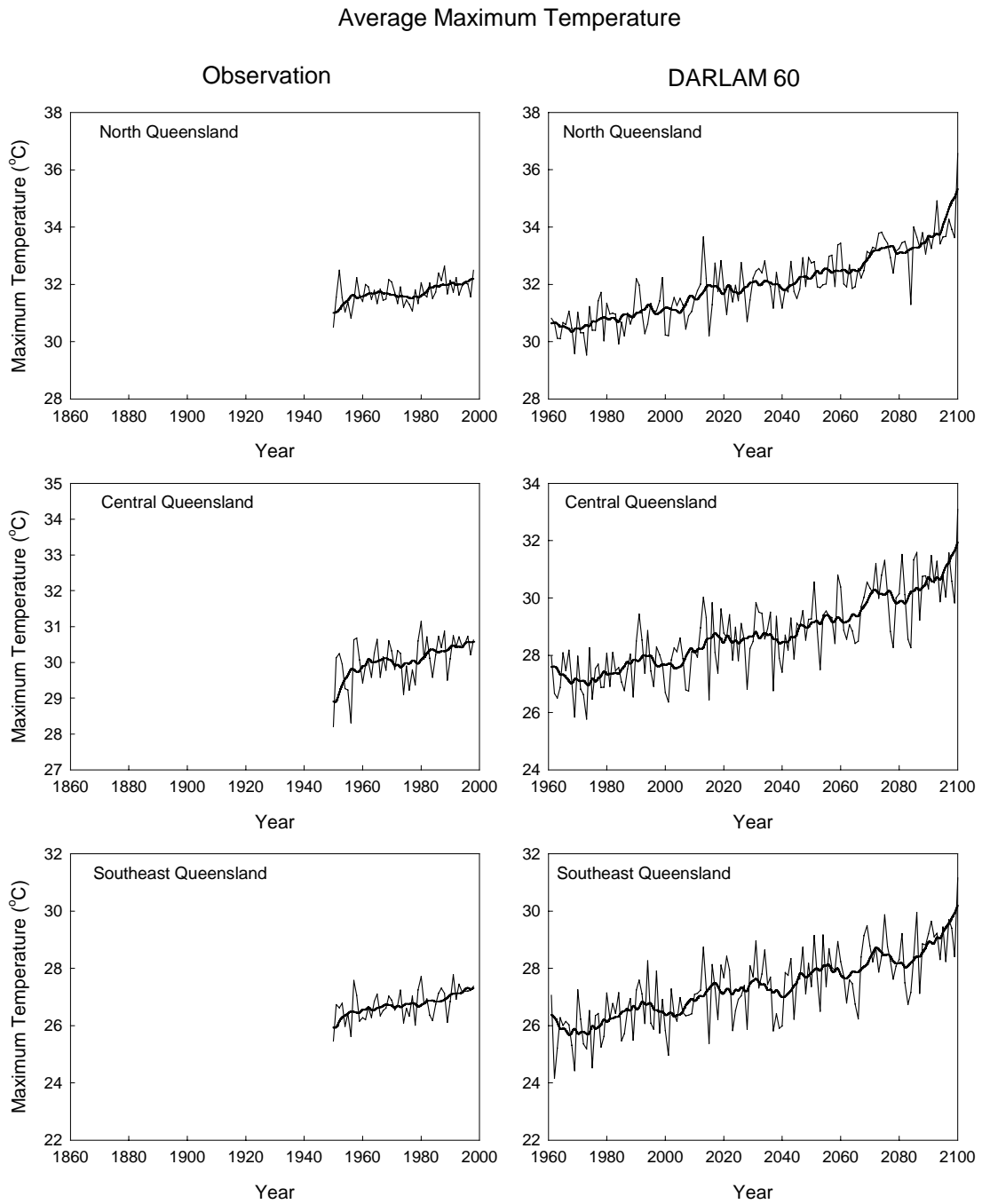
Figure 2.12. The same as Fig. 2.11 but for maximum temperature.

rnd_obs
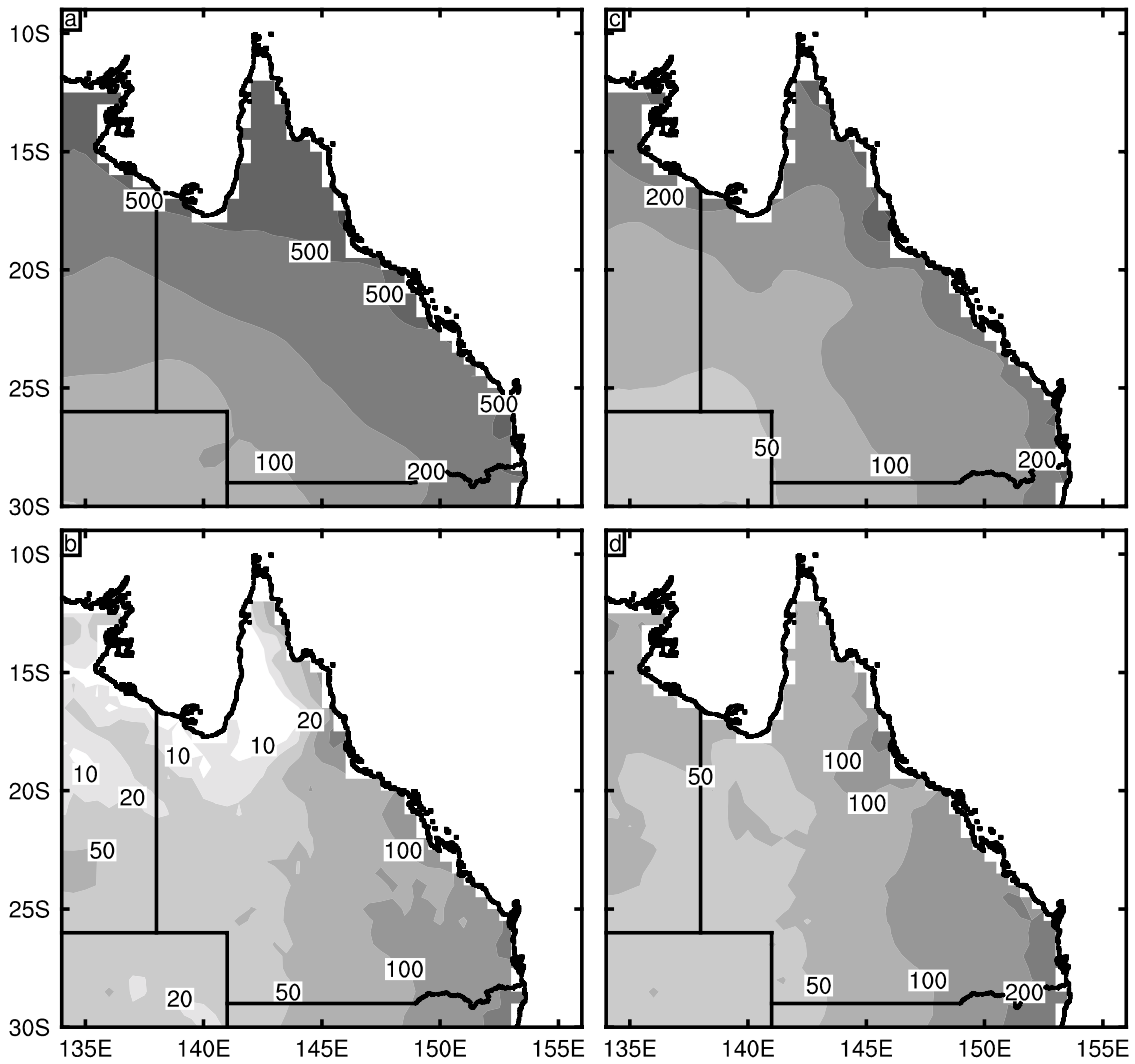
Figure 2.13. Observed rainfall for (a) summer (Dec.-Feb.); (b) winter (June-Aug.); (c) Autumn (Mar.-May); and (d) spring (Sep.-Nov.). Units are mm.

rnd_qld60
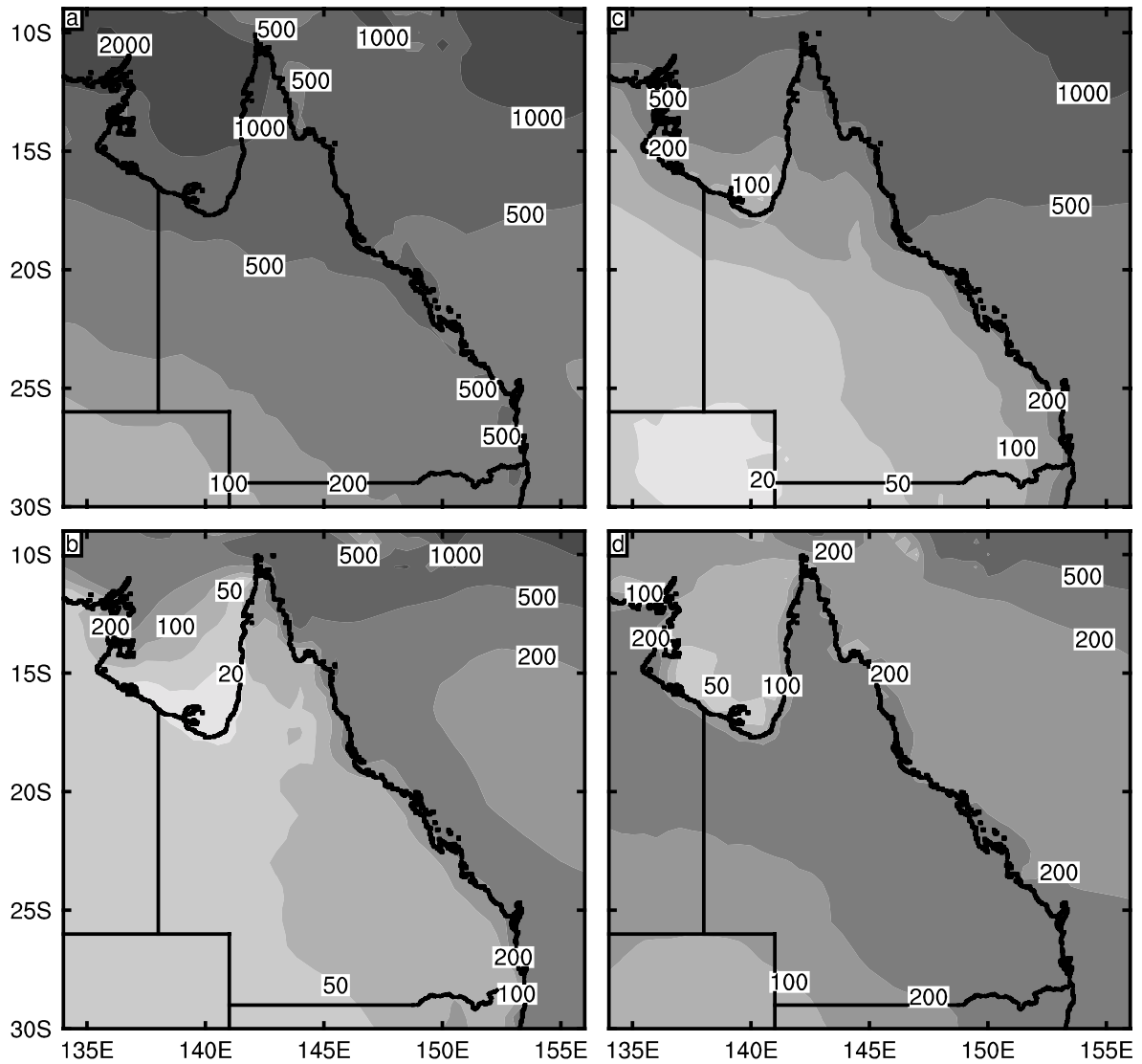
Figure 2.14. The same as Fig. 2.13 but for DARLAM-60 simulation (model equivalent of 1961-1990).
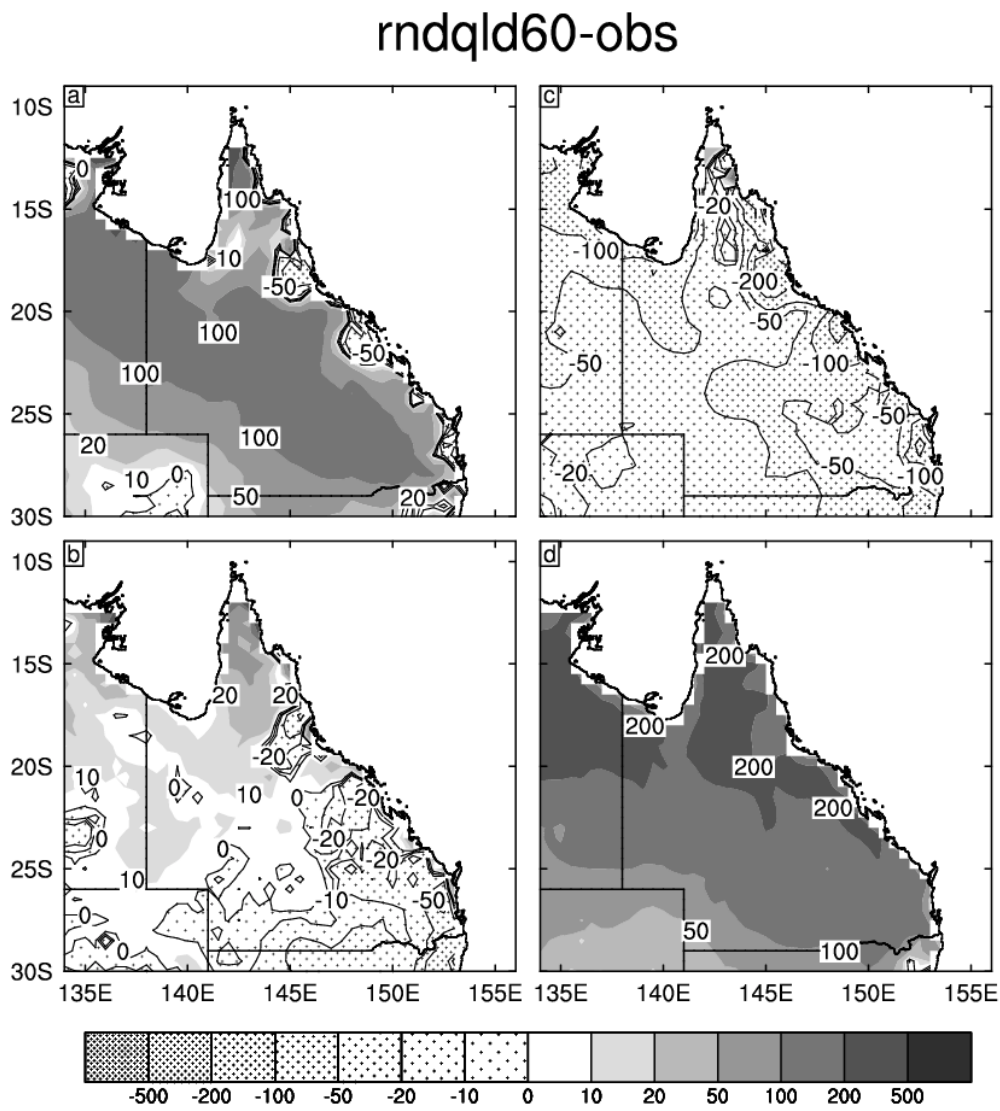
Figure 2.15. The same as Fig. 2.14 but for the difference, DARLAM-60 simulation minus observed.

The origin of these differences in precipitation between the simulation and observations has been examined. Analysis shows that much of the bias evident in the DARLAM-60 simulation is due to biases in the forcing GCM (Mark 2). The GCM transports too much moisture into the interior of the continent, causing too much rainfall to be simulated in both the GCM and in DARLAM-60. Further GCM development is addressing this issue. Although the DARLAM simulation is able to partially correct for these forcing biases, its ability to do so is not perfect.

Changes in mean rainfall under enhanced greenhouse conditions

Figure 2.16 shows the changes in rainfall simulated by DARLAM as a percentage per degree of global warming. In other words, for a 1°C global warming, the rainfall would change by the percentages indicated. In summer, the model predicts relatively small changes in rainfall in a warmer world over much of the State. Some increases are simulated in autumn, with percentage changes ranging from 0-10% per degree of global warming. Winter sees some fairly large decreases in the seasonally dry sections of Queensland, with values up to 10-15% in the north-west of the state. The south-east in winter experiences no change or slight increases, in contrast to the southern inland regions, where decreases are simulated. Finally, for spring, rainfall changes are neutral or slightly negative throughout the state.

The time evolution of rainfall and the remaining model biases at this resolution are illustrated in Figs. 2.17 and 2.18, for each of the three defined regions of the State, for the winter and summer halves of the year. The summer half-year is from October through March, while the winter half is April to September. For the winter half of the year (Fig. 2.17), the model overestimates rainfall in the northern and central regions; the mean rainfall is well simulated in the south-east. Few large rainfall trends are simulated between the years 2000 and 2100. There are large simulated interannual and decadal variations in the simulated rainfall towards the end of this century. In the summer half of the year (Fig. 2.18), the model overestimates rainfall in all regions. Again, few trends in rainfall are seen, with the exception of slight downward trends towards the end of this century in the north and south-east regions. Model decadal variability exists but it is smaller than that seen in the observations, especially towards the end of the 20th century.

In interpreting these predicted changes, we note again that DARLAM is one climate model among many, although it is particularly detailed and thus best equipped to be used for simulating regional climate changes. Temperatures in Queensland are confidently predicted to increase in a warmer world. To maintain the same level of soil moisture as in the current climate, an increase in rainfall would thus be required. However, no substantial increases in rainfall are predicted for Queensland in this simulation of the kind that would be required to counteract the drying effect of the predicted increase in temperatures. The precipitation does not change much when the year is taken as a whole. This means that soil moisture is still predicted to decrease. The balance of evidence from recent climate model simulations suggests a change to drier conditions over Queensland in a warmer world (see Section 2.4). The simulations shown here do not provide a strong contradiction of this conclusion. Further DARLAM results will be obtained using an improved GCM forcing (Mark 3) in the next year of the project.

In summary, rainfall is well simulated by DARLAM-60 in summer and winter. Simulated autumn rainfall is generally less than observed, and simulated spring rainfall is too great. Under enhanced greenhouse conditions, relatively small changes in rainfall are simulated in summer. Some increases are simulated in autumn, and decreases in spring and winter. DARLAM-60 does not simulate the consistent increases in rainfall required to counteract the drying effect of predicted temperature increases.
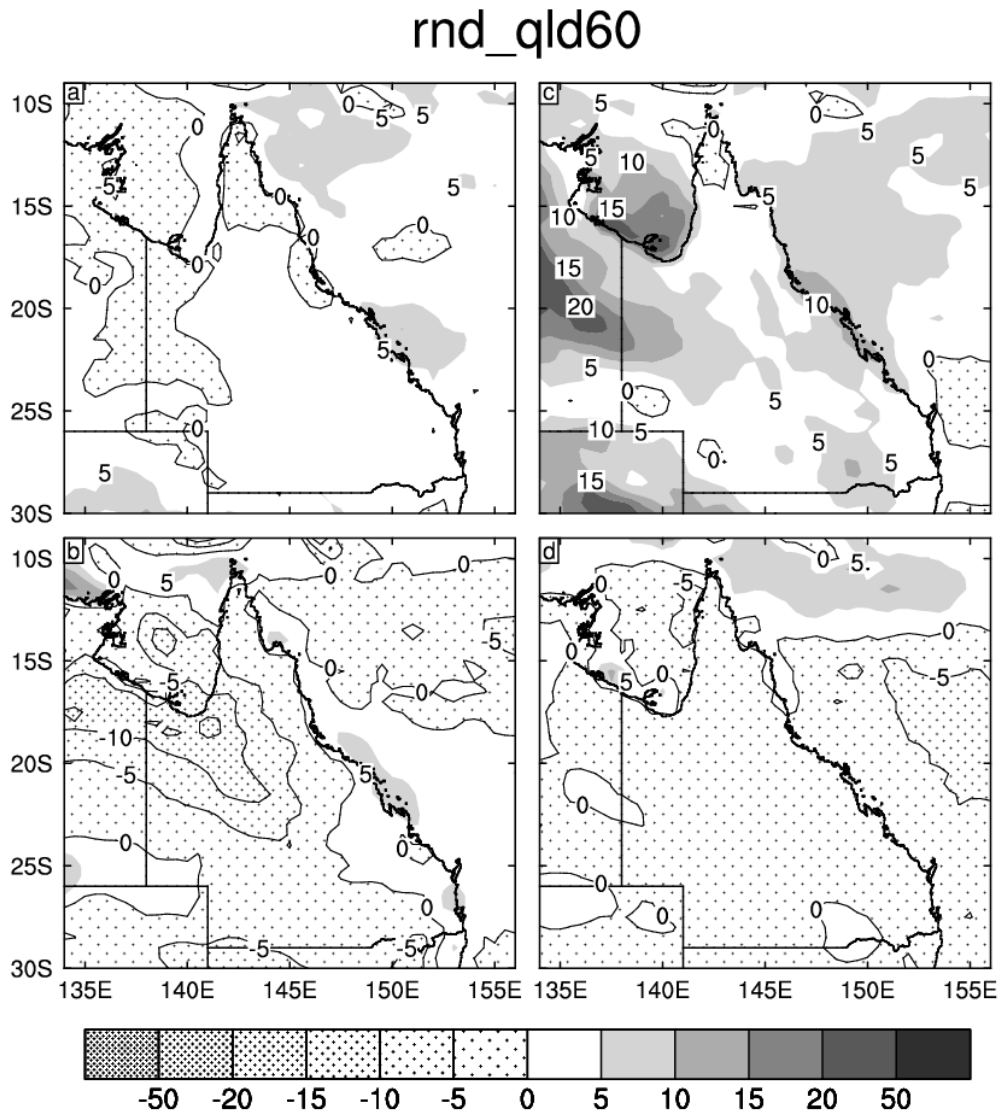
rnd_qld60

Figure 2.16. The same as Fig. 2.13 but for percentage change of rainfall per degree of global warming.
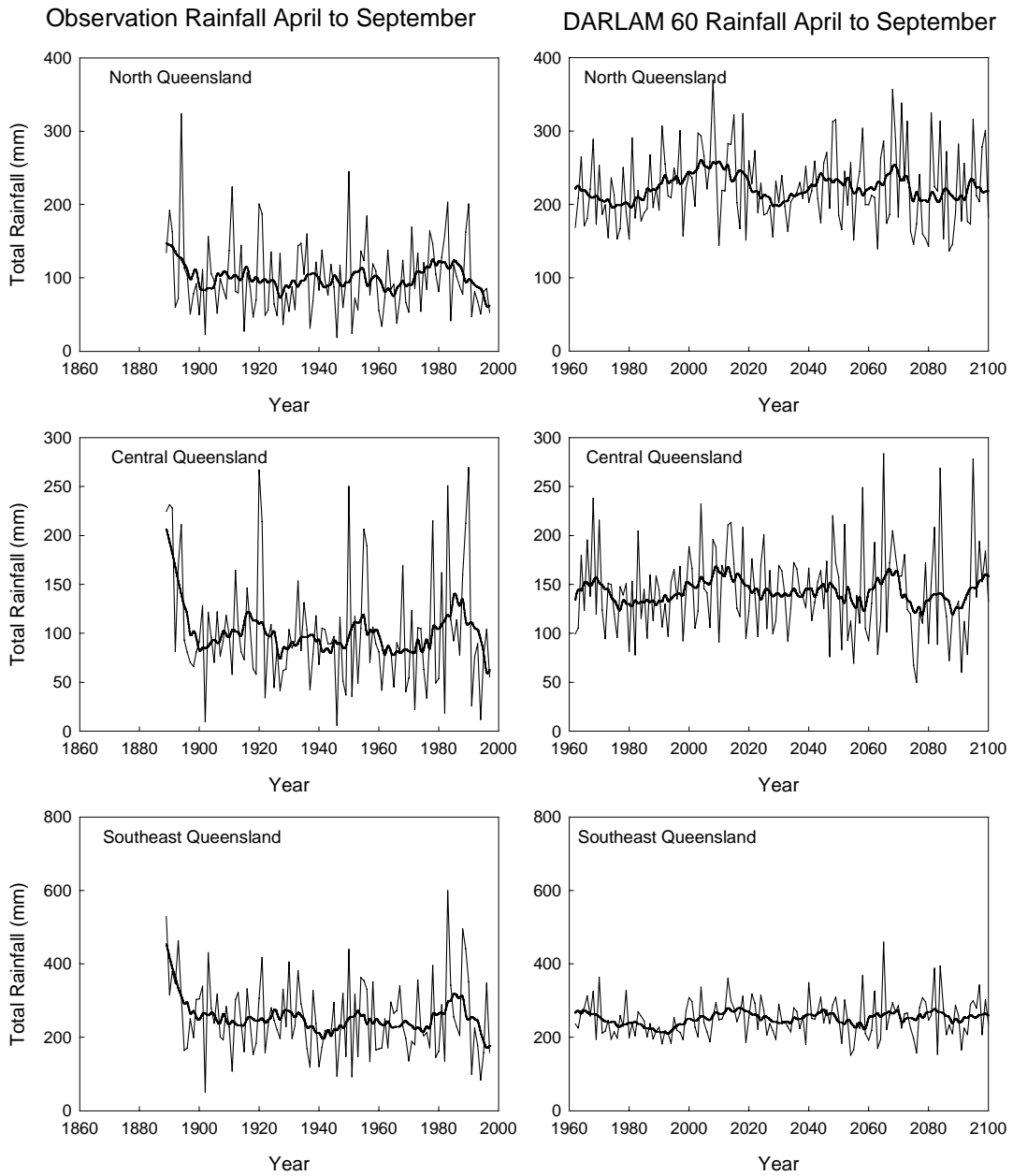
Figure 2.17. Observed and simulated rainfall for the winter half of the year, for the three regions of Queensland. Solid line gives the 11-year running mean.
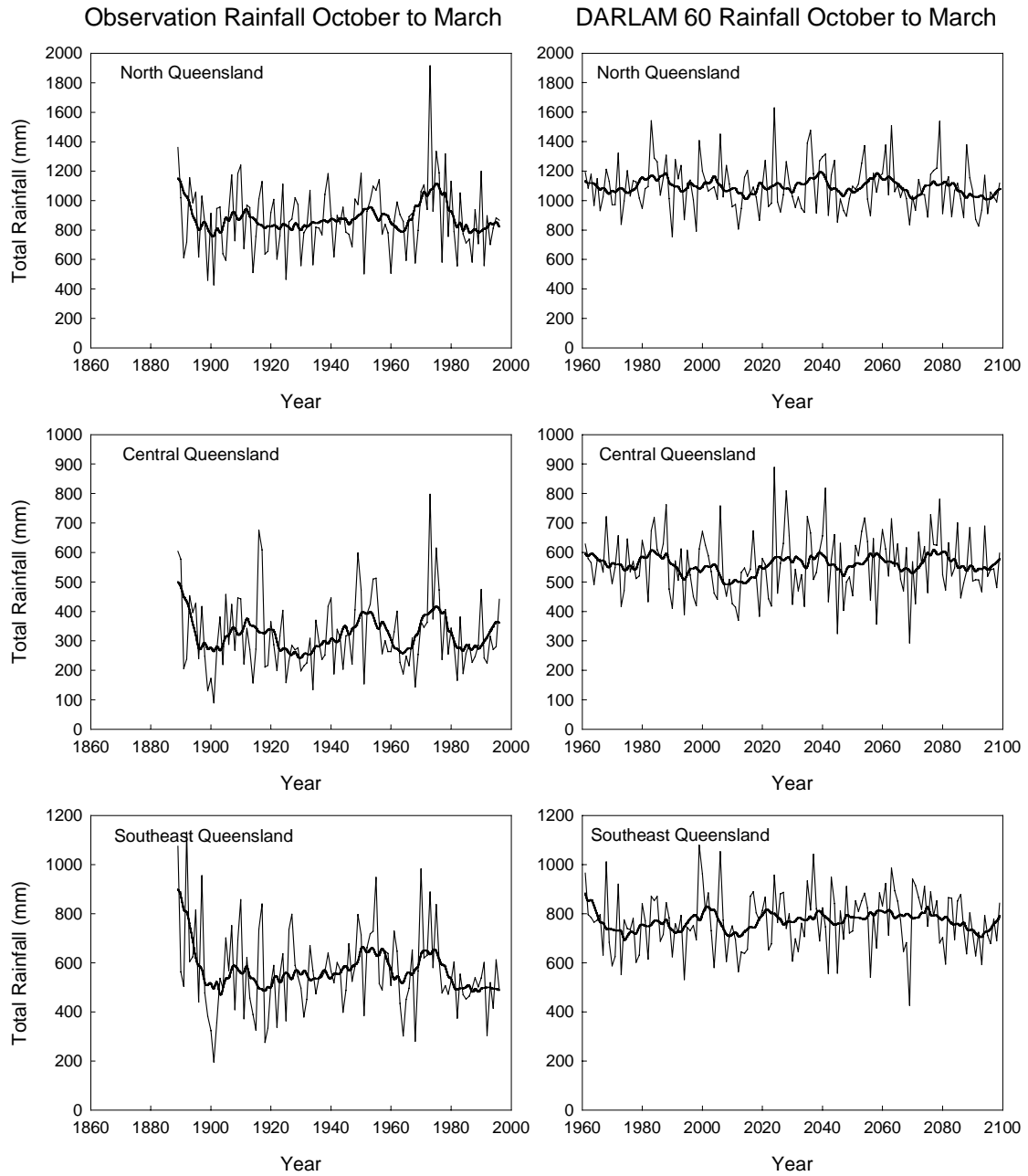
Figure 2.18. Observed and simulated rainfall for the summer half of the year.

2.2.2   Observed and simulated variability

Comparison is made between the observed and DARLAM-simulated variability at 60-km resolution. Figures 2.19 and 2.20 compare observed and simulated rainfall for the summer half of the year. As shown previously, the model somewhat overestimates the observed rainfall for the period 1960-2000, particularly in the central region. Also overlain as a continuous line on the observed and simulated data is a weighted 31-year running mean, with the weights chosen to exclude variations with periods less than 10 years (Neil Flood, personal communication, 2001). This gives an indication of long-term trends or decadal fluctuations. Figure 2.19 shows some decadal fluctuations in each region but little long-term trend. Simulated decadal variations are relatively small.

Additionally, as expected, the simulated record has smaller year-to-year fluctuations in rainfall than observed. This is most clearly shown in Fig. 2.21, which shows the variability expressed as the coefficient of variation CV, defined as

$$CV = 100(\sigma/\chi)$$

where σ is the standard deviation and χ is the mean of the time series. The coefficient of variation is displayed as a percentage and measures the variability of 31-year running portions of the time series as a ratio of their averages.

Fig. 2.21 shows rainfall variability for the summer half of the year. It is clear that the simulated year-to-year variability over the period 1960-2000 is considerably smaller than observed. This is a result of the small size of the ENSO variations generated in the forcing CSIRO Mark 2 GCM, which gives SST variations in the equatorial Pacific region only about a third of the size of those observed.

October to March

Figure 2.19. Observed rainfall (dashed line) from 1889 to 1996 during the summer-half year of the three regions in Queensland. The smooth line shows the weighted 31-year running mean.

October to March

Figure 2.20. DARLAM-simulated rainfall (dashed line) from 1961 to 2100 during the summer-half year for the three regions in Queensland. The smooth line shows the weighted 31-year running mean.

October to March

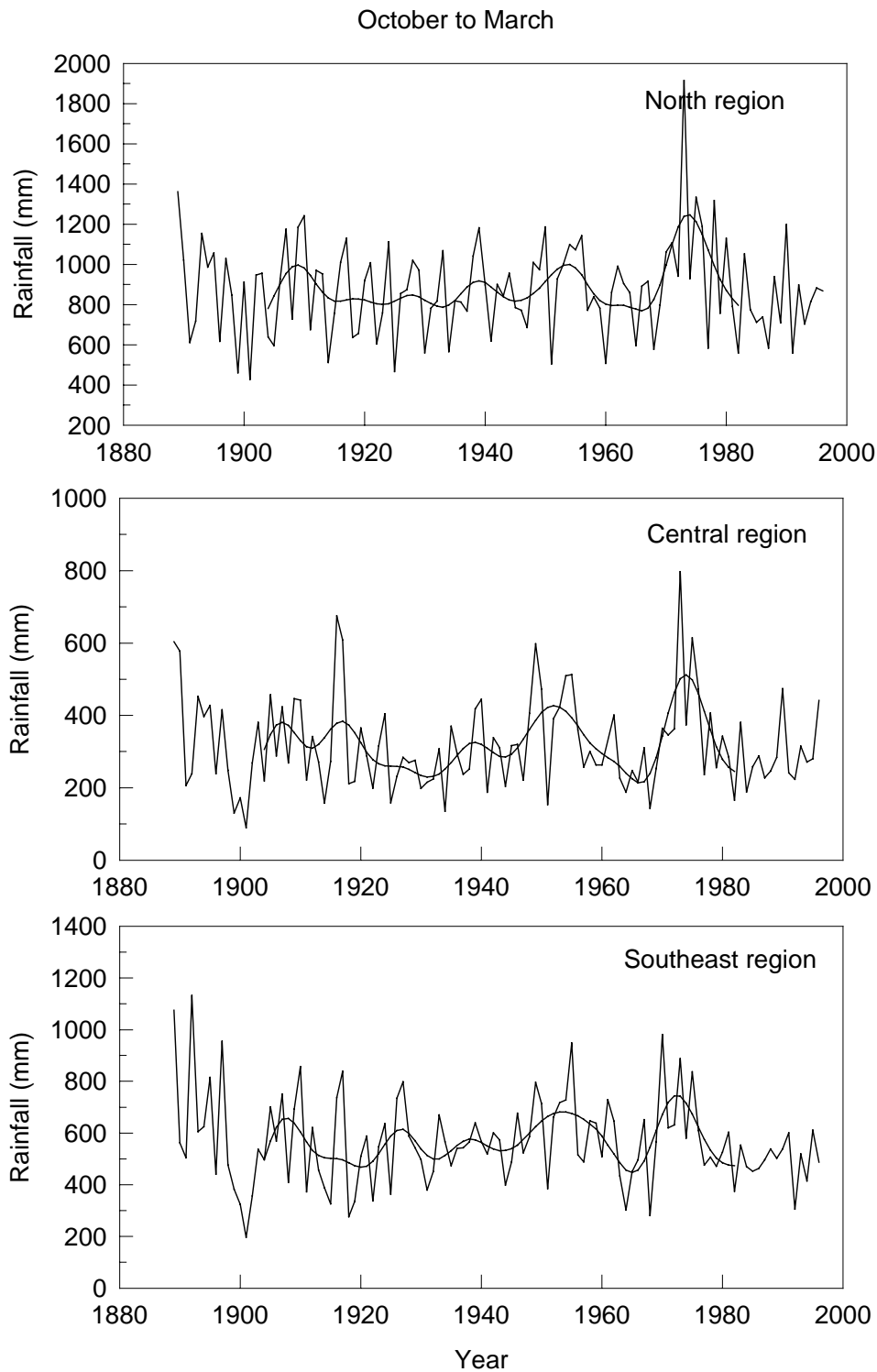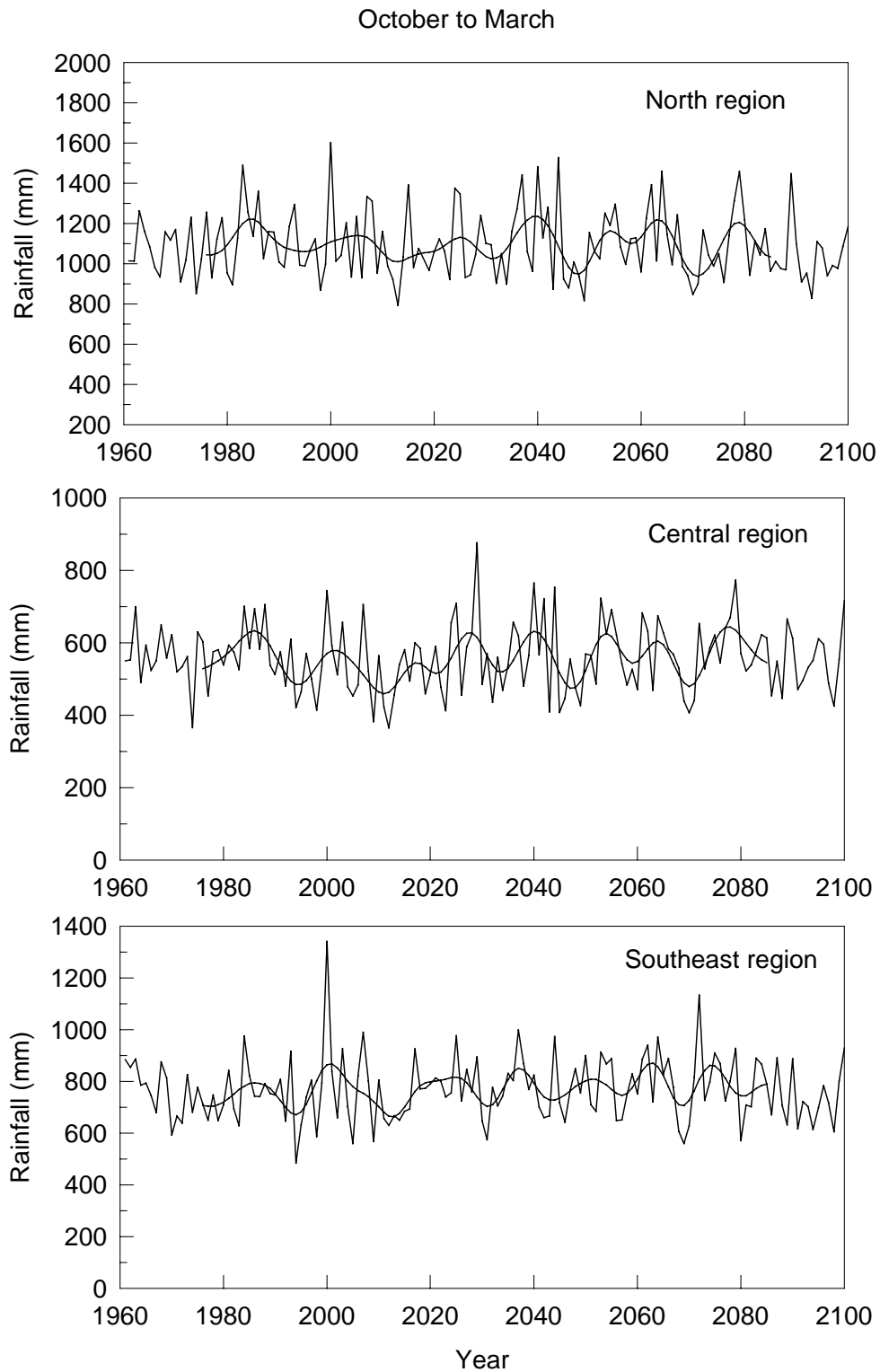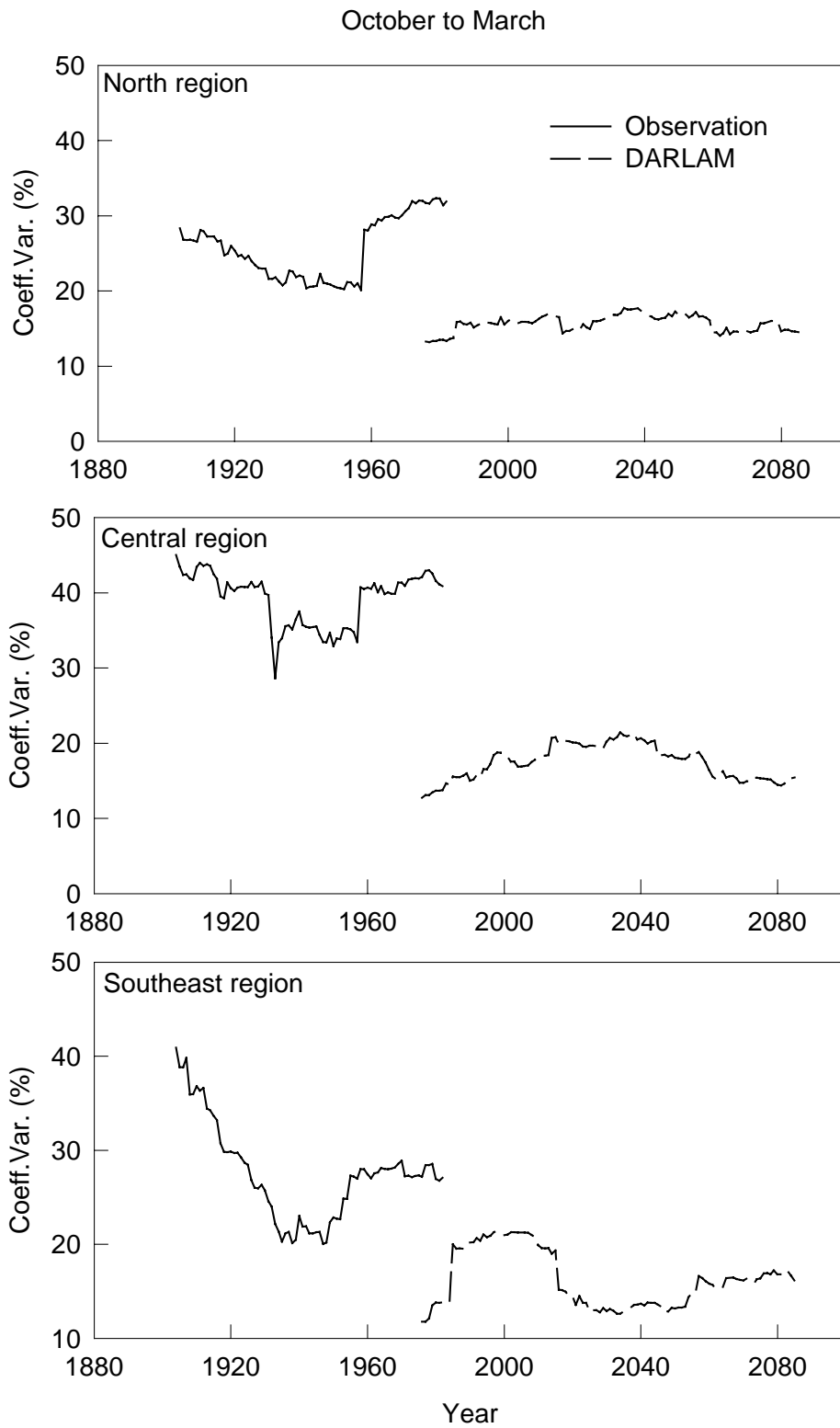**Figure 2.21.** Observed changes during the summer-half of year in the 31-year running mean of the coefficient of variation, for observations (solid line) and model simulation (dashed line).

There are some curious trends in year-to-year variability in the observed record (Fig. 2.21). Both the north and central regions experience almost a step jump in variability at about 1960. This is because the 31-year running values centred near this year suddenly incorporated the very variable rainfall experienced in the mid-1970s. Additionally, in the south-east region there has been a strong downward trend in year-to-year rainfall variability in the period 1900-1940, with variability rising slightly since then.

In general, the DARLAM-simulated rainfall variability is about half of that observed. Predictions of trends of variability into the next century must therefore be treated with caution. DARLAM predicts variability to remain roughly constant in all regions into the next century, with the possible exception of the central region, where variability is predicted to fall.

Turning to the winter half of the year, Figures 2.22 and 2.23 compare observed and simulated rainfall. In the north and central regions, the model again overestimates rainfall, particularly in the north. The model appears to have a good simulation of average rainfall in the south-east region, however. The observed rainfall in Fig. 2.22 does not appear to have substantial trends, and simulated trends into the next century (Fig. 2.23) remain modest, although there appears to be some substantial multi-decadal variability. Comparing the observed and simulated coefficients of variation (Fig. 2.24 and 2.25), again simulated variability is consistently lower than observed in all regions. Observed variability in the winter half of the year (Fig. 2.24) has shown some trends: there appears to be a downward trend in variability towards the year 2000 in the north region, while in the central and south-east regions the winter rainfall has been becoming slightly more variable in the past few decades. The model-predicted trends (Fig. 2.25) show increases in rainfall variability in all regions towards the end of the next century. Because of the model's weaker than observed variability, however, confidence in these predictions must be regarded as quite low.
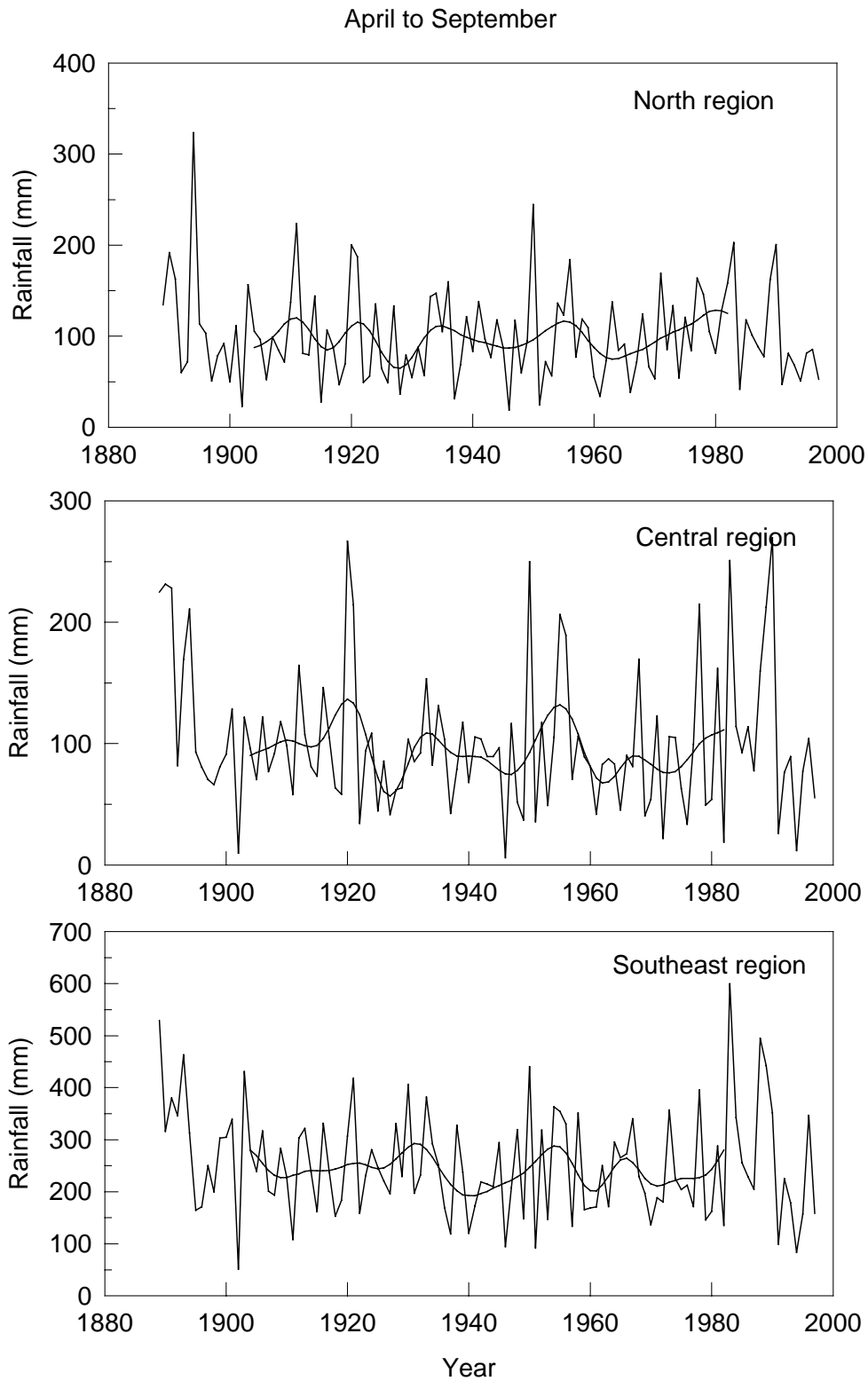
Figure 2.22. The same as Fig. 2.19 but for April-September.
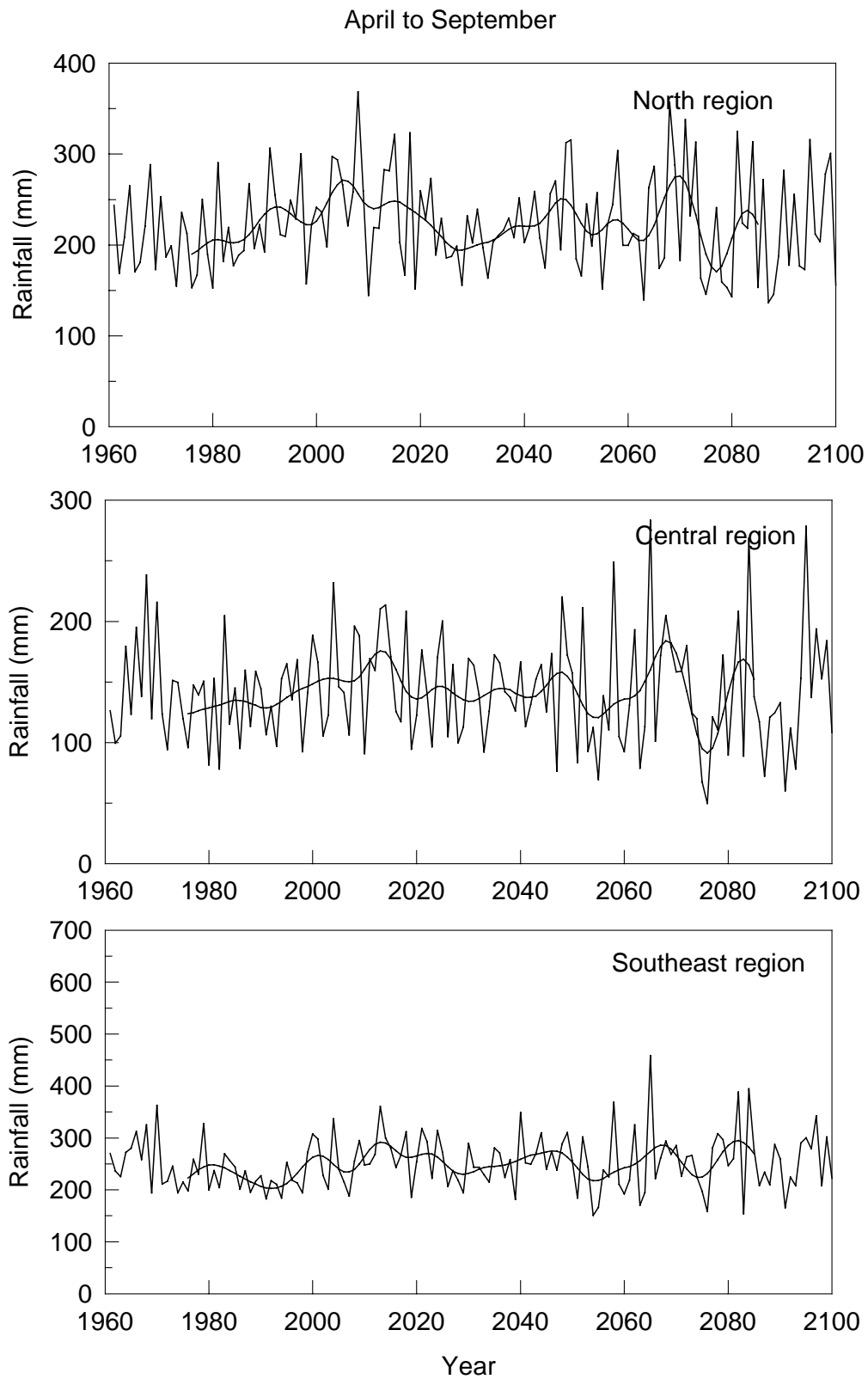
Figure 2.23. The same as Fig. 2.20 but for April-September.
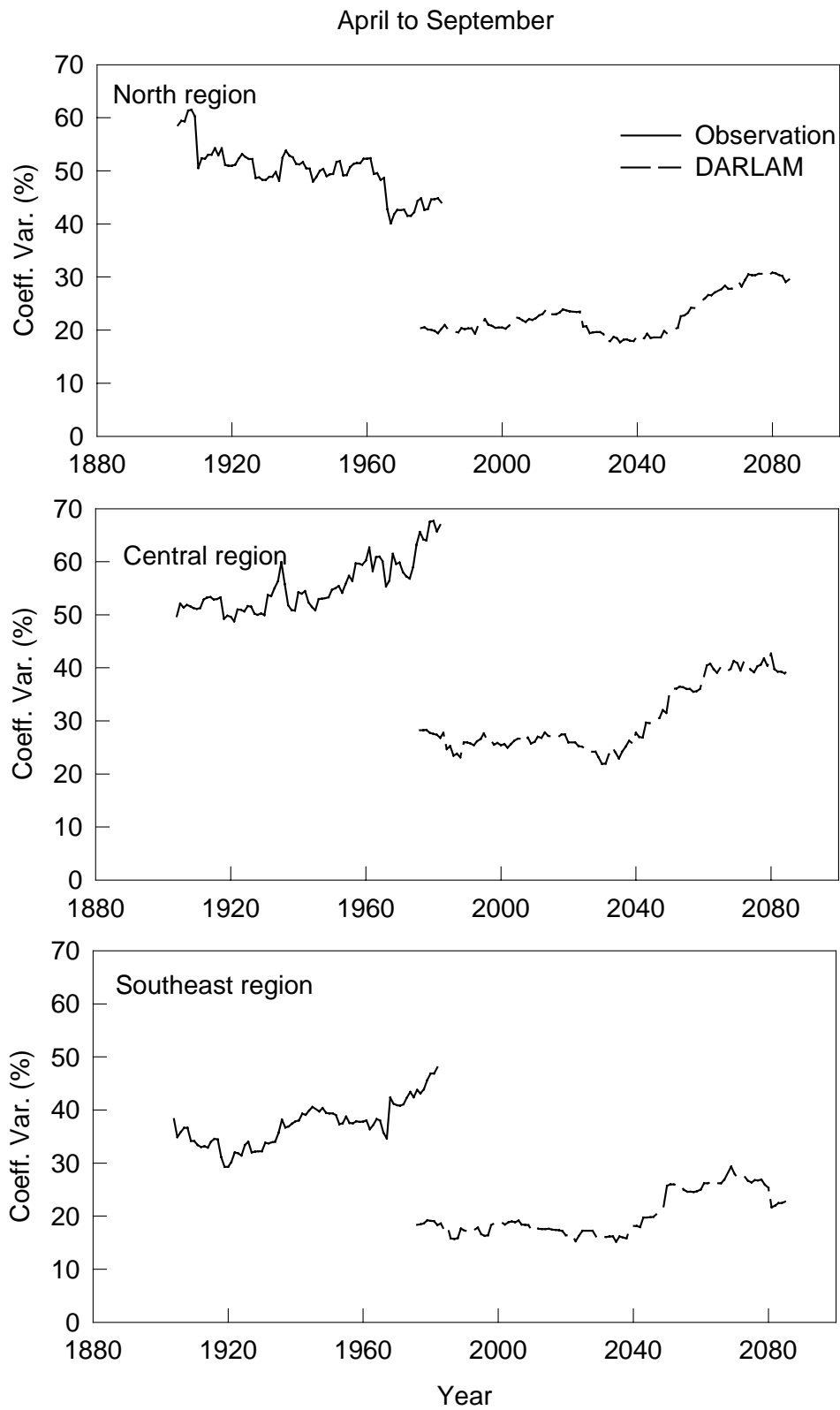
April to September

Figure 2.24. Same as Fig. 2.21 but for April-September.

2.2.3 Extreme events

Many of the important impacts of climate change rely on estimates of changes in the frequency of extreme temperature and rainfall rather than changes in averages or variability. Even relatively small changes in averages can cause large changes in extreme events, as illustrated in Fig. 2.25. This section summarizes the DARLAM-60 simulation of these quantities and the implications for future climate.

Temperature

Simulations of temperature extremes from the DARLAM 60-km simulation are shown in Figs. 2.26 and 2.27. Comparison with observed station data suggests that numbers of days over 35°C are overestimated in south-east Queensland, while the other regions are better simulated. However, all regions show consistent strong upward trends in the number of extreme temperature maxima and consistent downward trends in the number of extreme minima.
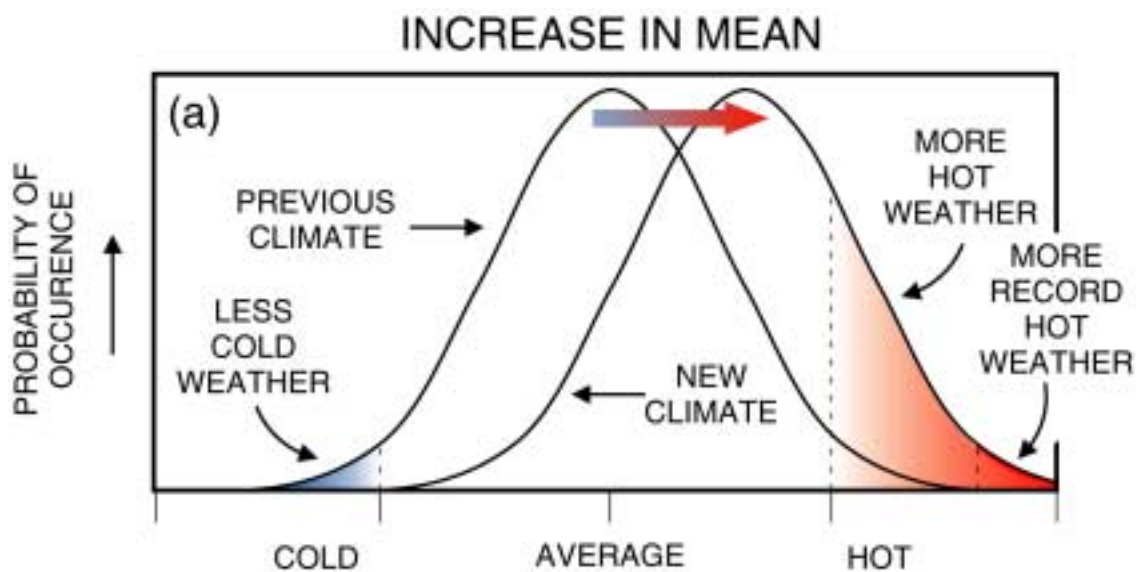
Figure 2.25. Illustration of large changes in extremes that can occur with only modest changes in mean conditions.

Maximum Temperature Extremes
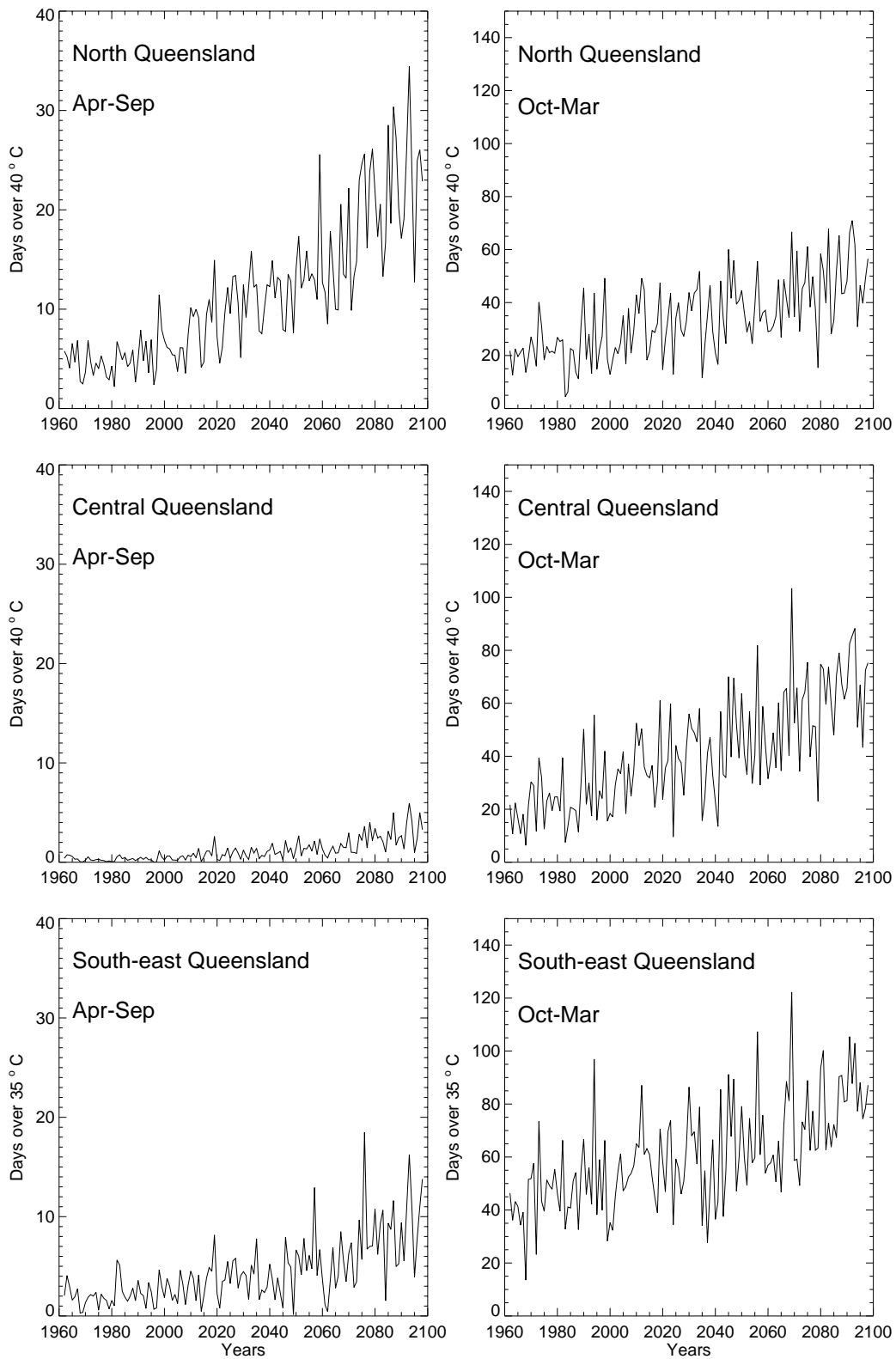
Figure 2.26. Simulated number of days in each half year of extreme maximum temperature events, defined as maximum temperatures greater than 40°C (north and central regions) or 35°C (south-east region).

Minimum Temperature Extremes
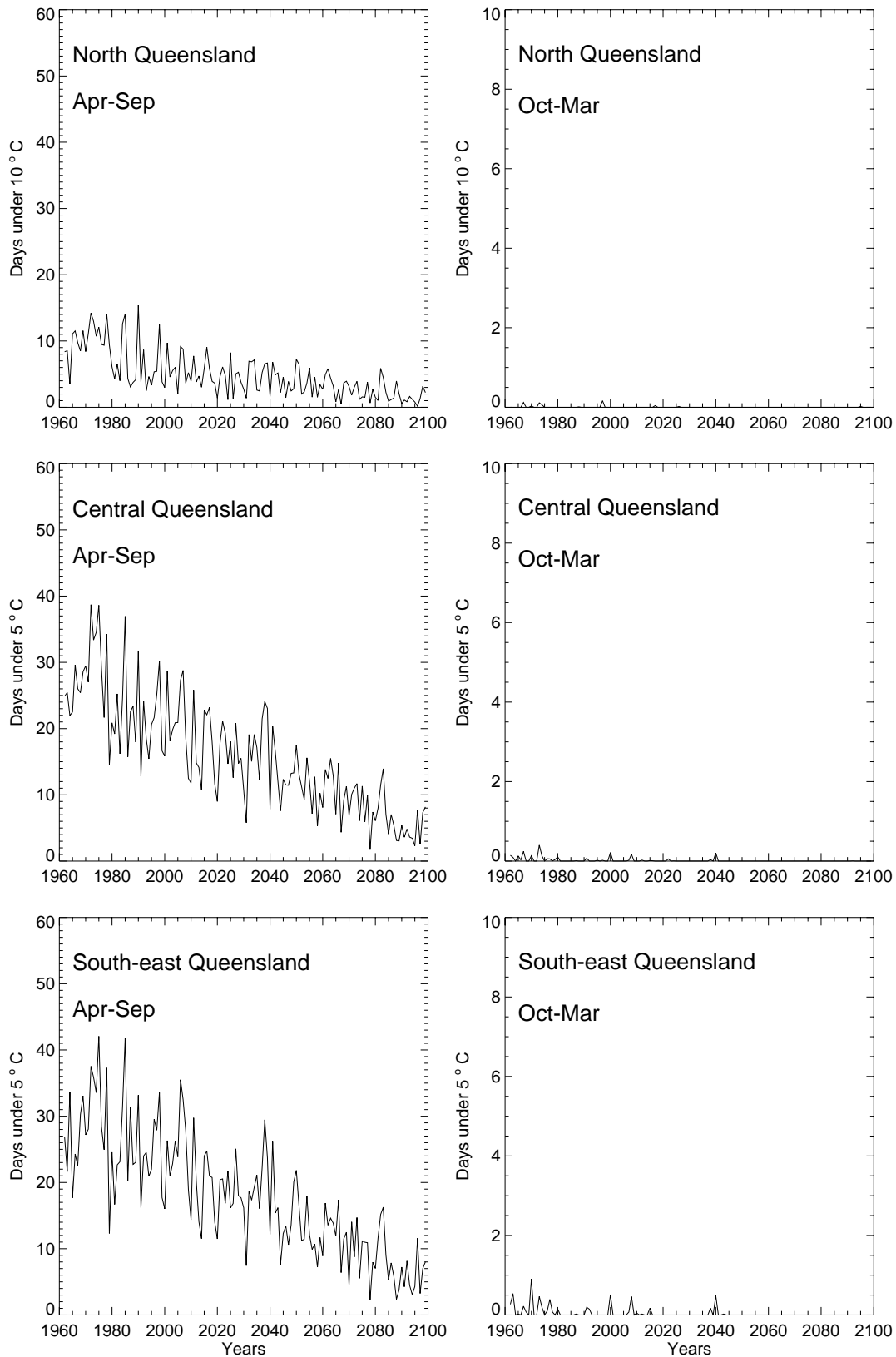
Figure 2.27. The same as Fig. 2.26 but for extreme minimum temperatures (less than 10°C for north Queensland, less than 5°C for central and south-east Queensland).

Impact of different emission scenarios and differing model predictions

The impact of differing emissions scenarios on extreme temperature events can be substantial. Figures 2.26 and 2.27 are based on the IS92a scenario, assuming a mid-range increase in emissions (IPCC, 1996). Using the lower IS92c emission scenario, the number of extreme maximum temperatures only rises slightly by the year 2000. Using the higher emission IS92e scenario, large increases in the frequency of extreme temperature events are simulated, with numbers of days of greater than 40°C in summer in north Queensland more than quadrupling by 2100.

Additional uncertainty arises from the lack of knowledge of the exact response of the Earth's climate to increases in greenhouse gases, known as the *climate sensitivity*. This quantity is different in each climate model. These two uncertainties are combined and the results for extreme temperatures are summarized in Tables 2.1 and 2.2. These tables were constructed assuming a range of emissions scenarios (IS92c, IS92a and IS92e, as described above).

Table 2.1*. Changes in daily temperature indicators between two 40-year periods: 2031-2070 and 1961-2000, during April to September. The indicators are average maximum temperature, average minimum temperature, percentage changes in number of extremely hot days (over 35°C in the south-east, over 40°C in the central and northern regions), and number of extremely cold days (below 10°C in the north and below 5°C in the central and south-east). The range of values reflects uncertainty in greenhouse gas emission scenarios and climate sensitivity.*

	South-east	Central	North
Ave. max temp (°C)	↑ 0.4 to 1.9	↑ 0.6 to 2.1	↑ 0.7 to 2.2
Ave. min temp (°C)	↑ 0.7 to 2.1	↑ 0.8 to 2.3	↑ 0.7 to 2.3
No. of hot days (% change)	↑ 30 to 162%	↑ 92 to 411%	↑ 62 to 216%
No. of cold days (% change)	↓ 18 to 56%	↓ 20 to 58%	↓ 27 to 61%

Table 2.2*. Changes daily temperature indicators between two 40-year periods: 2031-2070 and 1961-2000, during October to March. The indicators are average maximum temperature, average minimum temperature, number of extremely hot days (over 35°C in the south-east, over 40°C in the central and northern regions), and number of extremely cold days (below 10°C in the north and below 5°C in the central and south-east). The range of values reflects uncertainty in greenhouse gas emission scenarios and climate sensitivity.*

	South-east	Central	North
Ave. max temp (°C)	↑ 0.7 to 2.2	↑ 1.0 to 2.5	↑ 0.8 to 2.2
Ave. min temp (°C)	↑ 0.7 to 2.2	↑ 0.9 to 2.4	↑ 0.7 to 2.1
No. of hot days (% change)	↑ 16 to 46%	↑ 49 to 128%	↑ 35 to 83%
No. of cold days (% change)	↓ 72 to 89%	↓ 75 to 93%	↓ 100%

Extreme Rainfall Events

Extreme rainfall events also become more frequent in a warmer world. Figure 2.28 shows the return periods in years of rainfall events for the three regions. The 40-year event increases substantially in north Queensland in both seasons, and slightly in central and south-east Queensland. These results are similar to those from the DARLAM 125-km simulation from Walsh et al. (2000) (Figure 2.29[1]), except that the extreme events for the DARLAM-60 simulation are somewhat less than in the DARLAM 125-km simulation. In both models, the maximum daily rainfall expected over a certain period of time increases in a warmer world. This indicates that present-day heavy rainfall events should become heavier.

---

[1] These plots are a corrected version of Figs. 2.3 and 2.4 in Walsh (2000), the previous year's report, as these were plotted incorrectly in that report.
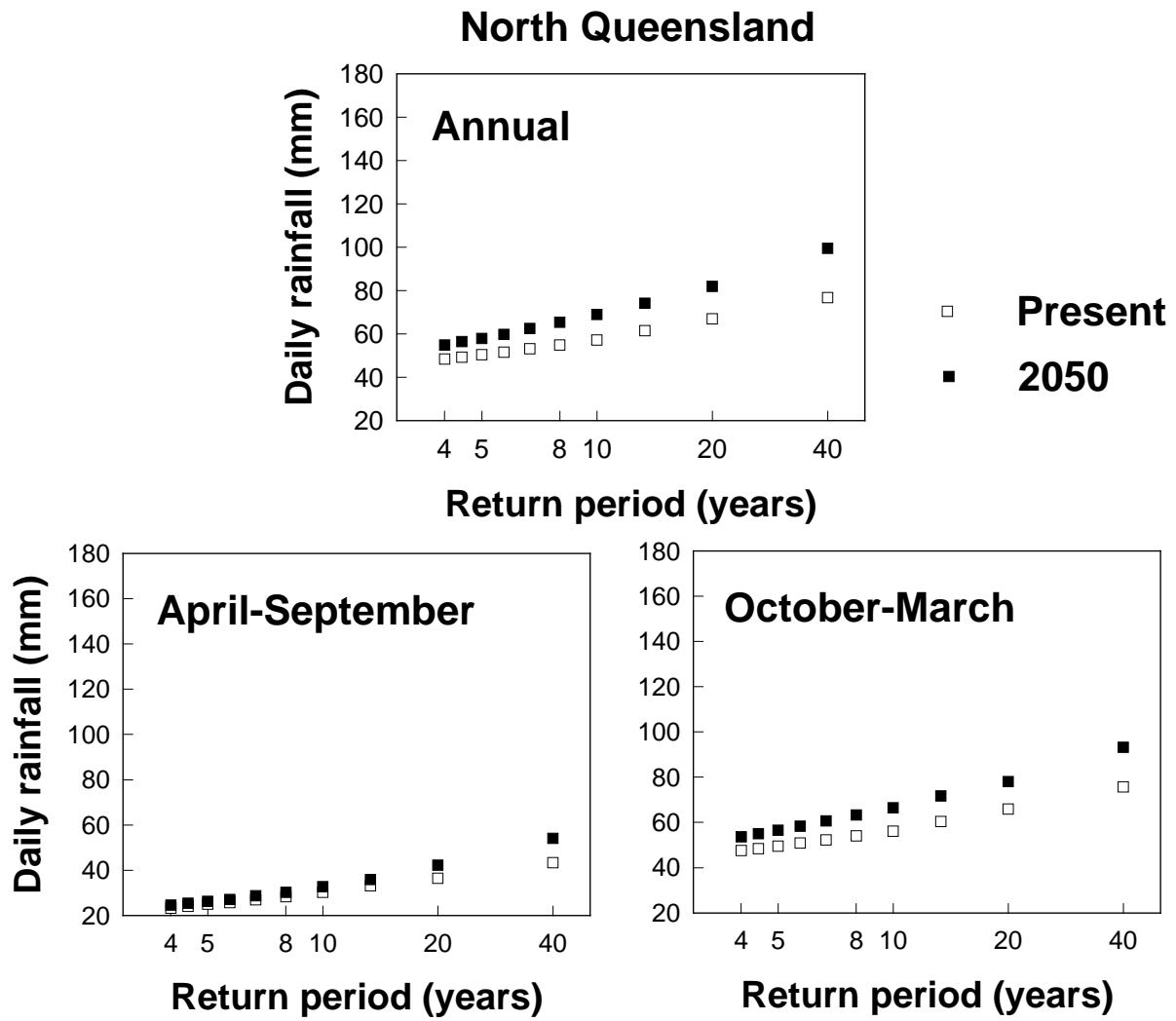
North Queensland

Figure 2.28. Return periods of rainfall events for north Queensland, for present and enhanced greenhouse conditions.
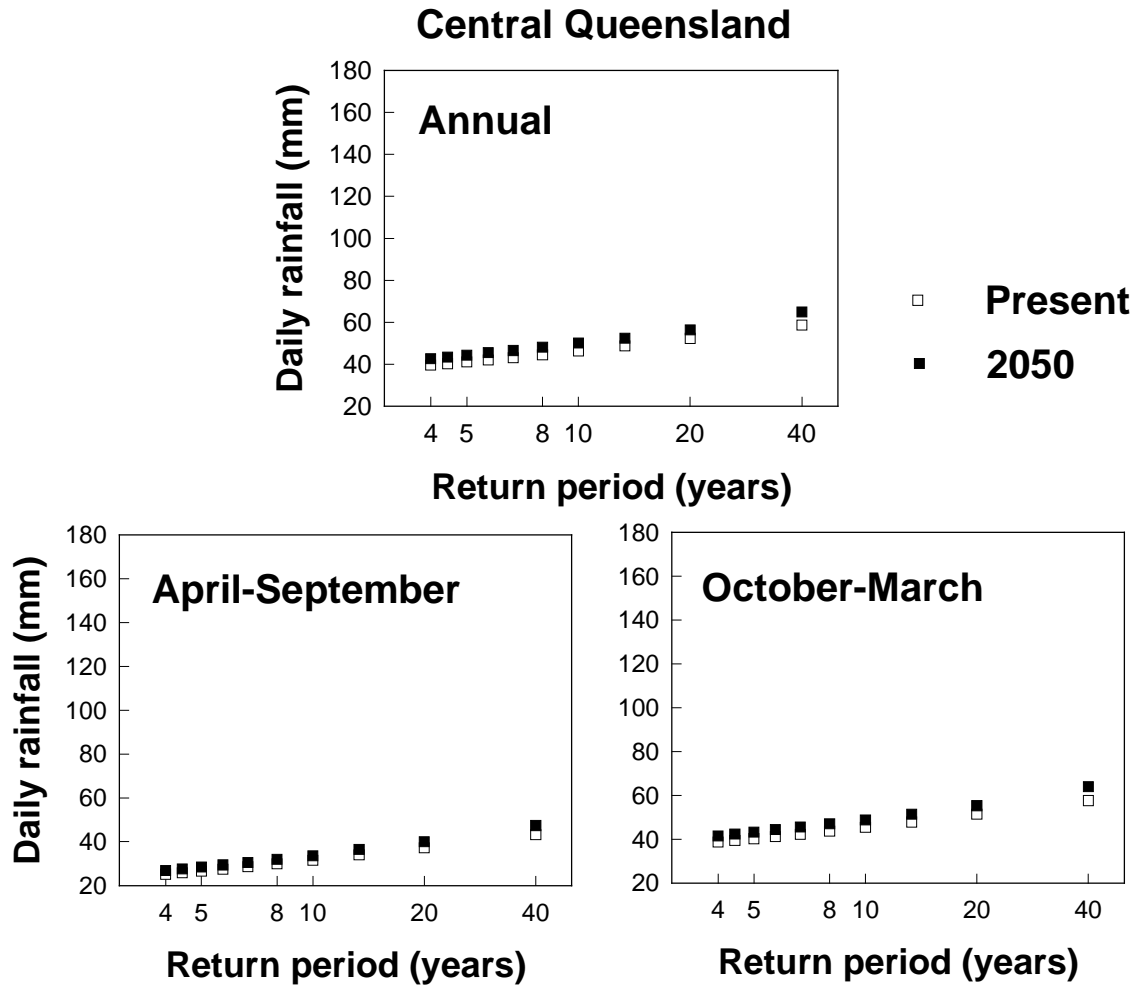
Figure 2.28 (continued).
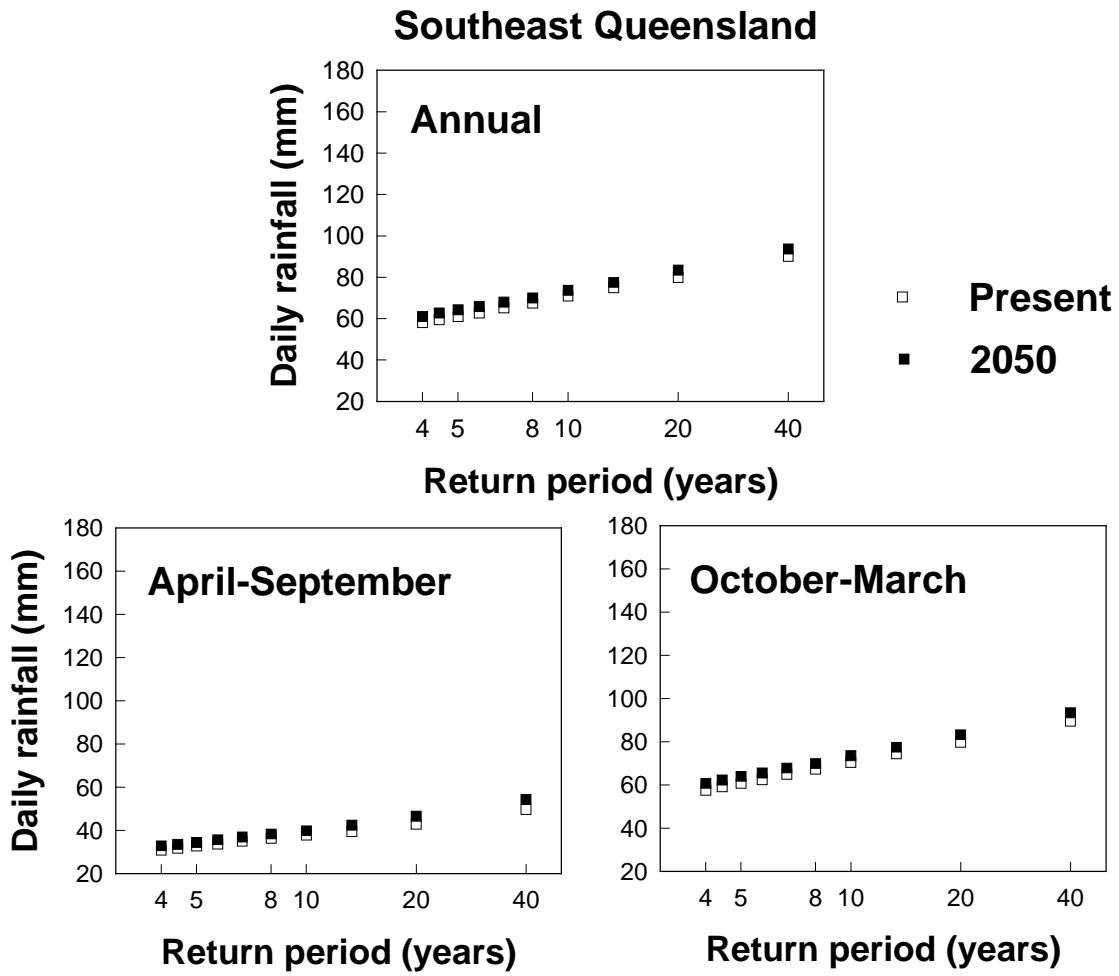
Figure 2.28 (continued).
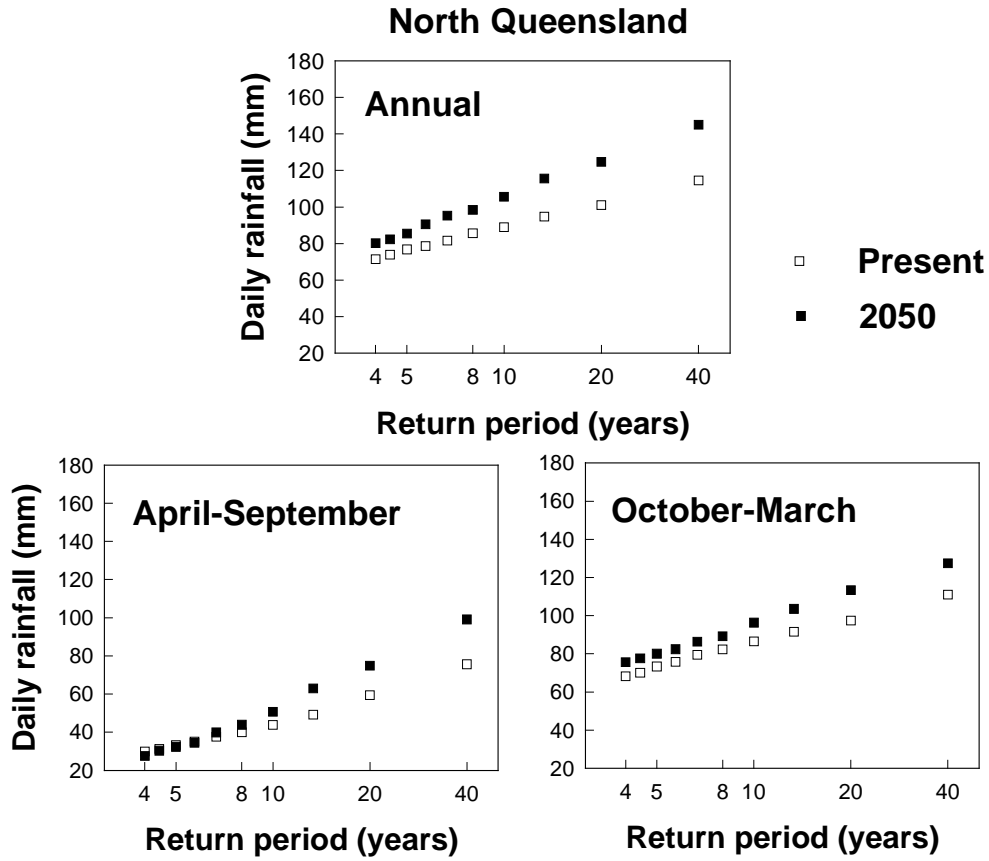
Figure 2.29. DARLAM 125-km simulation, return period of extreme rainfall.

Figure 2.29 (continued).
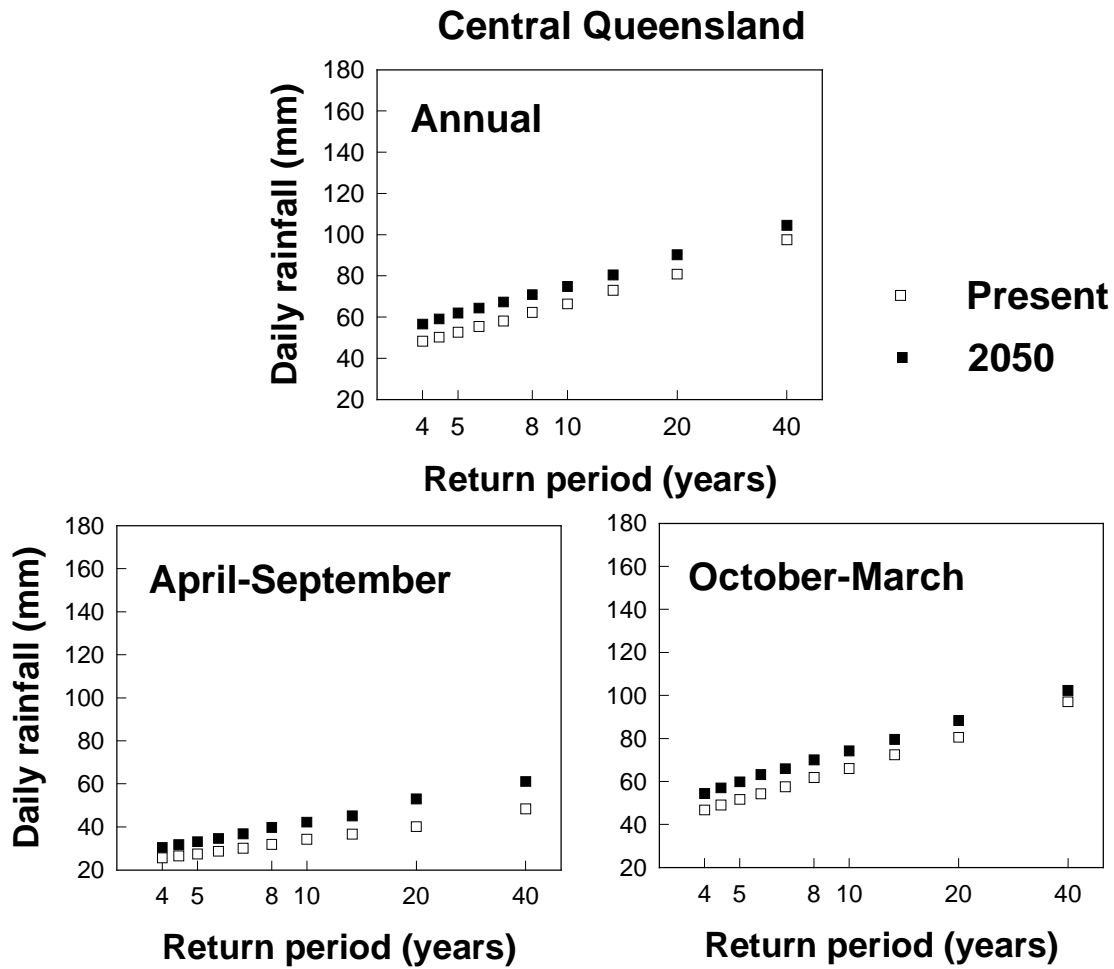
Southeast Queensland
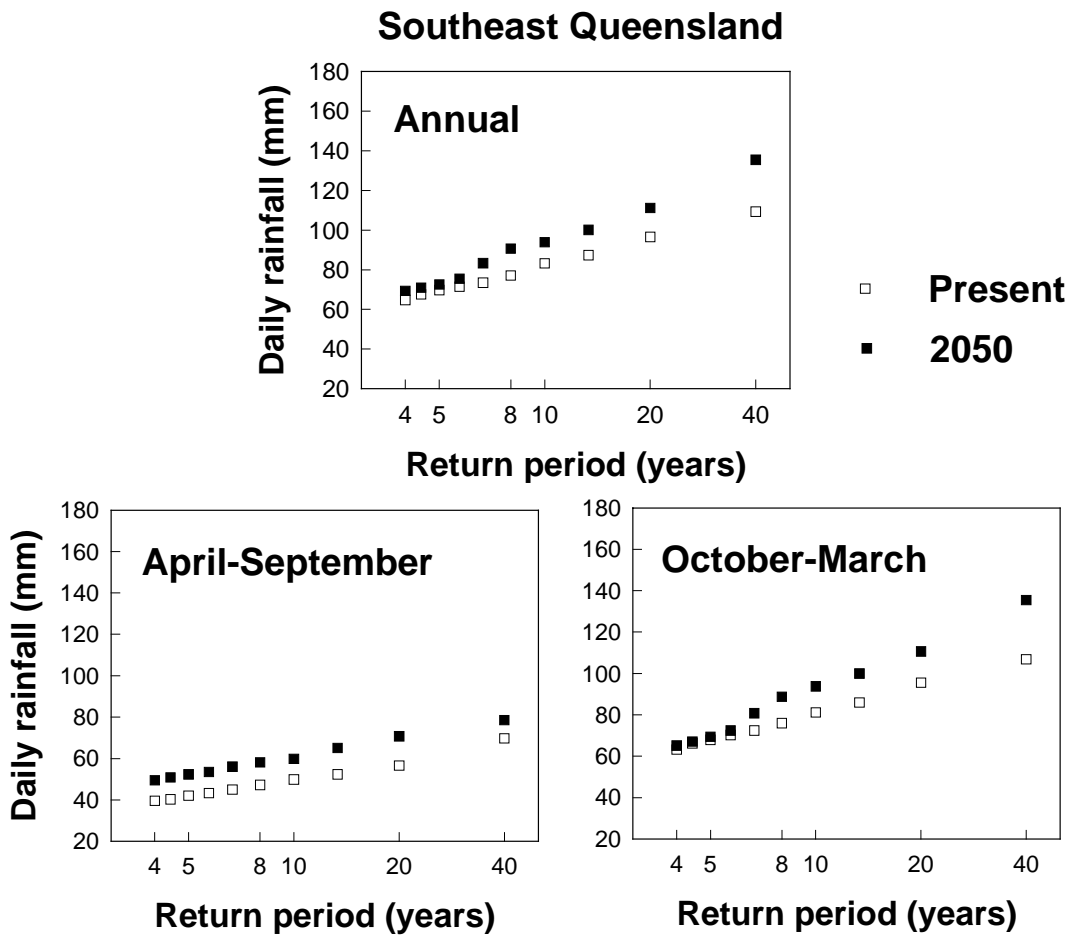
Figure 2.29. (continued).

2.3 Intercomparison of Model Results

2.3.1 Introduction

The intercomparison of model predictions is an important process in the construction of climate change scenarios (e.g. Whetton et al., 1994). Different climate models have different simulations of climate change, as they are constructed with differing representations of the physical processes governing such phenomena as clouds and rainfall. As climate models improve, a more discriminating evaluation can be performed of their strengths and weaknesses, even to the point of leaving out a model when constructing a climate change scenario. This section updates previous work (Walsh et al., 2000, Section 2.4) by considering the results of further models and making a judgement regarding their suitability for inclusion in climate change scenarios.

2.3.2 Model characteristics

The models evaluated in this section are listed in Table 2.3. Four new models are added to the results presented in Walsh et al. (2000).

Table 2.3. *Model runs used in intercomparison. "Letter in Figures" indicates the letter designating the model run in the subsequent figures contained in this section.*

Centre	Letter in Figures	Model	Emission Scenario	Features	Years
Canadian CCMA[5]	(a)	CGCM1	1% CO_2 pa	No sulfates	1900–2100
CCSR/NIES, Japan[8]	(b)	CGCM	IS92a	No sulfates	1890-2099
DKRZ, Germany[7]	(c)	ECHAM3/LSG	IS92a	No sulfates	1880-2085
GFDL[2]	(d)	GFDL CGCM	1% CO_2 pa	No sulfates	1958–2057
Hadley Centre, UK[4]	(e)	HADCM2	1% CO_2 pa	Ensemble of four simulations, no sulfates	1861–2100
Hadley Centre, UK[6]	(f)	HADCM3	IS95a, individual gas concentrations specified	No sulfates	1861-2099
DKRZ, Germany[3]	(g)	ECHAM4/OPY C3	IS92a	No sulfates	1860–2099
NCAR	(h)	CGCM	IS92a	No sulfates	1900-2035
CSIRO, Australia[1]	(i)	Mk2	IS92a equivalent CO_2	No sulfates	1881–2100

[1]Gordon and O'Farrell (1997)
[2]See http://ipcc-ddc.cru.uea.ac.uk/index.html
[3]DKRZ-Model User Support Group (1992), Oberhuber (1992)
[4]Cullen (1993)
[5]Flato et al. (2000)
[6]Gordon et al. (2000)
[7]DKRZ-Model User Support Group (1992); Maier-Reimer and Mikolajewicz (1991)
[8]Emori et al. (1999)

2.3.3 Model validation

Temperature

Mean temperature patterns in each of the models have reasonable agreement with observations, although variation amongst models is up to 5°C. An intermodel comparison for winter is shown in Fig. 2.30. The GFDL model (Fig. 2.30d) has the strongest cool bias. Given the reasonable quality of the temperature simulations in all models, it may not be justifiable to exclude any of them.
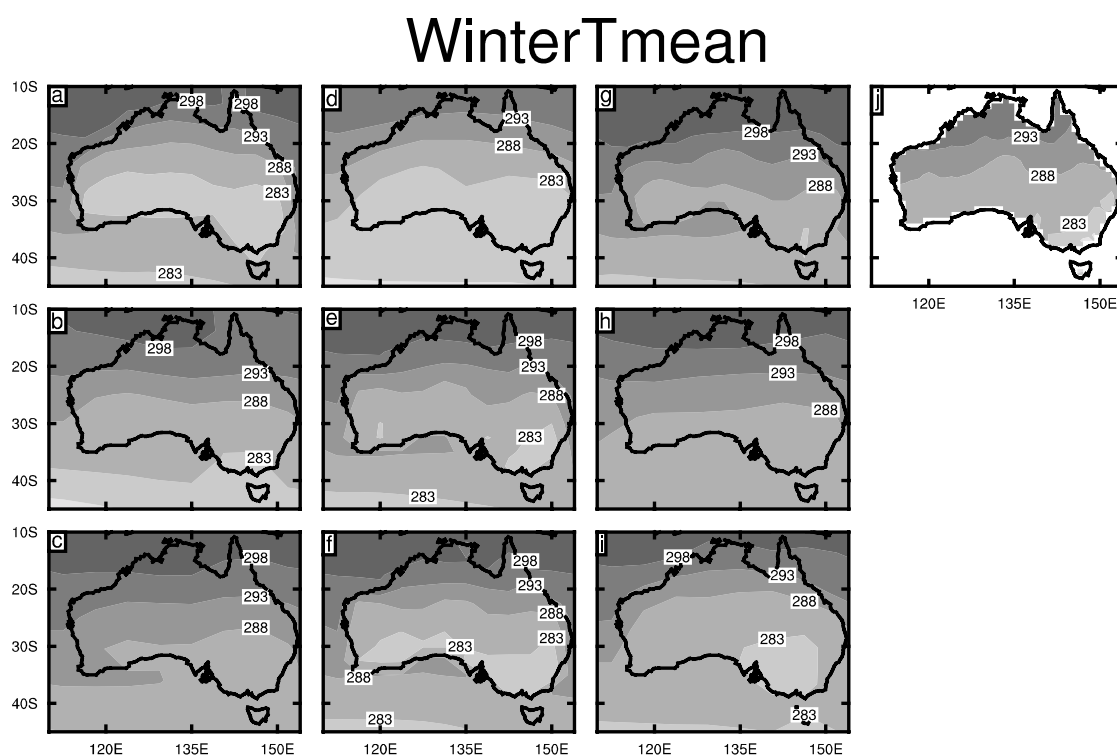
Figure 2.30. Winter simulated temperature for models detailed in Table 2.3, compared with observations (Fig. 2.30(j)). Contour interval is 5°K.

Precipitation

There is considerable variation amongst models in the simulations of summer and winter precipitation (Fig. 2.31). At points over Queensland, the range in simulated rainfall among models can be 100% or more. In agreement with the observations, all models simulate more rain in summer than in winter and more in the north and east of the State than inland. Although all simulations have their good and bad features, the GFDL simulation (Fig. 2.31(d)) is notably poor in its simulation of the seasonality of rainfall. In this model, rainfall in spring is higher than in summer in much of the State and that of winter is only a little less than summer (not shown).

General circulation

Rainfall variations are often determined by changes in the mean pattern of pressure and winds, known as the general circulation. Here, fields of mean sea level pressure are evaluated for the selected models (Fig. 2.32). By the criteria used in Whetton et al. (1994), the Japanese model's simulation of mean sea level pressure (Fig. 2.32(b)) would have excluded it from consideration. In this model, there are no trade winds in the Queensland coast in summer. Instead, there are north-westerlies, which result from the model connecting the continental heat low over the north of Australia directly with the midlatitude westerlies. All the other models simulated all of the main observed features of the mean sea level pressure, with the exception of the GFDL model, for which mean sea level pressure fields were not available. This model will be evaluated in subsequent work.

In summary, it is reasonable to conclude that the Japanese model and, to a lesser extent, the GFDL model are less reliable than the other models on the basis of their simulation of the current climate. A more complete evaluation of performance will be made in conjunction with the construction of new CSIRO climate change scenarios for Australia, in early 2001.

Summer
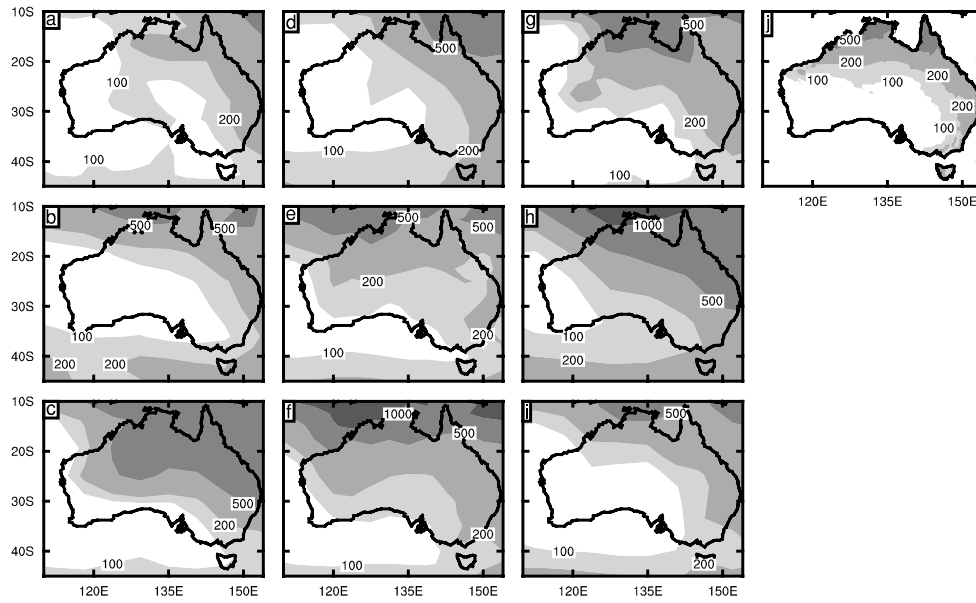
Winter
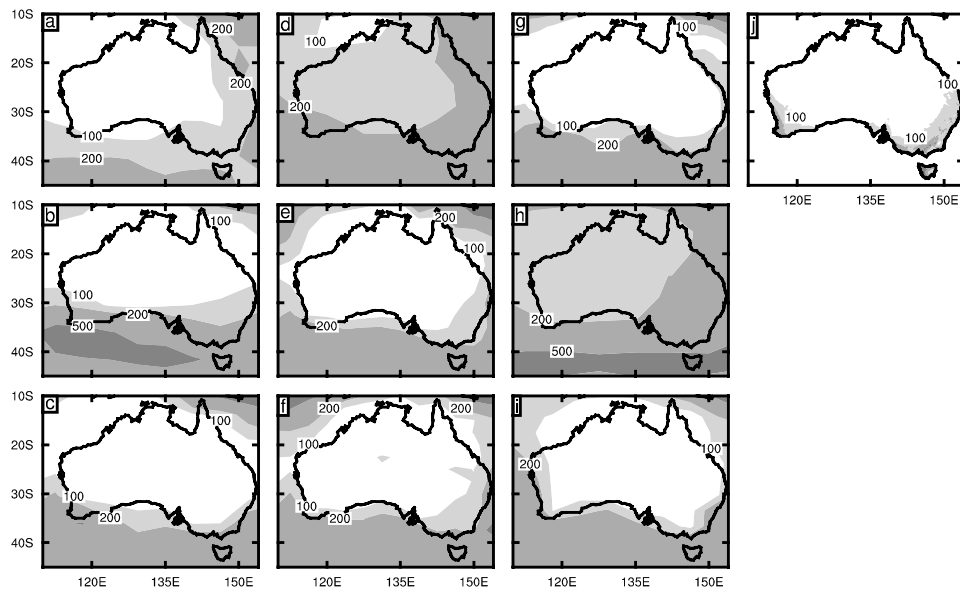
Figure 2.31. (top) Intercomparison of summer rainfall; (bottom) the same for winter. Contour interval is variable, in mm.

mslp
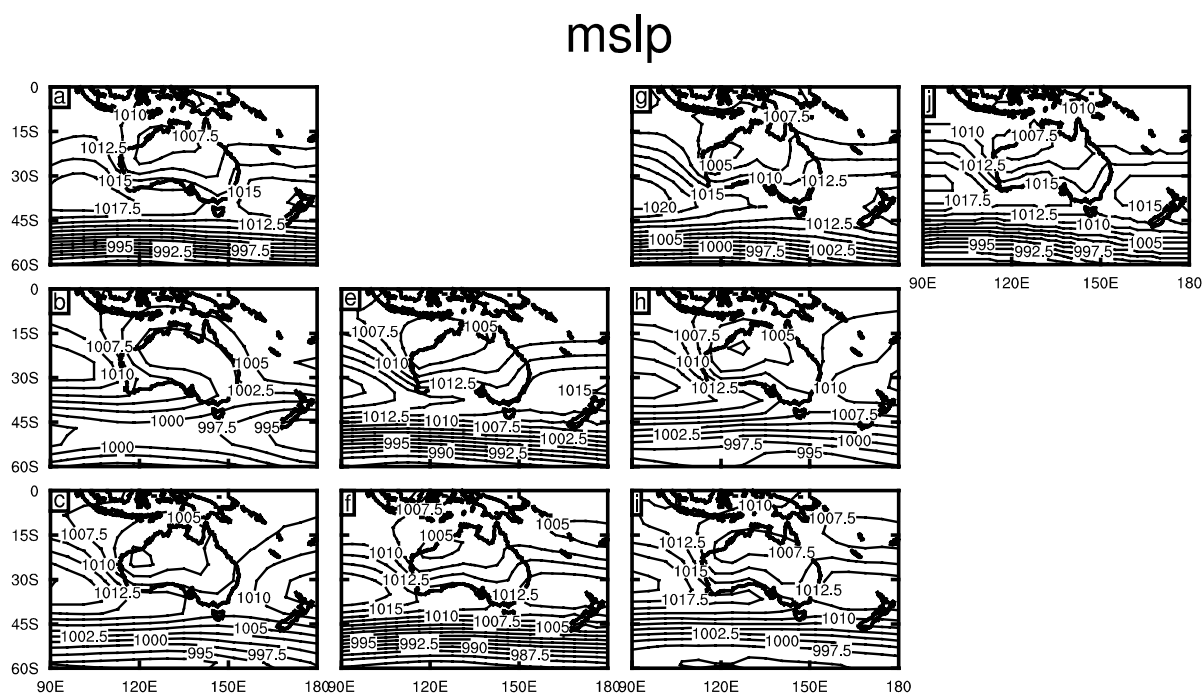
Figure 2.32. Comparison of observed and simulated summer mean sea level pressure. The GFDL model simulation (d) is missing. Contour interval is 2.5 hPa.

2.3.4 Climate change simulations

Figure 2.33 shows changes in mean temperature over Queensland simulated by the models. These are changes in °C per degree of global warming. The magnitude of the temperature changes are reasonably similar across Queensland in each of the models. The patterns of change also are generally similar, with largest increases inland and smaller increases towards the coast and in the tropics. The warming range is 0.9 to 1.5°C per degree of global warming in inland areas and 0.7 to 1.3°C in coastal areas. These ranges are similar to those reported in Walsh et al. (2000), using a sample of five models. Exclusion of the GFDL or Japanese models would not much affect these ranges.

Seasonal variations of average temperature changes simulated by each model over the three regions of Queensland are also shown in Fig. 2.33. There is considerable similarity among the model results for each season and region, although individual models exhibit consistently weaker or stronger responses. Some regional variations can be seen, with warmings slightly greater in the central region. Variations in the seasonal response are minor compared with the differences between models, although winter warmings tend to be less than warmings in the other seasons.
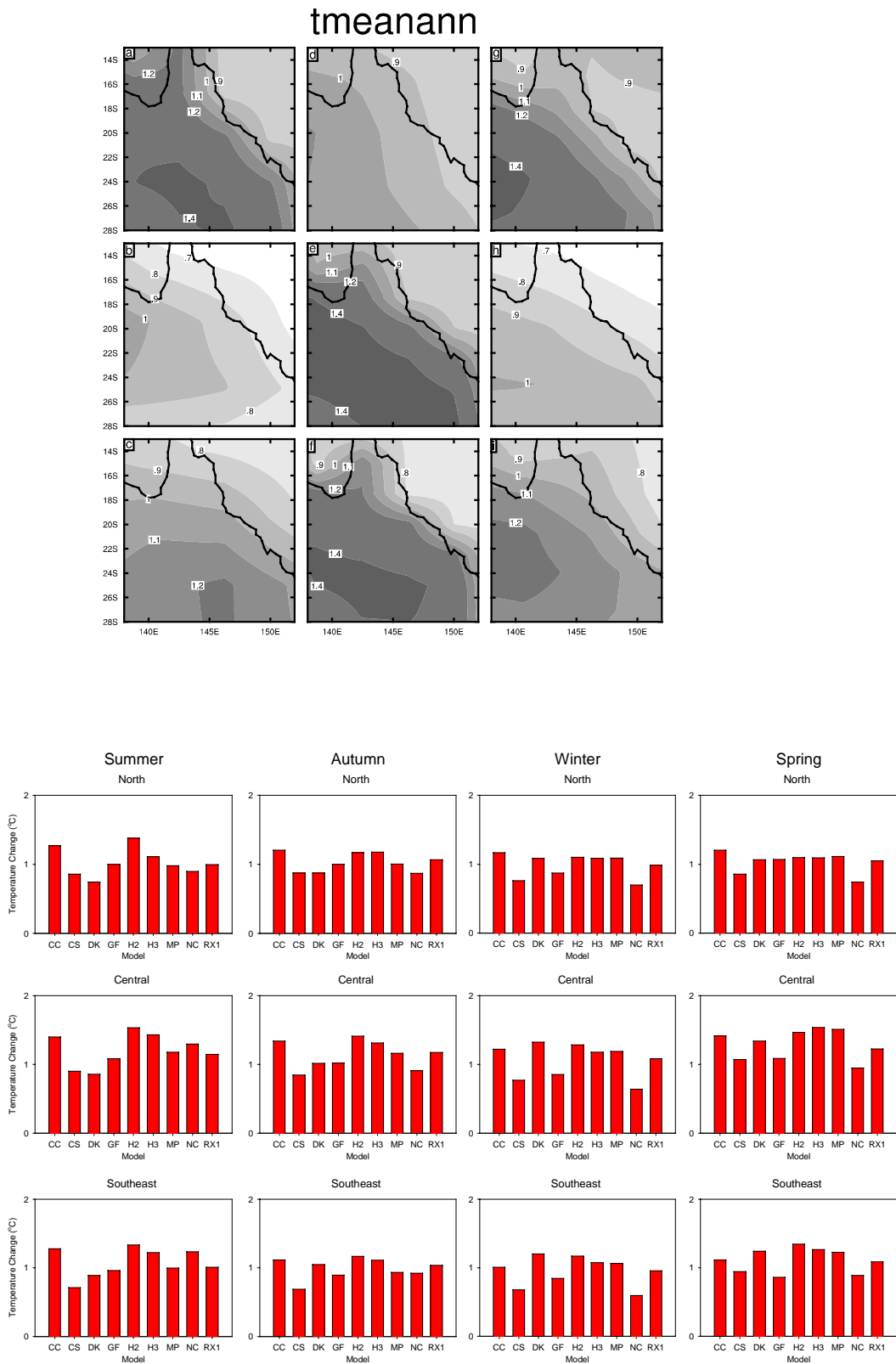
Figure 2.33. (top) Simulated change in temperature (°C per degree of global warming) for each model; (bottom) average change in temperature for each model by season and region.

Variations in the precipitation response of the models is much greater (Fig. 2.34). In both summer and autumn, the models predict the possibility of either rainfall increases or decreases in most areas of the state. In all three regions and in both of these seasons, the changes are in the range of +10 to –10% per degree of global warming. Although some models simulate rainfall increases in winter, the predominant tendency is one of decrease: across the three regions the results are in the range of +5% to –10%. There is strong and consistent tendency for rainfall decrease in spring, with changes across the three regions of +2 to –15%.

As mentioned in the previous section, inclusion of these model results in the construction of a climate change scenario depends upon their ability to simulate well the current climate. The results for the predicted precipitation response to global warming would not be much affected if the Japanese CCSM results were excluded, as this model is not an outlier in the climate change simulations. However, exclusion of the GFDL results would have a significant impact, as this model is one of those predicting rainfall increases. In particular, the exclusion of the GFDL model would increase consistency amongst models in predicting rainfall decreases in winter.

In summary, most models are predicting similar temperature increases over Queensland, with increases larger in the interior than along the coast. Models differ in their prediction of precipitation changes, but the predominant tendency is for rainfall decreases, particularly if one model is excluded from consideration on the basis of its less than adequate simulation of the current climate. A final decision on this will be made in conjunction with the construction of new climate change scenarios by CSIRO.
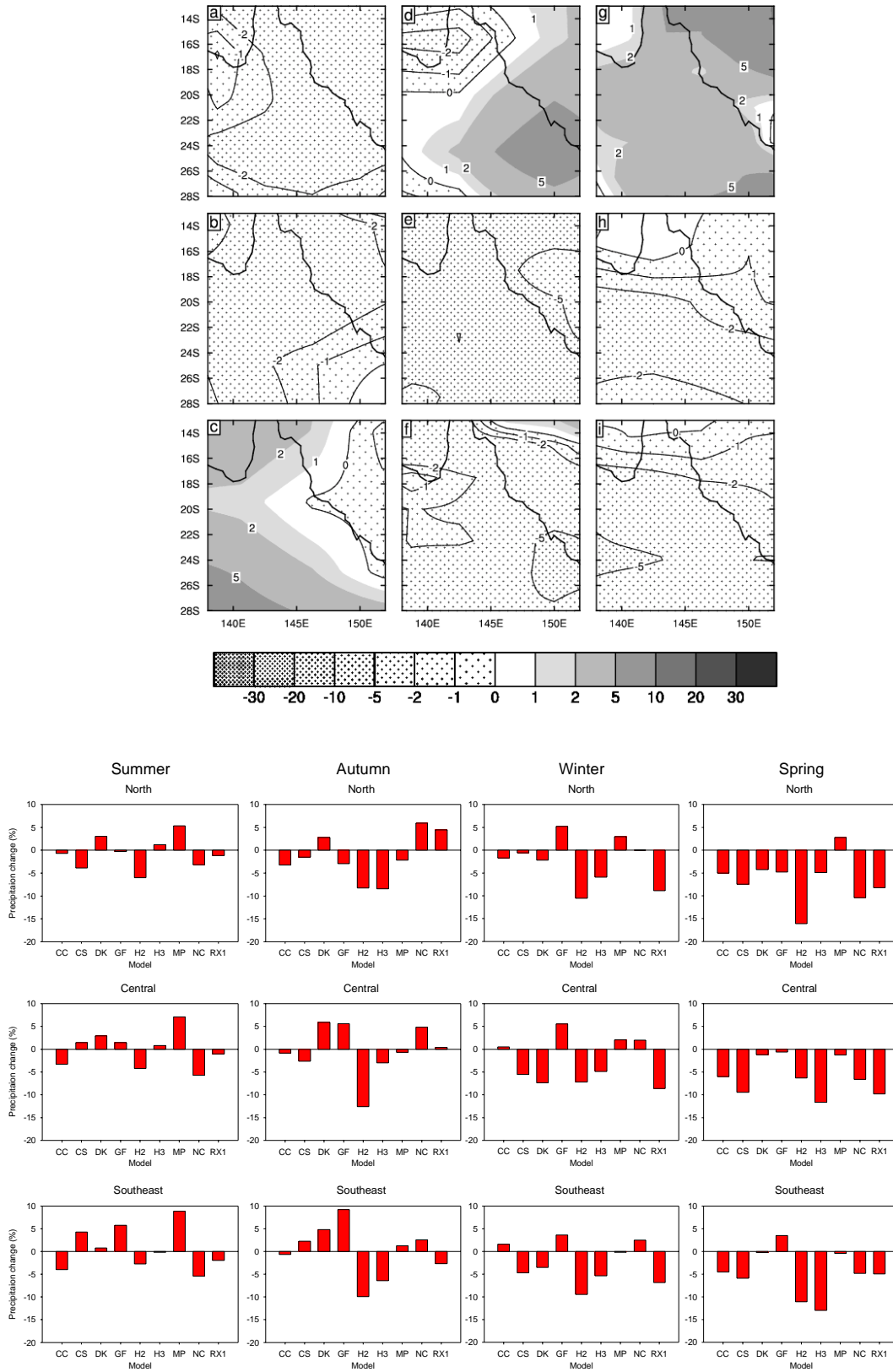
Figure 2.34. The same as Fig. 2.33 for precipitation changes, in percent per degree of global warming.

2.4   ENSO and climate change

As in the previous year's report (Walsh et al., 2000), we will discuss the possible effects of climate change on ENSO in terms of both possible changes in the average state of ENSO and of changes in its variability. Here, new results are discussed that have a bearing this issue.

2.4.1   Change in the average state of ENSO

In general, while the balance of evidence suggests a trend towards an average climate that is more El Niño-like (e.g. Hulme and Sheard, 1999), it is still true to say that consensus has not yet been reached that climate change will definitely lead to such conditions. Despite most GCM simulations suggesting such a trend, there are still some differences between various models in terms of their simulation of the effect of climate change on ENSO. Collins (2000) notes that the response of the Hadley Centre model at $4xCO_2$ conditions gives a mean pattern that is somewhat El Niño-like, in agreement with the recent results of Timmermann et al. (1999). In contrast, Meehl et al. (2000) compare the results of two climate models, the National Center for Atmospheric Research (NCAR) U.S. Department of Energy (DOE) model and the NCAR Climate System Model (CSM). They show that while the DOE model produces an El Niño-like response as a result of global warming, the CSM model does not. They attribute the differing model response to substantial differences in the way that the clouds simulated by each model respond to increasing CO_2.

Whether a SST signature that is more El Niño-like has yet emerged in the observed record remains a controversial issue. Lau and Weng (1999) note that analysis of observed SSTs from 1955-97 suggests that the rapid warming since the 1970s is a manifestation of a decadal or multidecadal signal. Thus, in their view, the more frequent El Niños observed since the 1970s may be related to the modulation of the ENSO interannual variability by interdecadal variations, rather than caused by global warming. They detected relatively little change in the east-west temperature gradient across the Pacific in their analysis; a decrease in the gradient would have indicated a trend to more El Niño-like mean conditions, but this was not shown in their analysis.

On the other hand, some recent evidence from climate of the past suggests that the warming since the 1970s may be unusual compared to typical natural variability. Hughen et al. (1999) examined the ENSO variations measured in oxygen isotopes and elemental ratios extracted from fossil coral that grew 124,000 years ago in the central Indonesian region, near the island of Sulawesi. The measured frequency pattern of ENSO variability at that time is similar to the variability in modern instrumental records, but distinct from that in the period since the mid-1970s. These results tend to support the hypothesis that ENSO behaviour since that time has been unusual with respect to normal interannual variability.

2.4.2   Changes in the variability of ENSO

Recent work has thrown more light on possible changes in ENSO variability in a warmer world. In the previously-mentioned simulations described in Collins (2000), no statistically significant changes in ENSO variability occur until $4xCO_2$ conditions are reached. At this level of CO_2 concentration, the simulated ENSO has a frequency about double that of the simulated ENSO in the current climate – in other words, with a period reducing from 3-4 years in the control simulation to 2-3 years in the $4xCO_2$

simulation. The model ENSO also becomes about 20% stronger than the control simulation. The increased strength of the simulated ENSOs is attributed to the increased vertical temperature difference across the thermocline, or the region of strong vertical temperature gradient in the upper ocean. A sharper thermocline has been previously shown to give stronger ENSO fluctuations (Münnich et al., 1991; Wilson, 2000).

A sharper thermocline and stronger ENSO variations in a warmer world were also simulated by Timmermann et al. (1999), although the resulting stronger ENSO variations occurred earlier in their model simulation, as they presented results only out to 2100 (slightly later than equivalent $3xCO_2$ conditions). The stronger thermocline in their simulations is caused by temperatures rising near the surface but falling at deeper ocean levels. They attributed the deeper ocean cooling to a greater inflow of cold waters caused by an intensification of the atmospheric Hadley circulation, particularly in the Southern Hemisphere.

Again, the confidence of these predictions may depend on processes that are not entirely understood, such as cloud feedbacks in the equatorial Pacific. The continued development of improved models, such as the CSIRO Mark 3 GCM, will be important in building a consensus for changes in ENSO variability in a warmer world.

2.5   Simulation of current climate by CSIRO Mark 3 GCM

One of the main tasks undertaken recently by CSIRO Atmospheric Research is the development of a new, state-of-the-art coupled ocean-atmosphere GCM. The main motivation for this task has been to develop a model that has a good simulation of ENSO variations so that more confidence can be placed in its predictions of the effect of climate change on ENSO, and how this affects the predicted patterns of rainfall change over Queensland. The previous Mark 2 version of the coupled model (Gordon and O'Farrell, 1997) produced ENSO-like variations, but these had some deficiencies, most notably their small amplitude compared to those observed. In this section, aspects of the Mark 3 GCM simulation of ENSO in the current climate are presented, showing that Mark 3 produces ENSO variations of more realistic size. The climatology of the Mark 3 model is still being improved at this time, but already it simulates many aspects of the observed ENSO variability.

The experiments described in this section use a high-resolution version of the Mark 3 CSIRO GCM. The horizontal resolution of the atmospheric component is approximately 200 km, with 18 vertical levels. It contains a land-surface scheme (Kowalczyk et al., 1991, 1994) that simulates the effects of vegetation. Precipitation is calculated in the model using the methods described in Rotstayn (1997) and Rotstayn et al. (2000). The main difference between the Mark 3 GCM and the Mark 2 version (apart from the finer horizontal resolution) is the maintenance in the Mark 3 ocean GCM of a sharp thermocline (Wilson, 2000). This has been shown to make the ENSO variations larger than in Mark 2 and thereby more realistic.

Figure 2.35 shows a comparison between the observed and simulated global rainfall for January. The observed rainfall (1979-1995) is from Xie and Arkin (1997), and the simulated rainfall is for twenty-four years of the Mark 3 simulation. Many features of the observed global pattern of precipitation are well reproduced, including the sharp gradient of rainfall in the central Pacific region from the high-rainfall region of the Intertropical Convergence Zone (ITCZ) just north of the equator to the dry region immediately to the north of the ITCZ. Rainfall over northern Australia is overestimated but the pattern of rainfall is good. For July (Fig. 2.36), the simulated rainfall pattern is good over both northern and southern Australia, while again the global patterns of rainfall are generally well reproduced. Rainfall is overestimated over the west coast of South American and over southern Africa, however.

The model is also able to simulate year-to-year variations quite well. A standard test of the atmospheric part of the model is to force it with observed SSTs over a number of years and see if model variations in atmospheric parameters are similar to those observed. Figure 2.37 shows the Mark 2 and Mark 3 atmospheric model's simulation of the observed Southern Oscillation Index (SOI), as defined by Troup (1967). Both models simulate the observed SOI variations well, with Mark 3 giving a particularly good simulation of the 1982 El Niño event.

(a) Observed rainfall for January
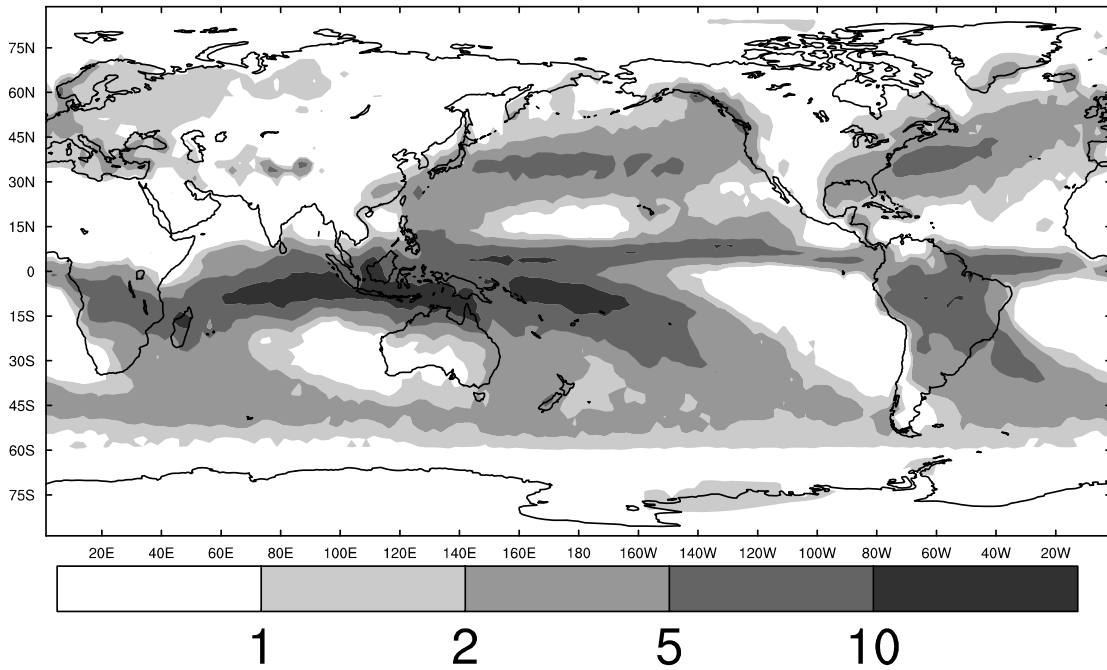
(b) Simulated rainfall for January
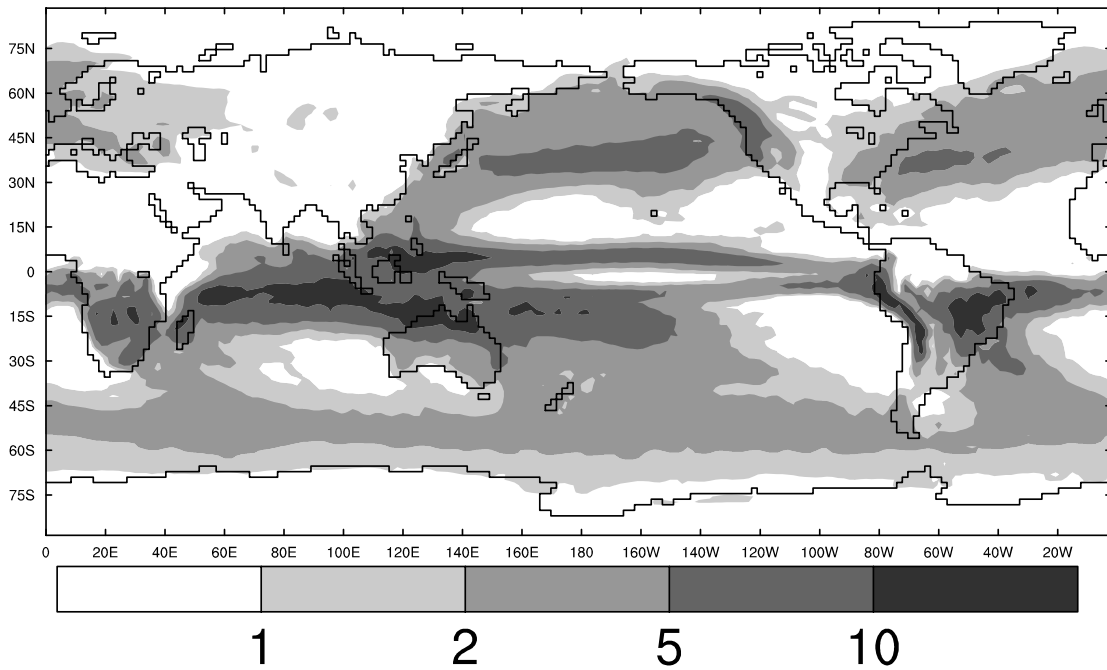
Figure 2.35. January rainfall in mm per day for (a) observations (Xie and Arkin, 1997); and (b) Mark 3 coupled model simulation.

(a) Observed rainfall for July
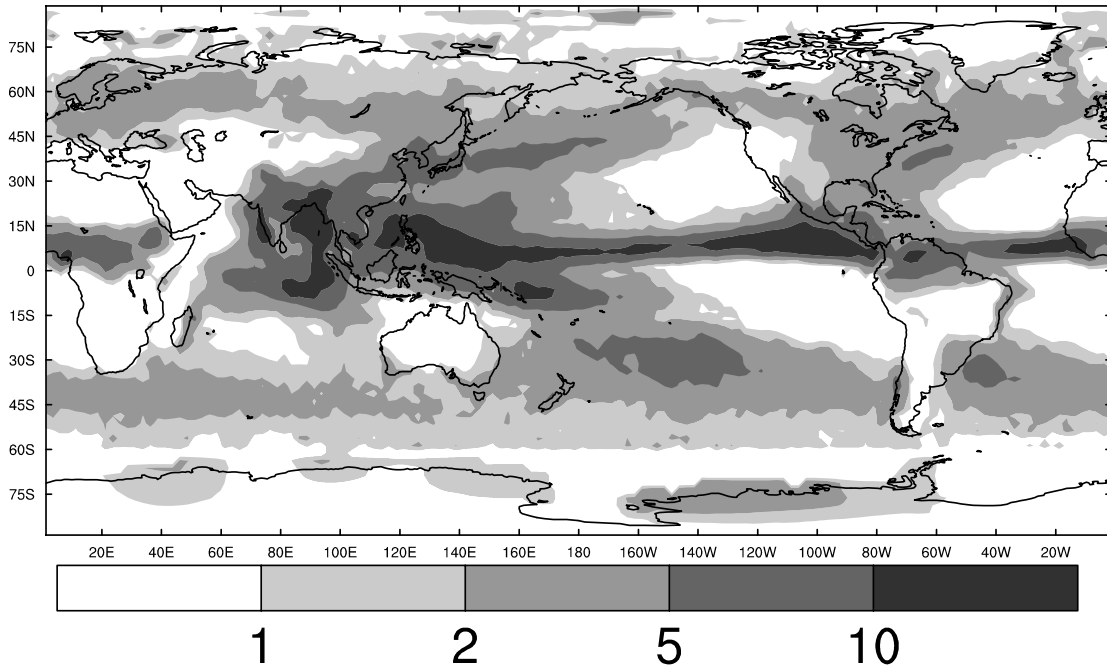
(b) Simulated rainfall for July
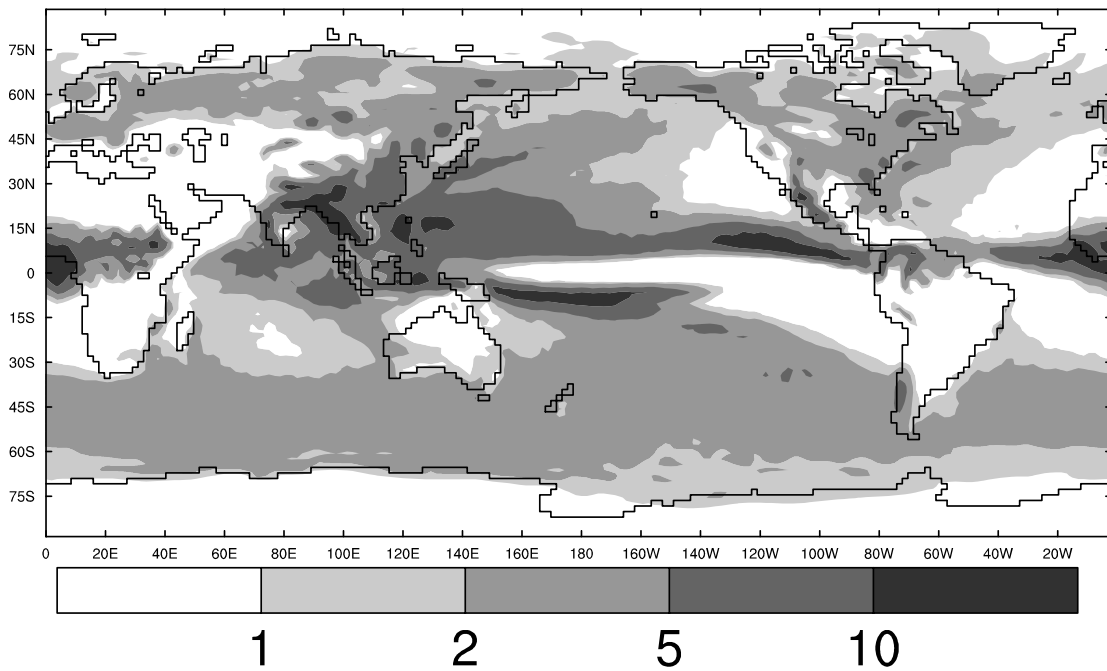
Figure 2.36. The same as Fig. 2.35 for July.

In addition to giving an excellent simulation of the observed SOI when forced by observed SSTs, the unforced coupled ocean-atmosphere version of the Mark 3 GCM produces large amplitude variations in central Pacific SSTs, internally generated by the model, of the kind observed in reality. Figure 2.38 shows the simulated year-to-year variations in Niño 3.4 SSTs, where Niño 3.4 is defined as the average SST over the region 5°N-5°S, 170°W-120°W. The first five years of this run are omitted as the GCM was still "spinning up" during this time. Positive SST anomalies averaged over this region are more than 2° in year 28 of the model run; this would correspond to a model-generated El Niño. There are also substantial model-generated La Niña events, where the Niño 3.4 SST anomaly goes below -1°C. The period of the ENSO variations is also reasonable, typically 2-3 years, which is similar to observations (e.g. Allan et al., 1996).

There is also a substantial model-generated SOI, shown in Figure 2.39. Values in year 28 of the model run are lower than –20, which compares well with observed El Niño variations of this quantity: for instance, during the 1982 El Niño, which was particularly severe, SOI values dipped to a little less than –30. Another way of showing these variations is in Figure 2.40, which shows global SST patterns for a typical model El Niño and La Niña. For the El Niño occurring in year 28 of the model run (Fig. 2.40a), peak SST anomalies are more than 2°C across a large region of the central and eastern Pacific. Negative SST anomalies are also generated in the Australian region, as observed. For the simulated La Niña of year 26 (Figure 2.40b), anomalies are more negative than –3°C in one region of the eastern Pacific. These are substantial anomalies compared with observations and indicative of the ability of Mark 3 to generate large ENSO variations.

Figure 2.41 shows global rainfall anomalies for model-generated El Niño and La Niña conditions. For simulated El Niño conditions (Fig. 2.41a), January rainfall anomalies are strongly negative over much of northern Australia, similar to observed. There is also a large negative anomaly over the South Pacific region adjacent to Australia, with positive anomalies further eastwards in the South Pacific past the dateline, generally as observed. In contrast, for simulated La Niña conditions (Fig. 2.41b), rainfall anomalies over much of northern Australia are strongly positive, with accompanying positive anomalies in the adjacent South Pacific region. In general, these are also in agreement with observed ENSO variations (e.g. Allan et al., 1996).

In summary, while further work is still being performed on the CSIRO Mark 3 GCM, its present simulation of ENSO variations has a good representation of a number of the characteristics of the observed ENSO.
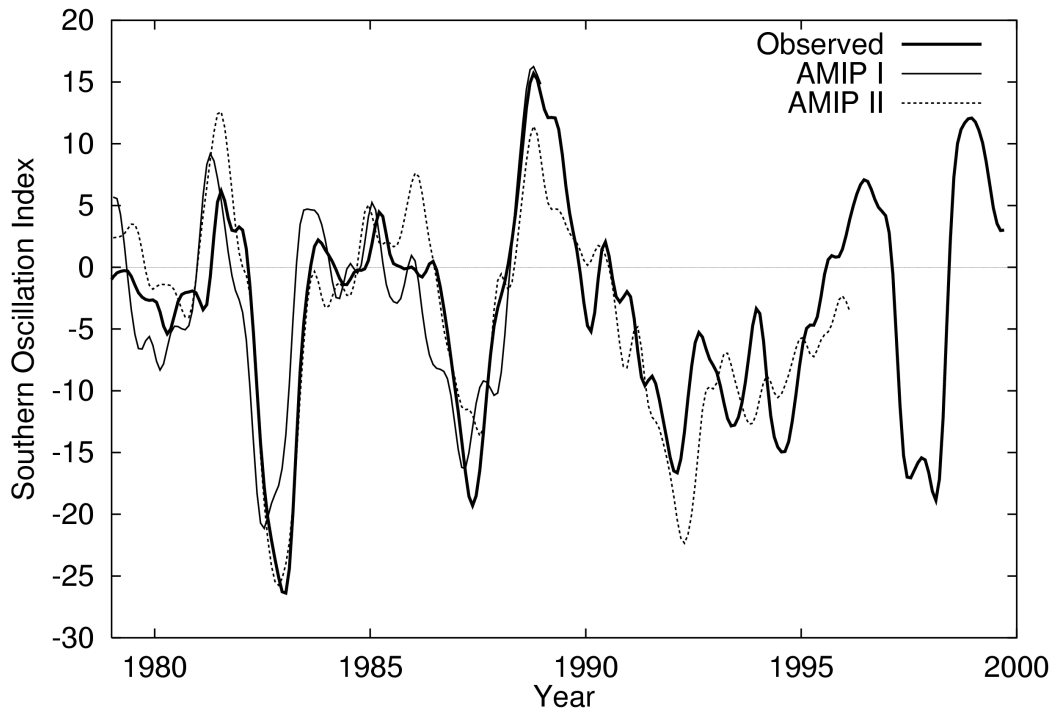
Figure 2.37. CSIRO Mark 2 and Mark 3 atmospheric GCM simulation, when forced with observed SSTs, of the observed SOI. The bold line is the observed SOI. The line marked "AMIP I" is the SOI simulated by the Mark 2 atmospheric GCM; the line marked "AMIP II" is that simulated by the Mark 3 GCM. AMIP I and II are two international model comparison experiments, with AMIP I simulating the period ending in 1988, and AMIP II in 1996.
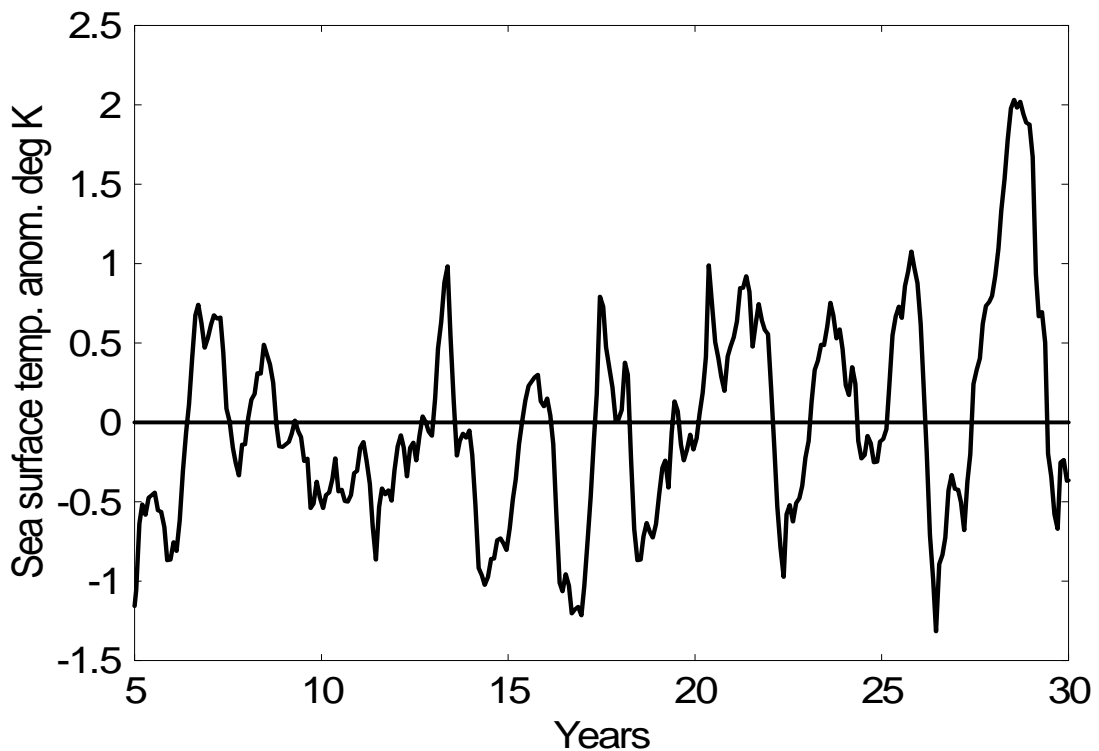
Figure 2.38. Variations in the "Niño 3.4" index of equatorial SST as simulated by Mark 3.
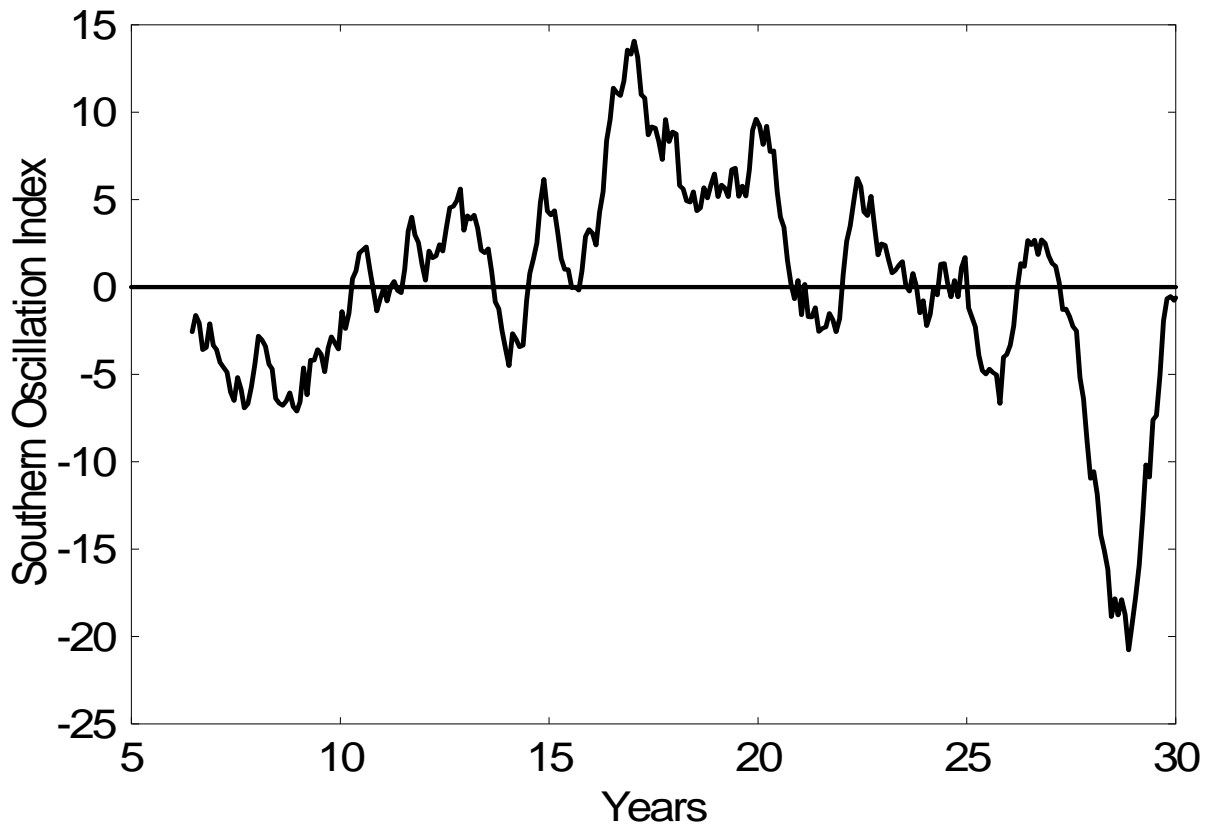
Figure 2.39. SOI generated internally by Mark 3 coupled ocean-atmosphere GCM, rather than from specified SSTs as in Fig. 2.37.

(a) El Nino sea surface temperature anomalies for June of year 28
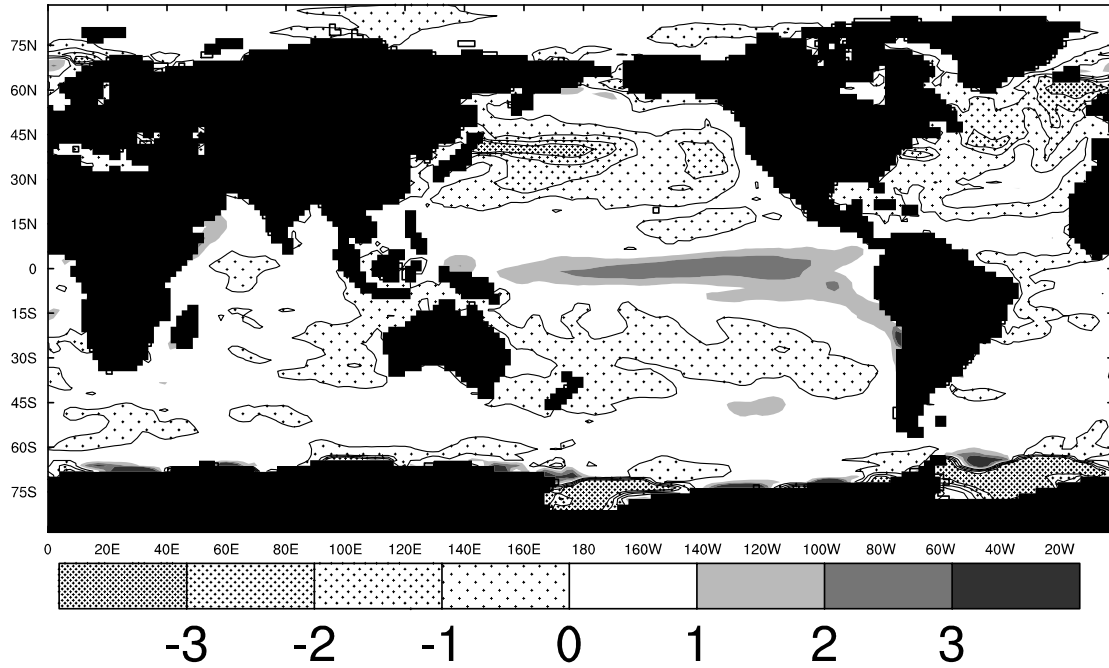
(b) La Nina sea surface temperature anomalies for June of year 26
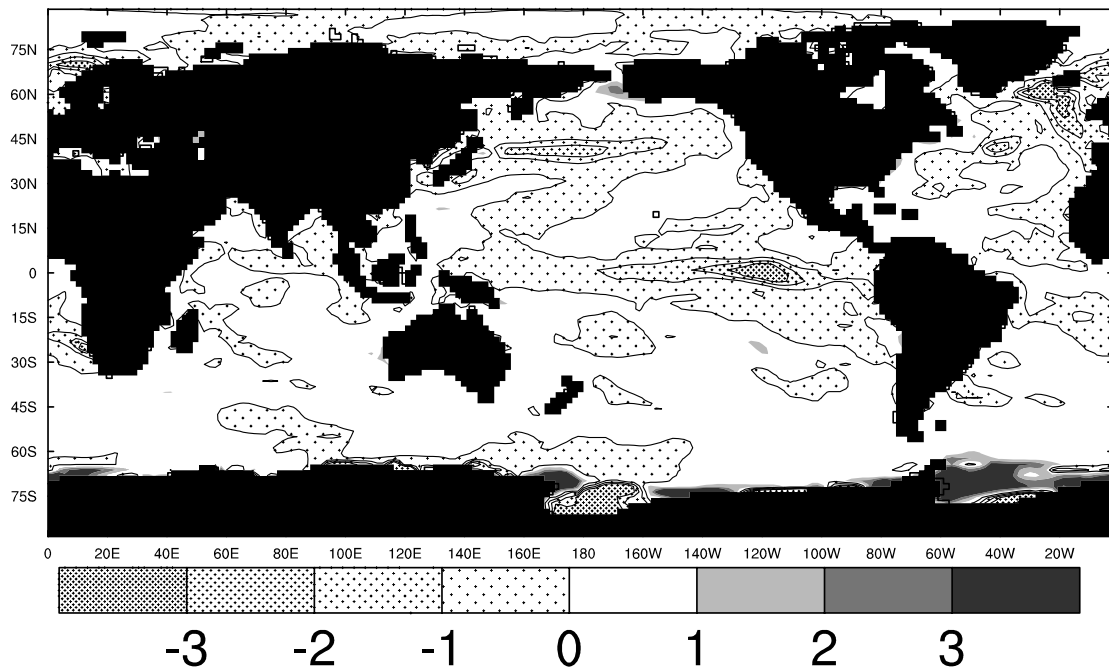
Figure 2.40. SST anomalies generated by Mark 3, for (a) a selected model El Niño year; and (b) a model La Niña year. Contour interval is 1° C.

(a) El Nino rainfall anomalies for January of year 28
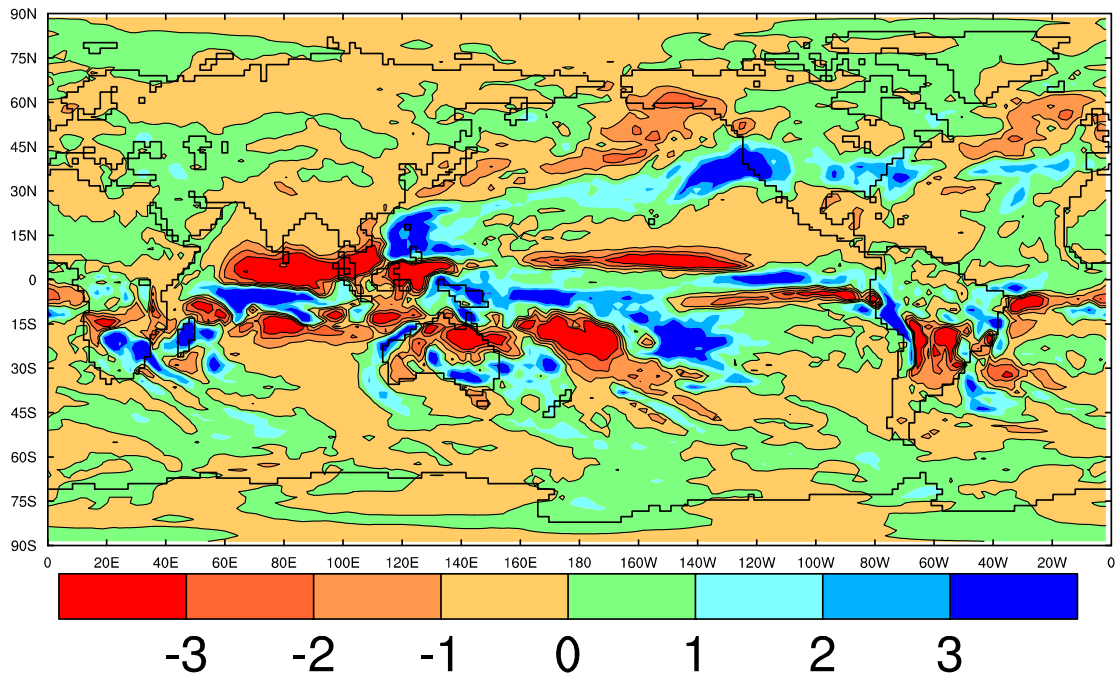
(b) La Nina rainfall anomalies for January of year 26
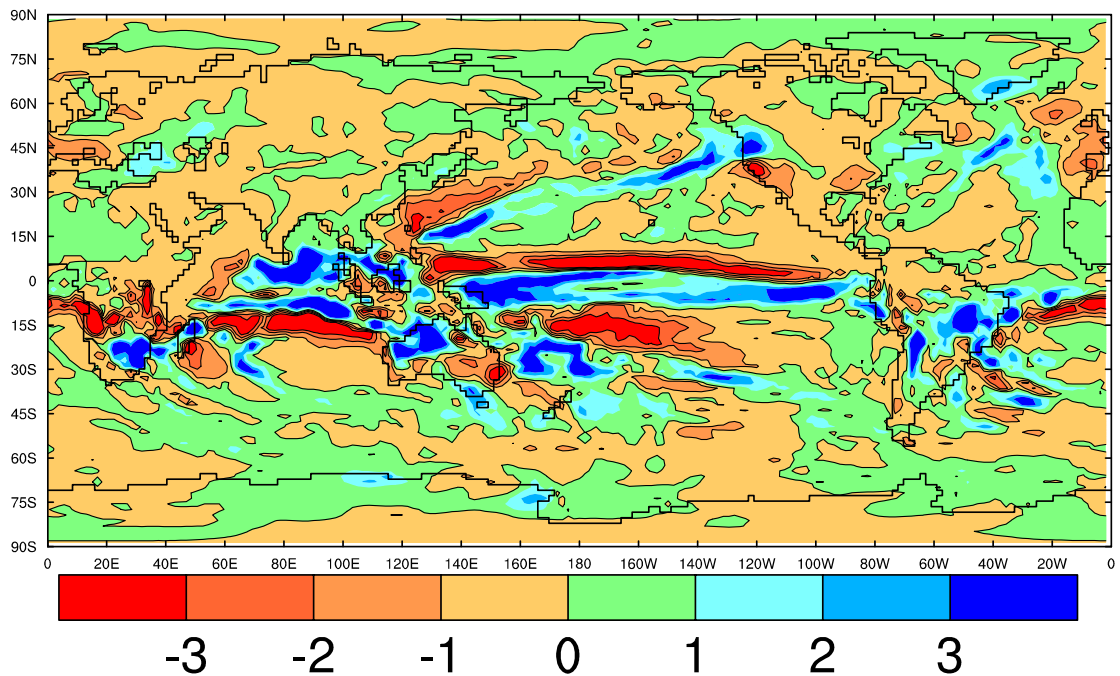
Figure 2.41. Rainfall anomalies in mm per day for (a) a selected Mark 3 model-generated El Niño year; and (b) the same for La Niña conditions.

3. Climate change and tropical cyclones (Item 2.3.2)

3.1 Introduction

In addition to reviewing the latest understanding of the effect of climate change on tropical cyclones, this section details the results of new simulations, as well as making an estimate of the effect of climate change on the return periods of tropical cyclone winds in several locations along the coast of Queensland. The return period, the average time between events of a certain magnitude, is an important variable in assessing the impact of climate change because of its role in design standards and planning.

Recent results continue to suggest that there are likely to be some increases in tropical cyclone intensities in a warmer world (Knutson et al., 1999; Walsh and Ryan, 2000). Building on previous work, Knutson et al. (2000) incorporated an ocean that interacts with the atmosphere into simulations of the effect of climate change on tropical cyclone intensities; previous simulations used sea surface temperatures (SSTs) as specified from the forcing GCM. Their results suggest that the inclusion of ocean/atmosphere interaction has only a minor effect on previous results that simulated the intensification of tropical cyclones in a warmer world, with the predicted intensification slightly reduced compared with that predicted by a model with no ocean/atmosphere interaction. In other words, the prediction of stronger tropical cyclones is supported by a number of different approaches, from theoretical techniques (e.g. Holland, 1997) to the above-mentioned numerical studies. Because these studies have been performed with different climate models in different regions of the globe, and yet have obtained similar results, this strengthens the consensus on this issue.

3.2 Further simulations of tropical cyclones under climate change

Previous work in the Australian region (Walsh and Katzfey, 2000) suggested that tropical cyclones might track further poleward in a warmer world. However, at the time of writing this is the only climate model in the world displaying this behaviour. In addition, this simulation was performed using DARLAM at a horizontal resolution of 125-km, which is adequate for simulation of tracks but not for intensities. This limits the interpretation of the results, particularly when the physical reasons need to be investigated for the dissipation of storms at the poleward limit of their tracks. As a result, in Walsh and Katzfey (2000) it was not possible to determine unambiguously the reason for the simulated poleward shift of cyclone occurrence simulated in a warmer world. Analysis showed that the southward shift in occurrence could be explained by a slight southward shift in formation combined with tracks that were more southward under enhanced greenhouse conditions. The analysis did not answer the question of why the storms were able to maintain their intensities further south in a warmer world despite atmospheric conditions that remained unfavourable for the maintenance of storm intensities, namely high vertical wind shear, the difference in wind speed and direction between upper and lower levels in the troposphere.

Accordingly, similar simulations at higher horizontal and vertical resolutions were undertaken. It was found in previous work (Walsh and Ryan, 2000) that a horizontal resolution of 30 km is adequate (although not ideal) for the simulation of tropical cyclone intensities. The simulations described in this section are at this resolution and

are implemented over the domain shown in Fig. 3.1. These simulations are driven at their boundaries by the 125-km resolution DARLAM simulation whose characteristics were described in Nguyen and Walsh (2001), which in turn is forced at its boundaries by the CSIRO Mark 2 coupled ocean/atmosphere GCM. In other words, these are "multiply-nested" simulations. So far, 30 Januaries have been simulated for 1x and $3xCO_2$ conditions. These results are presented and discussed in this section.
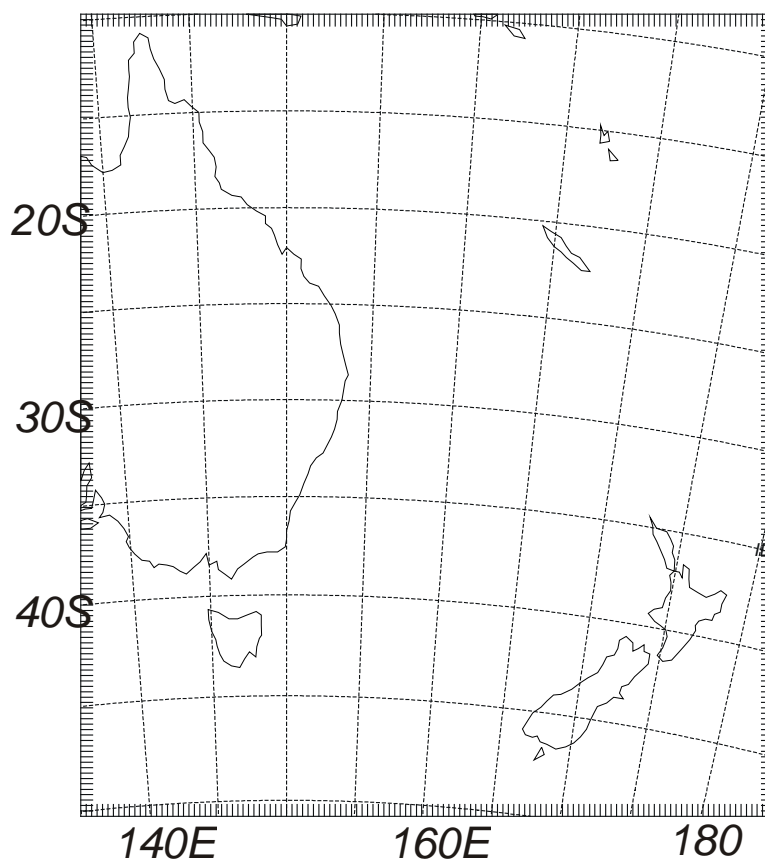
Figure 3.1. Domain for 30 km DARLAM simulations described in the text.

Figure 3.2 shows the detected tracks of the "tropical cyclone-like vortices" (TCLVs) in the 30-km DARLAM simulations. Here we show all TCLVs that have low-level wind speeds of at least 17 ms^{-1}, the observed tropical cyclone intensity threshold. Numerous TCLVs are generated by the model, and their tracks follow paths that are similar to those observed. There are a couple of anomalies in the $3xCO_2$ simulation: TCLV formation is simulated near the coast of New South Wales, where it never occurs in reality in the current climate. Further analysis is required to investigate the reasons for this. Figure 3.3 compares the number of TCLVs formed and their occurrence to observed formation and occurrence by latitude band. Here, occurrence is defined as the number of cyclone-days in each latitude band. Figure 3.3 shows that cyclone formation and occurrence are generally well simulated, although formation is underestimated in the 10-15°S latitude band, and overestimated in the 20-25°S latitude band. Examination of Fig. 3.1 suggests that this latitude band is in close

proximity to the northern boundary of the DARLAM domain. This boundary is suppressing intense TCLV formation through the forcing by the coarser-resolution 125-km simulation, where considerably weaker vortices are generated. To avoid this problem, new simulations are under way where this boundary is extended further north.

(a)   **(b)**
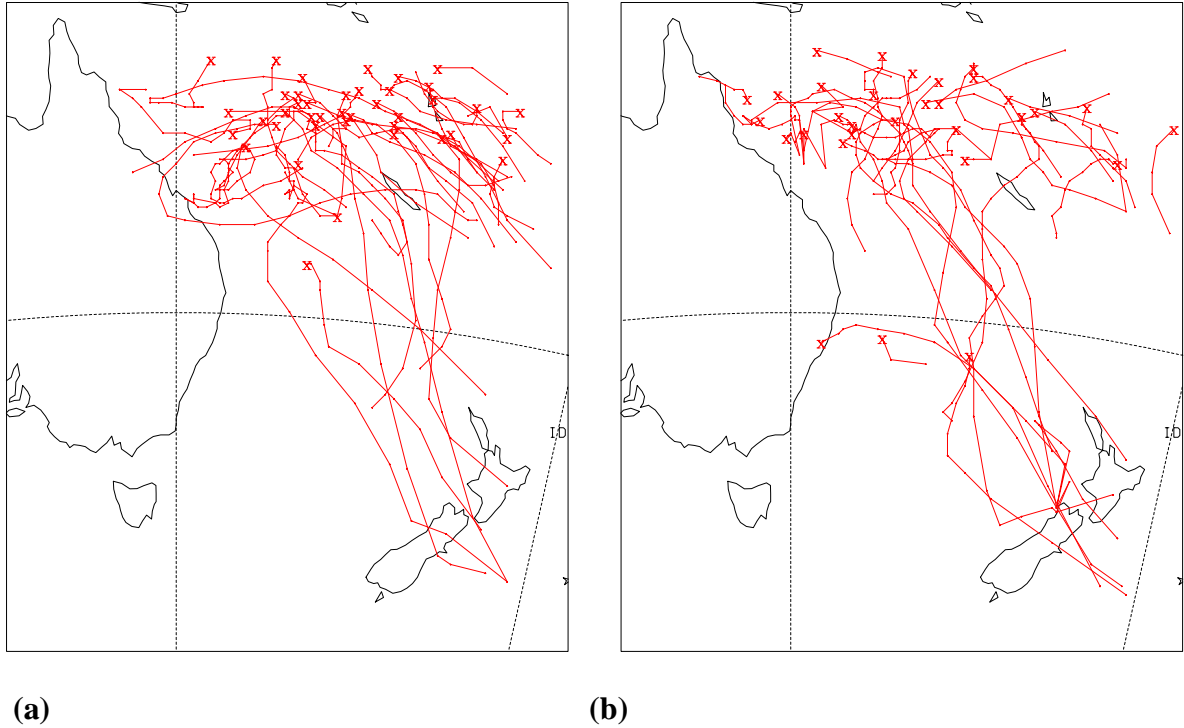
Figure 3.2. Tracks of simulated TCLVs, for (a) $1xCO_2$ conditions; and (b) $3xCO_2$ conditions. Crosses are formation locations.

(a)   **(b)**
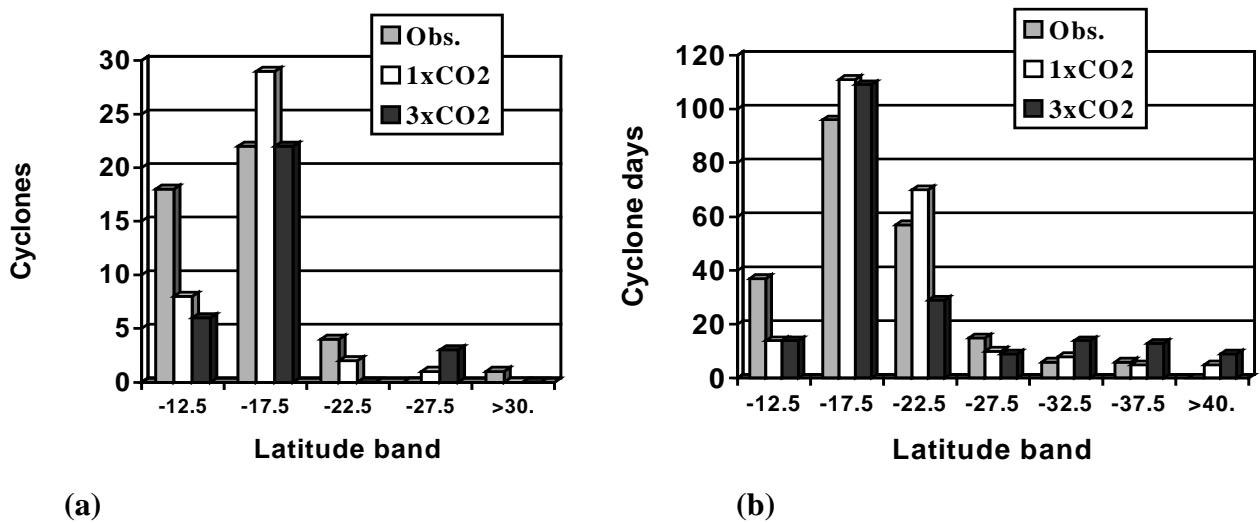
Figure 3.3. Comparison between observations, 1x and $3xCO_2$ simulations for (a) formation of cyclones; and (b) occurrence of cyclones.

Under $3xCO_2$ conditions, formation decreases. This was also simulated in the 125-km simulation using the same GCM forcing (Nguyen and Walsh, 2001). Note that these results may only be applicable to the south-west Pacific region over which DARLAM is implemented. A general decrease in tropical cyclone numbers in a warmer world has also been simulated by other models (Yoshimura et al., 1999); nevertheless, Tsutsui et al. (1999) and Walsh and Katzfey (2000) simulated little change in numbers in the south-west Pacific region. Therefore it is probably premature to state what the change of tropical cyclone numbers in a warmer world will be, particularly because the direction of change is likely to be different for various regions of the globe.

Depending upon the latitude band in question, the results of Fig. 3.3 suggest both increases and decreases in TCLV occurrence as a result of climate change. These results must be considered preliminary; simulations of other months besides January and a more detailed analysis needs to be performed before firm conclusions can be drawn.

What percentage decrease in cyclone occurrence would be required to negate the predicted increases in intensities? The damage caused by tropical cyclones increases very sharply as intensity increases. Therefore a 15% decrease in tropical cyclone occurrence would not be sufficient to negate a 15% increase in maximum cyclone intensity, an intensity increase within the range of current predictions. Clark (1997) suggests that a 15% increase in maximum cyclone intensity would cause more than double the amount of property damage caused by cyclones in the current climate. Thus to negate an increase in intensity of this size, the occurrence of tropical cyclones would have to fall by more than a factor of two, considerably larger than the changes in numbers simulated by recent model simulations.

In addition to increases in tropical cyclone intensities, simulations suggest increases in rainfall generated by tropical cyclones. Knutson and Tuleya (1999) showed that near-tropical cyclone precipitation increased by 28% in their enhanced greenhouse simulations compared to their current climate simulations. Similar results have been shown in the later, coupled ocean/atmosphere simulations of Knutson et al. (2000). Using a GCM, Yoshimura (2000, personal communication) simulated a 10% increase in precipitation near their model-generated tropical cyclones. Analysis of the TCLV simulations of Walsh and Ryan (2000) gives similar results, with the average of maximum daily rainfall rates near the simulated TCLVs being 29% greater under $2xCO_2$ conditions than in the current climate, a result that is statistically highly significant. There are good theoretical reasons why rainfall might increase in intensity in a warmer world, as there is a large increase in lower tropospheric water vapour content and greater environmental evaporation rates. This increase in tropical cyclone rain rates in a warmer world may have some implications for the estimates of maximum precipitation rates due to tropical cyclones and the subsequent effects on infrastructure.

3.3   Return period analysis of tropical cyclone winds

3.3.1   Introduction

In northern Australia, tropical cyclones are a major source of extreme winds that pose a threat to the built environment. As mentioned above, under enhanced greenhouse conditions, there is evidence to suggest that tropical cyclone intensities will increase.

Estimates of the return periods of extreme winds, the time between wind events of a specified intensity, are essential in the structural design of buildings. However, the current design standards for wind loading do not incorporate the issue of climate change. This study is the first to examine the possible changes to extreme wind return periods caused by tropical cyclones under enhanced climate conditions.

The technique used in the present study involves coupling a statistical model of tropical cyclone occurrence with a simple model of the cyclone vortex to randomly simulate maximum winds (see McInnes et al., 2000). Model-simulated winds are converted to wind gusts, the crucial variable for design standards. Estimates of cyclone intensity changes under enhanced greenhouse conditions are made and these are inserted into the statistical model. New return periods of extreme winds under enhanced greenhouse conditions are thereby calculated.

3.3.2   *Methodology for Evaluating Tropical Cyclone Extreme Winds*

Return periods of extreme winds under present and enhanced greenhouse climates have been determined for five locations along the Queensland east coast: Brisbane, Hervey Bay, Mackay, Rockhampton and Cairns.

The magnitude of the cyclone winds depends on the following factors:
- *intensity of the cyclone's central pressure;*
- *size of the cyclone (measured by the radius from the cyclone centre to the region of maximum winds);*
- *cyclone track,* including its direction of movement, forward speed and proximity to the location under consideration; and
- *speed of forward movement* of the storm.

In this study, tropical cyclone winds are generated by randomly selecting values of these parameters from statistical distributions calculated from observed historical records of cyclones. The selected parameters are then used in a simple model of the cyclone vortex to calculate the winds (Holland, 1980).

Cyclone Climatology

An analysis of the cyclone climatology was performed for each of the five study locations. Cyclone data in the Australian region are available from 1908, although data in the pre-satellite era (prior to the mid-1960s) are considered to be less reliable because a number of cyclones over the open ocean would not have been detected. However, in the interests of maximising the number of events so as to perform a meaningful statistical analysis in the present study, cyclones were selected from the 1953 to 2000 seasons inclusive. This is justifiable for this study, as cyclones are analysed here that approach the coast in populated regions, where few or no cyclones would have been missed during this period.

The boundary of cyclone influence can be defined as the distance from the location of interest at which the most intense storms produce no significant wind damage. The lower threshold of damaging wind speed is arbitrary, and here a lower limit of 20 m s^{-1} is used. Based on the size and strength of typical tropical cyclones that affect the Queensland coast, this requires even the most severe storm to pass within a specified radius of the location in question.

Because the number of cyclones that have travelled within this distance of each location is small, it is not possible to use them adequately to represent the long-term distribution of cyclone behaviour (defined by storm intensity, size, speed and direction of movement). Accordingly, the analysis region must be expanded to encompass a larger section of the coast. In doing this, it is assumed that cyclone behaviour is reasonably homogeneous over a small area surrounding each location. Thus the probabilities associated with cyclone activity in the expanded region can be appropriately scaled to represent cyclones affecting the location of interest.

For example, Figure 3.4 shows the storm analysis for Mackay. All storms that passed within two degrees of latitude (approximately 220 km) of the coast were included in the analysis. Cyclones crossing the straight line drawn along the coast were defined as 'coast-crossing'. Others crossing the line drawn perpendicular to the coast from the location of interest were defined as 'coast-parallel' cyclones. Table 3.1 summarises the latitude range from which coast-crossing and coast-parallel cyclones for each location are selected. The mean annual recurrence rates (the time interval between events) for each cyclone type are also given.
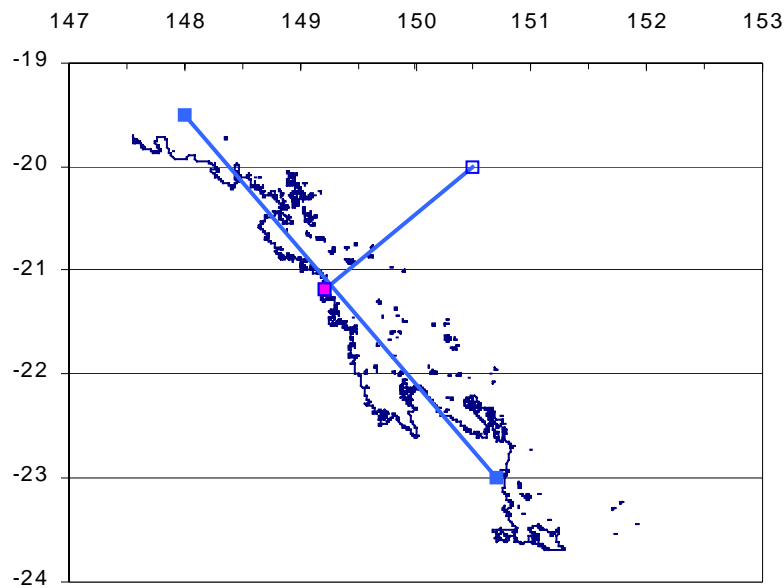
Figure 3.4. Cyclone analysis region for Mackay. Longitudes and latitudes (in degrees) are indicated.

Table 3.1. *Details of observed cyclones used in statistical analysis. Recurrence is defined as the average time between events.*

Location	Region	Number of Cyclones	Average Recurrence of Coastal Crossing Cyclones (years)	Average Recurrence of Coast-Parallel Cyclones (years)
Brisbane	25.8°S - 30°S	10	7.4	16.7
Hervey Bay	23.5°S - 28°S	19	4	8.8
Rockhampton	20.5°S - 25.5°S	16	5.5	14.7
Mackay	19.5°S - 23°S	22	4	14.7
Cairns	14.5°S - 19.2°S	26	3.7	7.4

Cyclone Intensity

Cyclone intensity, the maximum wind speed close to the surface, is directly related to the cyclone central pressure. An analysis of storm central pressure was made by obtaining the minimum pressure of each storm within the regions defined in Table 3.1 for each location. A statistical distribution was then fitted to the pressure data. The distribution used in the present study is the Generalised Pareto Distribution (GPD), which is of the form,

$$F(y) = \left\{ 1 - \left(1 - \frac{ky}{s} \right)^{\frac{1}{k}} \right\},$$ (3.1)

where s is a scale factor and k is a shape factor. The case $k < 0$ is the usual Pareto Distribution. Unlike the often-used Gumbel distribution, which is frequently used in extreme weather applications, the GPD has the advantage that it has an upper limit for extreme values. This is often more realistic in geophysical applications (Holmes and Moriarty, 1999), and is particularly important for tropical cyclones, as there are good physical reasons to believe that there are upper limits to the possible intensity of cyclones in any one location (e.g. Holland, 1997). The GPD also has an advantage over the Gumbel distribution in that all available data are used to fit the distribution rather than just the extreme value within a specified time interval. The fitted cumulative distributions are shown in Fig. 3.5.
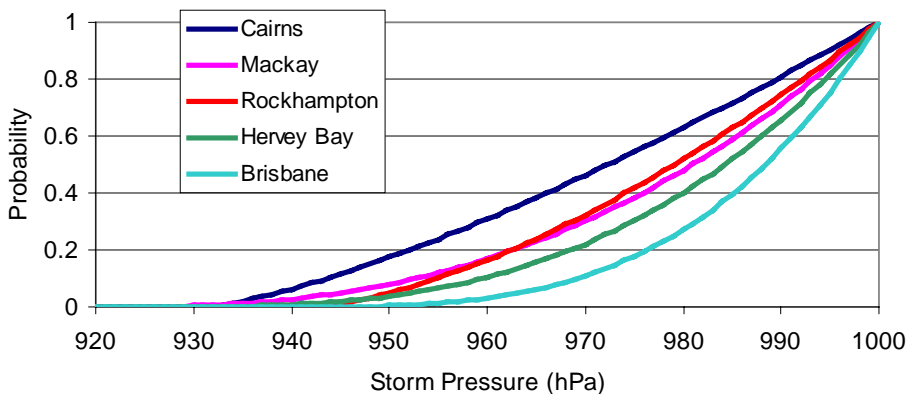
Figure 3.5. Cumulative probability of cyclone intensity for each location.

Translation Speed

The speed of movement of the cyclone is important as it contributes to the magnitude and distribution of wind speed around the storm. In the Southern Hemisphere, winds circulating around the cyclone centre on the left side of the storm (facing the direction towards which the cyclone is moving) are in the same direction as the movement of the storm. Therefore the direction of storm movement increases the speed of these winds. On the right side of the storm, the wind direction is opposite to the direction of movement, which reduces winds on this side. Thus the faster moving the cyclone, the greater the asymmetry in the wind field.

The average speed of movement was calculated over a period of twelve hours as the cyclones either moved across the coast (for coast-crossing storms) or near to the coast (for coast-parallel cyclones). Probability distribution functions were fitted to the results at each location by pooling both sets of cyclones and fitting a single distribution, shown in Figure 3.6.
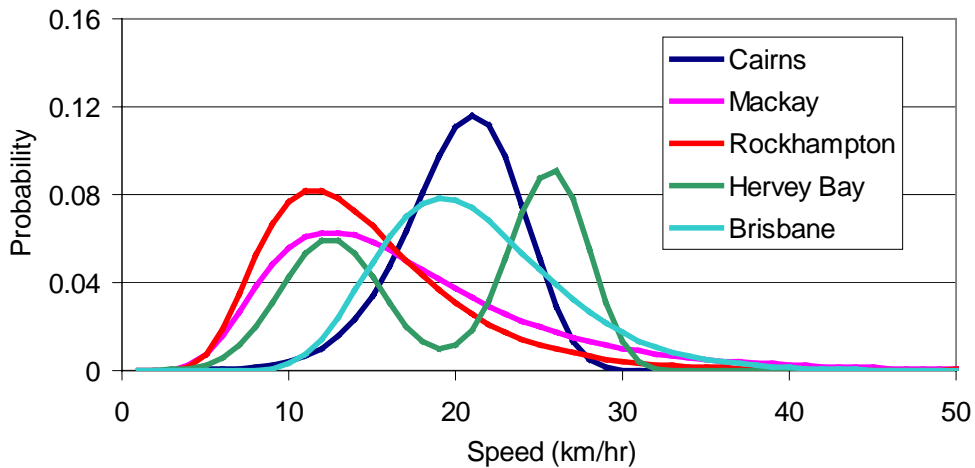
Figure 3.6. Probability distributions for storm speed at each location.

Direction of Approach

The direction of cyclone approach was determined by calculating the mean cyclone direction over the same twelve hour period centred on each cyclone's coastal crossing location (for coast-crossing cyclones) or the closest approach to the location of interest (for coast-parallel cyclones). Normal or log normal distributions were fitted to the results and these are shown in Figure 3.7. A bi-modal distribution was fitted for Mackay, where the orientation of the coast allows some storms to cross the coast from a more north-westerly direction, compared with the other locations.
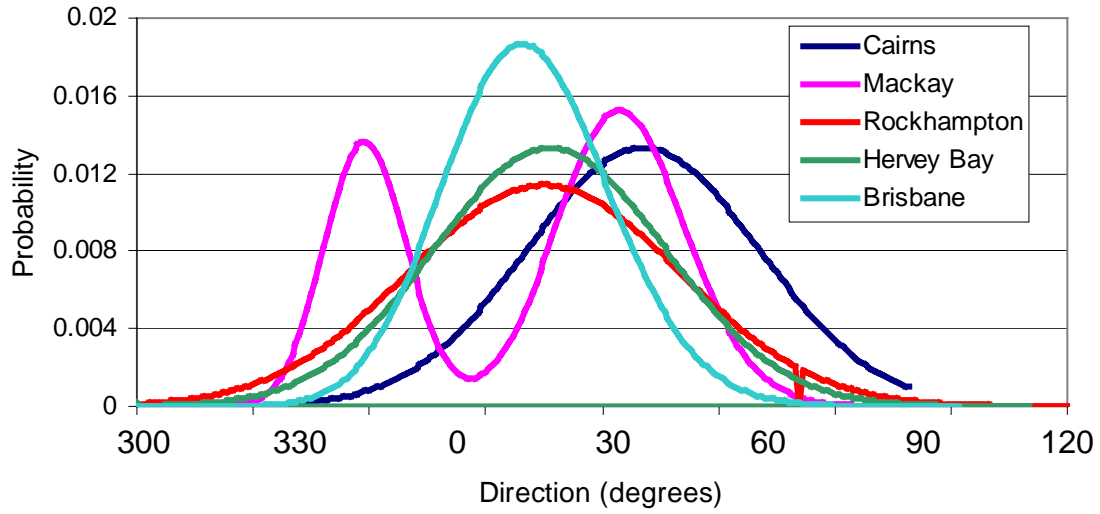
Figure 3.7. Probability distributions for storm direction at each location.

Radius of Maximum Winds

The wind field associated with a tropical cyclone depends on both its intensity and spatial extent. The latter is generally characterised by the radius of maximum winds (RMW), defined as the distance from the cyclone centre to the band of maximum winds. Due to the absence of data on cyclone size, a mean RMW of 30 km was applied to all cyclones in the current study.

Cyclone Filling

To account for the fact that storms lose intensity (i.e. 'fill') after crossing the coast, a statistical filling algorithm was applied in the numerical modelling procedure. This algorithm is based on an aggregated analysis of coast-crossing cyclones extracted from the cyclone data base.

The relationship between cyclone filling and both its time over land and distance from the coast was considered. However, best results were found by relating the filling rate directly to the speed of movement of the cyclone.

The filling algorithm is then given by:

$$\Delta p = a_0 v_c \left(\frac{p^*}{a_1} \right)^2 + a_2, \tag{3.2}$$

where a_0, a_1 and a_2 are empirically derived constants, v_c is the speed of the cyclone and p^* is the pressure deficit given by

$$p^* = 1000 - p, \tag{3.3}$$

p being the cyclone central pressure. Δp has units of hPa hr^{-1}.

Figure 3.8 shows the derived relationship for three cyclone speeds and Figure 3.9 shows predicted versus observed pressures for 10 randomly selected events. Good agreement is shown between the predicted filling based on equation 3.2 and the observations.
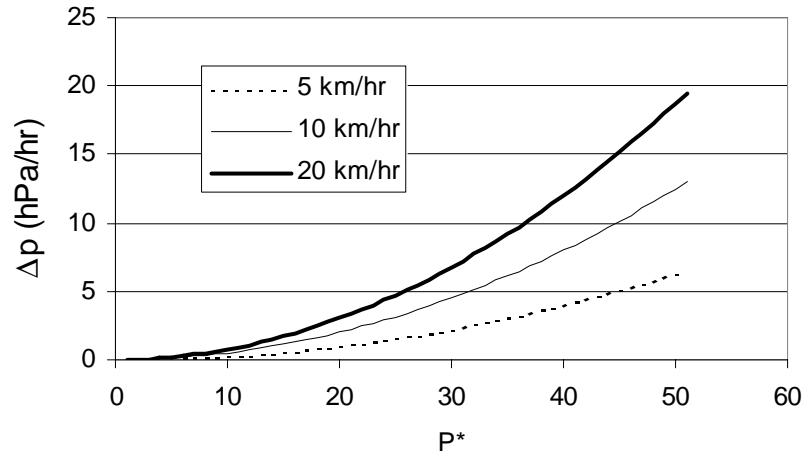
Figure 3.8. Relationship between cyclone filling rate and pressure as a function of cyclone speed as it moves inland (based on Eq. 3.2).
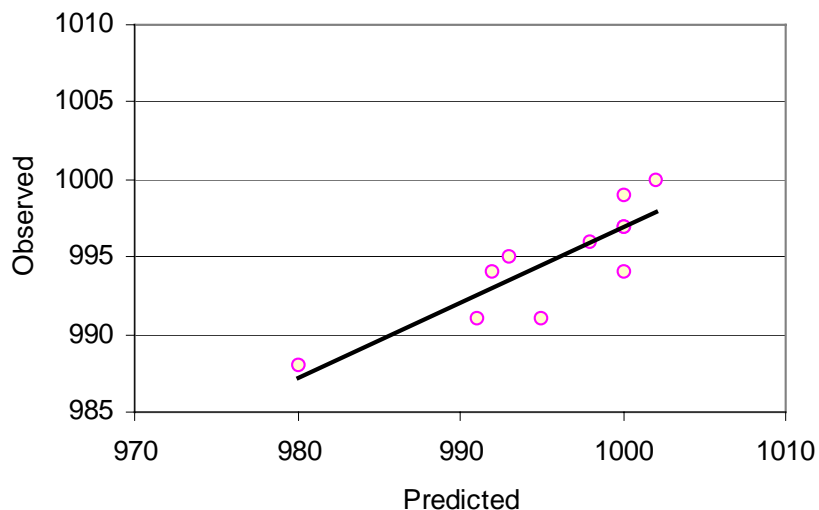
Figure 3.9. Predicted cyclone filling rates versus observed filling rates for ten randomly selected coastal crossing storms.

Monte-Carlo Simulations

The fitted probability distributions described above are used in a "Monte-Carlo" technique to generate individual synthetic cyclones. In this method, individual cyclone characteristics, including storm track, intensity, and speed of movement, are randomly selected and used to generate synthetic cyclones. A cyclone crossing point is also selected. In the case of coastal crossing cyclones, this is a location on the coastline that lies less than 1.0° to the north and south of the location of interest, as these are cyclones that are close enough to cause extreme winds. This is a smaller region than that over which cyclones from the observational record were extracted and this is taken into account by reducing the frequency of coast-crossing cyclones in Table 3.1 when calculating the return periods. In the case of coast-parallel cyclones, a crossing point is chosen along a fictitious line extending perpendicularly from the coast about 1.5° to the east. Once the crossing point is selected, a start and finish location and time for the cyclone is determined from the speed and direction parameters. A 24-hour cyclone simulation is performed for each selection of cyclone variables with the simulation commencing 15 hours before the cyclone reaches the crossing point. The maximum winds are recorded at the selected location in the 24-hour period of simulation and used in the return period analysis.

Approximately 2000 cyclone simulations were performed for each coastal location, comprising a mix of coast-crossing and coast-parallel cyclones depending on the average frequency of cyclones of each category observed in each location. The output of the model is the gradient wind speed, which is related to the surface pressure distribution in the cyclone.

3.3.3 Wind Loadings in Urban Design

The gust speed, $\hat{U}_{2\sec}$, is the wind speed used in the design of small buildings in the Australian Standard for Wind Loads (Standards Australia, 1989). In urban areas, the magnitude of wind gusts is reduced by the sheltering effect of buildings located upstream and by the adjustment of the boundary layer (the region of the atmosphere close to the surface) to the rougher terrain (if the distance travelled by the wind over land is large enough). In the present study, gust speeds are evaluated at 4-m height, which is appropriate for wind loads on low-rise buildings. The ratio of the gradient wind speed, $\overline{U}_\infty$, calculated in the cyclone wind model to the gust speed at 4 m, $\hat{U}_{2\sec,4m}$, can be determined as follows:

$$\frac{\hat{U}_{2\sec,4m}}{\overline{U}_\infty} = \frac{\overline{U}_{10\min,10m}}{\overline{U}_\infty} \cdot \frac{\hat{U}_{2\sec,10m}}{\overline{U}_{10\min,10m}} \cdot \frac{\hat{U}_{2\sec,4m}}{\hat{U}_{2\sec,10m}}. \tag{3.4}$$

Here, $\overline{U}_{10\min,10m}$ is the average wind speed over a period of 10 minutes at a height of 10 m. Following Standards Australia (1989), the ratio of the 10-m wind to the gradient wind is taken to be:

$$\frac{\overline{U}_{10\min,10m}}{\overline{U}_\infty} = \begin{array}{ll} 0.66 & \text{north of 25}^\circ \text{ S,} \\ 0.62 & \text{south of 25}^\circ \text{ S.} \end{array} \tag{3.5}$$

Studies into the relationship between wind gusts and mean wind speed have been undertaken by Deacon (1965) for mid-latitude gales in flat, open country, Ishizaki (1983) for Japanese tropical cyclones (typhoons), and Krayer and Marshall (1992) and Black (1992) for hurricanes in the United States. Based on these studies, the ratio of the 2-second, 10-m gust to the 10-m mean wind speed is found to range from 1.45 to 1.66 (John Holmes, personal communication, 2000). In the present study, the following ratios have been adopted:

$$\frac{\hat{U}_{2\sec,10m}}{\overline{U}_{10\min,10m}} = \begin{array}{ll} 1.60 & \text{north of 25}^\circ \text{ S,} \\ 1.50 & \text{south of 25}^\circ \text{ S.} \end{array} \tag{3.6}$$

Following Standards Australia (1989), the ratio of the 4-m gust to the 10-m gust is taken to be:

$$\frac{\hat{U}_{2\sec,4m}}{\hat{U}_{2\sec,10m}} = \begin{array}{ll} 0.925 & \text{north of 25}^\circ \text{ S,} \\ 0.88 & \text{south of 25}^\circ \text{ S.} \end{array} \tag{3.7}$$

Therefore the factors used in (3.4) are given as follows

$$\frac{\hat{U}_{2\sec,4m}}{\overline{U}_\infty} = \begin{array}{ll} 0.98 & \text{north of 25}^\circ \text{ S,} \\ 0.82 & \text{south of 25}^\circ \text{ S,} \end{array} \tag{3.8}$$

for winds over open country and coastal waters.

Over urban terrain, further modification to the wind reduction factors occurs due to the sheltering effect of upstream rows of houses. Standards Australia (1989) gives this reduction factor as 0.85, which is applicable for buildings at least one row downwind from the 'edge of town'.

There is also a gradual reduction in wind speeds as air travels over rough terrain such as urban buildings. Standards Australia (1989) allows for a linear reduction over a distance of 2.5 km. Table 3.2 gives the adjustment factors (multiplicative factors used to reduce gust strength) for gust wind speeds at a height of 4 m due to this effect.

Table 3.2. Adjustment for change of terrain.

Distance into urban terrain (m)	Adjustment factor (north of 25° S)	Adjustment factor (south of 25° S)
1000	0.95	0.94
2000	0.89	0.88
> 2500	0.86	0.85

Since there is little difference in these values north and south of 25° S, the more conservative values (the higher ones) are used. These additional adjustments are incorporated into the wind reduction factors used for each of the five coastal locations by taking into account the terrain features of each location. These factors are summarised in Table 3.3. For each location, only the highest and lowest values are shown and refer to the most and least vulnerable areas within each location. For example, in Cairns, the suburbs that are most exposed to wind effects are the hillside suburbs, especially when the wind is from the east. Those least exposed are situated more than 2.5 km from the edges of the main urban area and are afforded some sheltering by the surrounding housing.

These factors are applied to the winds generated over each location during the cyclone simulation and the maximum values of the low and high 4-m gusts are extracted and stored for later analysis.

Table 3.3. Ratio of $\hat{U}_{2\sec,4m}$ to $\overline{U}_\infty$ for the five locations indicated. The high value applies to residential areas that are most exposed to wind effects and the low value to residential areas that experience the maximum sheltering effects.

Location	High		Low	
	Directions	Gust factor	Directions	Gust Factor
Brisbane	all	0.60	all	0.49
Hervey Bay	all	0.70	all	0.62
Rockhampton	N,S,W	0.83	N,S,W	0.72
	E	0.75	E	0.67
Mackay	all	0.83	all	0.74
Cairns	N,S	0.83	N,S	0.72
	E	0.90	E,W	0.64
	W	0.75		

3.3.4 *Impact of Climate Change*

Some additional assumptions need to be made about the effect of climate change on tropical cyclone intensities in each location. In McInnes et al. (2000), which examined the effects of climate change on the tropical cyclone climate in the Cairns region, tropical cyclone mean central pressures were assumed to decrease by 10 hPa (i.e. become more intense), and the standard deviation of tropical cyclone intensities was assumed to increase by 5 hPa. These results were derived from previous climate model simulations by Walsh and Ryan (2000). In that study, a large number of TCLVs in both the present and enhanced climate simulations of a regional climate model were selected for re-simulation at a higher model resolution. Cyclones of central pressure 985 hPa were then inserted at the position of the original TCLV and a higher-resolution simulation conducted to allow the cyclone to develop to its maximum intensity. This is a relatively intense cyclone for the region. Comparing the maximum intensities of the cyclones in the two climates indicated that under enhanced greenhouse conditions, the average intensity of cyclones was 10 hPa deeper and the standard deviation had increased by 5 hPa.

These figures are appropriate for Cairns, which is in a region where the most intense cyclones occur off the Queensland coast. Some adjustments need to be made for the other locations, however, where intensities are generally lower. This is especially true in the far southern regions of tropical cyclone occurrence. If tropical cyclones do not travel further south in a warmer world, then their typical latitude of dissipation will remain the same. Thus at this latitude, the change in tropical cyclone intensity in a warmer world will be zero. If we assume a maximum central pressure for tropical cyclones of 1000 hPa, then the amount that the central pressures of cyclones are less than 1000 hPa in the current climate can be used to scale the assumed changes in intensity under enhanced greenhouse conditions. This amount would be different at each location. For example, at Mackay the mean cyclone intensity in the current climate is 22.4 hPa less than 1000 hPa (an "exceedance" of 22.4 hPa). Since the exceedance at Cairns is 29.3, we calculate a change in mean at Mackay under climate change conditions of 10x(22.4/29.3) = 7.6 hPa. Similar scalings for all locations are shown in Table 3.4.

The changes in mean and standard deviation in Table 3.4 are used to generate a modified Pareto distribution of cyclone intensity based on those determined for the five locations for the current climate on the basis of historical cyclone information. From these modified distributions, additional Monte-Carlo simulations can be performed.

We note, however, that these changes represent an upper threshold for changed climate conditions because, as discussed above, in Walsh and Ryan (2000) the changed means and standard deviations were derived after inserting relatively intense (985 hPa) cyclones. For less intense cyclones, it is possible that the average increase in intensity in changed climate conditions would be less than this. Thus, in the present study, a lower threshold was also determined for increases in cyclone intensity under changed climate conditions. This was achieved by taking the population of cyclone intensities selected via the Monte-Carlo process for Cairns under present climate conditions and reducing the intensity by 10 hPa for all cyclones with an intensity of 985 hPa or deeper and then re-calculating the population mean and

standard deviation. This assumes that no change in intensity of cyclones weaker than 985 hPa occurs, and therefore constitutes a lower threshold of possible cyclone intensity change. It is expected that under actual changed climate conditions, the modified Pareto curve for each location would lie somewhere between the upper and lower limit. For locations to the south of Cairns, the lower threshold values of mean and standard deviation are once again scaled on the assumption of no change in the dissipation latitude. The resulting values are given in Table 3.4.

Using the changes in mean and standard deviation indicated in Table 3.4, two modified Pareto distributions of cyclone intensity are derived for each location and two sets of changed climate Monte-Carlo simulations were performed representing an upper and lower limit of likely occurrence.

Table 3.4. *Summary of changes to cyclone climatology under enhanced greenhouse conditions. Units are hPa.*

Location	Present Climate Average Intensity (μ)	Present Climate Standard Deviation (σ)	$\Delta\mu$ (Changed Climate)		$\Delta\sigma$ (Changed Climate)	
			Upper	Lower	Upper	Lower
Cairns	971	18.6	-10.0	-7.2	5.0	3.5
Mackay	978	16.7	-7.6	-5.4	3.8	2.7
Rockhampton	977	15.1	-7.8	-5.6	3.9	2.7
Hervey Bay	981	14.5	-6.4	-4.6	3.2	2.2
Brisbane	986	11.2	-4.9	-3.6	2.4	1.6

3.3.5 *Results*

The 10-m winds from the 2000 cyclone simulations in each region under present climate conditions are ranked and fitted to a Pareto Distribution, as shown in Figure 3.10. This figure shows wind speed return periods for current climate for both high and low exposures (i.e. the amount of sheltering by other buildings; black curves); and the same for changed climate conditions, with the lower limit shown by the green curves and the upper by the red curves. The location exhibiting the lowest probability of tropical cyclone wind damage is Brisbane, owing to the relatively low number of tropical cyclones that affect this location. Cairns experiences not only the greatest threat from cyclone wind damage, but also the largest range of wind exposure.

The maximum 10-m wind return periods for each location are compared with the current wind code guidelines (Fig. 3.11). This figure compares the wind speed design standards over open ground for similar wind speeds generated by the model. For Brisbane, the cyclone wind gusts calculated in the present study are considerably lower than the wind design standards. However, we note that the code estimates are based on all wind gusts including those due to thunderstorms, while the current study considers only gusts caused by tropical cyclones.

In an analysis of thunderstorm related wind gusts based on anemograph records (Bureau of Meteorology, 1997), 1000-year average gust predictions (based on several fitting methods) were approximately 56 m s^{-1} (48 years of record) and 46 m s^{-1} (33 years of record) at Brisbane and Gladstone respectively. These results, combined with those of the current study, suggest that thunderstorm winds dominate extreme wind statistics in south-east Queensland while cyclone activity dominates to the north. Combining the cyclone predictions from the current study with the thunderstorm

related predictions from the earlier study would produce a result consistent with the Wind Code Region B standard.

The results of Fig. 3.11 show that increases in tropical cyclone wind speeds, by themselves, are unlikely to have an impact on building design standards in south-east Queensland, because projected increases in intensities still leave an adequate safety margin below the design standard. Further north, wind speeds in a warmer climate exceed the design standards, with the greatest impact likely in Cairns. This also occurs to a lesser extent in Mackay. The practical implications of these results for design standards need to be assessed.
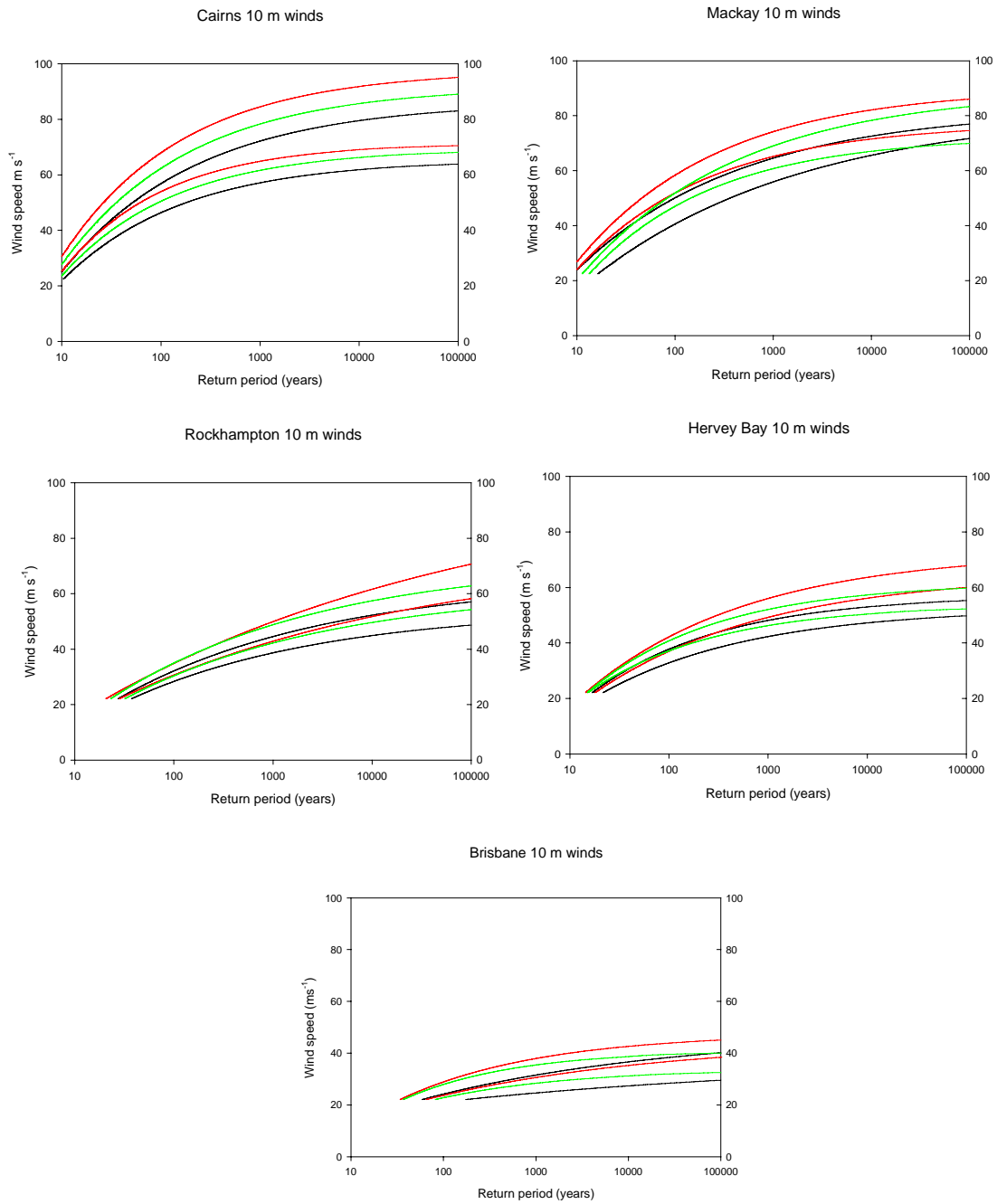
Figure 3.10. Distributions of 10-m wind gusts at the five locations. Black curves are current climate (high and low exposure, as described in the text); green curves $2xCO_2$ climate, lower limit of intensity increase (high and low exposure); and red curves are the same for the upper limit of intensity increase.

Cairns

Mackay

Rockhampton

Hervey Bay

Brisbane
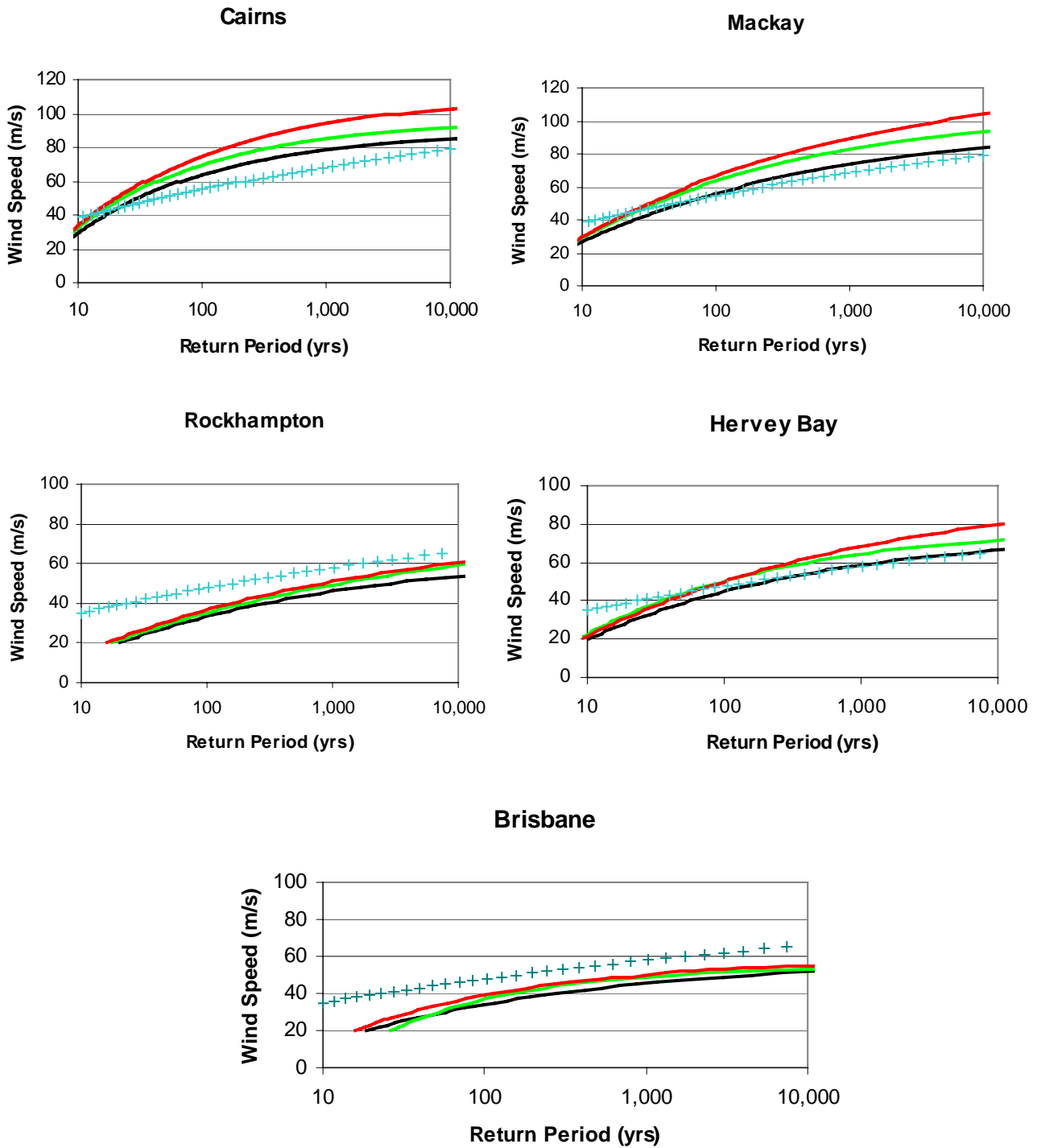
Figure 3.11. Wind speed return periods over open ground compared with design standards. Design standards are indicated by crosses, while the calculated wind speeds are for the current climate (black curve); enhanced greenhouse climate, lower limit (green curve) and upper limit (red curve).

3.3.6   Discussion and Conclusions

The level of confidence of these results can only be described as moderate. This is because of combined effects of uncertainty in the predictions of the effect of climate change on tropical cyclone intensities and the assumptions made about the regional variation of this change. Additionally, another source of uncertainty is the possible effect of climate change on ENSO. If climate change leads to more El Niño-like conditions (see Section 2.4), this would likely reduce the number of tropical cyclone affecting the Queensland coast, all other things being equal. This would reduce the changes in wind gusts shown here; however, the possible reduction in total numbers of tropical cyclones close to the coast of Queensland in a warmer world has not been realistically quantified yet (e.g. Nguyen and Walsh, 2001).

In addition, the impact of these predicted wind gust changes on the building design standard would have to be considered in the context of whether changes of this magnitude could lead to practical changes in design standards, given the level of uncertainty of the predictions.

In summary, the predictions of climate model simulations have been used in conjunction with a statistical modelling technique to deduce changes in return periods of wind gusts at five locations in coastal Queensland under enhanced greenhouse conditions. Substantial increases in wind gusts for the same return period are shown for Cairns and Mackay, with smaller increases further south. The impact of these changes on building design standards is yet to be assessed.

4. OzClim and scenario development (Item 2.3.3)

This section describes advances in scenario development, particularly regarding their applicability to impact studies and the management of uncertainty. Analysis is presented that delineates the relationship between precipitation and evaporation as simulated in climate models, showing that their changes in a warmer world are not independent. Using these relationships, it is also shown that most climate models are predicting drier soil conditions in Queensland in a warmer world.

As part of this analysis, potential evaporation (E_p) climate change scenarios are created, building on the uncertainty analyses presented in Section 6 of Walsh et al. (2000). Potential evaporation is the evaporation that would occur from a surface if that surface were perpetually saturated and if the evaporation was quickly carried away by the wind so that it could not moisten the air enough to reduce further evaporation. Climate change patterns have been created for potential evaporation, vapour pressure, downward shortwave radiation, precipitation and temperature for a number of models, and these have been incorporated into OzClim, the interactive climate change scenario generator. Extra functionality has been built into OzClim, including interactive regridding and extraction of data for use in impact assessment.

In addition, a CD containing the new release of the OZCLIM scenario generator (Version 2.0.1 Beta) is included with this report. In this section, some of the new features of this version are described.

4.1   Potential evaporation scenarios

4.1.1   Introduction

In last year's report, the use of output from the DARLAM 125-km regional climate model to simulate potential evaporation (E_p) using the Complementary Relationship Areal Evaporation (CRAE) method (Morton, 1983) was described. An error analysis compared the results with those computed from observed climate records. It was concluded that climate scenarios of E_p could be calculated from climate models and used to construct E_p climate change scenarios. This is important as E_p is a crucial variable in many climate impact models. In this report, the results from seven climate models are presented and the relationship between E_p, precipitation (P) and temperature (T) delineated, showing that these variables are not independent of each other. This interdependence reduces the possible range of future climate states.

It is well understood that climatic variables show dependency between each other in the real world, and that this should be reflected in individual climate models. What is not so clear is whether this co-dependency is shared between models under climate change. If this is the case, one may hypothesise that if one climate variable changes by a certain amount then other variables showing dependence are more likely to change in some ways than others. For example, if P increases, then E_p may decrease if there is an accompanying increase in cloudiness, as would normally be expected.

Reducing this type of uncertainty is important for at least two reasons:
1. Current strategies applying constructed ranges of P and T in risk assessment assume that these two variables are independent (see Jones, 2000).

2. Scenarios of precipitation change for Australia have been equivocal about the direction of change (CSIRO, 1996). This has created a great deal of uncertainty about impacts on variables such as water supply and crop and pasture yield.

If co-dependency between rainfall and other variables can be established, then the total uncertainty affecting such impacts can be reduced. This increases confidence in estimates of probability for certain outcomes, and while not directly reducing the uncertainty associated with P, can reduce the uncertainty surrounding impacts where it is a major driver.

4.1.2   Method

Changes in E_p were calculated for 7 models: the CSIRO Mark 2 AOGCM, CSIRO DARLAM 125 km, Deutsches Klimarechenzentrum DKRZ ECHAM4/OPYC3 and ECHAM3/LSG, Hadley Centre for Climate Prediction and Research HADCM3, Geophysical Fluid Dynamic Laboratory CGCM and the Canadian Center for Climate Modelling and Analysis CGCM. Details of the climate change simulation of these models are shown in Table 2.3. The changes in E_p are shown in Figure 4.1, and predominantly show increases in E_p, or mostly drier conditions. Most changes are in the range of 2 to 10% per degree of global warming. The construction of multiple model scenarios for climate change allowed the question of dependence between different variables under climate change to be explored.

To do this, P and E_p changes per degree of global warming were spatially sampled at grid intervals of 3° over Queensland from the 0.25° resolution surfaces created for OzClim. These samples were taken quarterly at 23 grid points in Queensland and came from the outputs of 7 climate models, making a total of 644 samples. Note that although P and E_p are inversely correlated over the seasonal cycle (in any one season, when P is high, E_p is low), the analysis of model output is based on δP and δE_p, or changes to these variables. The complementary relationship of Bouchet (1963) on which the CRAE model is based (Morton, 1983) offers an indication of whether δP and may be inversely correlated. This is illustrated schematically in Figure 4.2, which shows how E_p may be expected to change with respect to moisture availability, or in other words changes in rainfall. If there is no moisture available, then E_p is high and actual evaporation (E_a) is zero. As moisture availability increases through increasing rainfall, actual evaporation increases and potential evaporation decreases. Finally, an equilibrium situation is reached for high moisture availability, where E_p is equal to E_a and is now defined as E_w, the evaporation that occurs over a wet surface that is large enough to modify the atmosphere. The inverse correlation between E_p and E_a in Australia was also noted by Beer and Williams (1995).
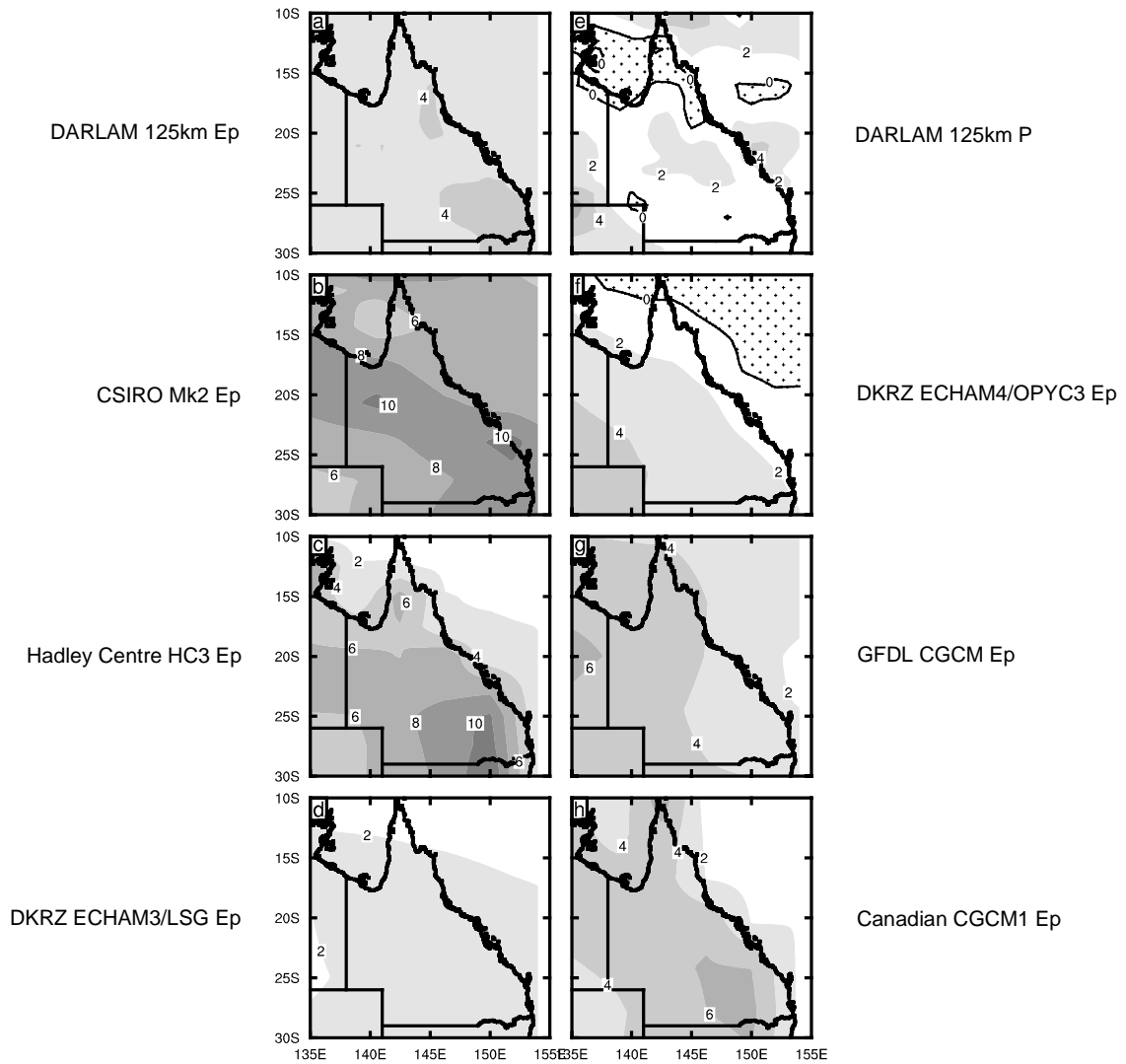
Figure 4.1. Annual percentage change per degree of global warming to E_p in percentage for seven climate models. DARLAM 125 km annual percentage change in P is also shown for comparison with E_p changes.
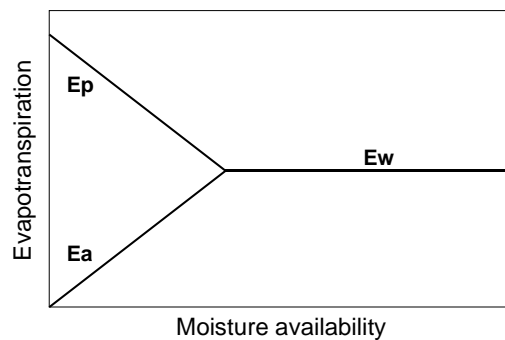
Figure 4.2. Schematic diagram of CRAE relationship (adapted from Morton, 1983) where $E_p + E_a = 2 E_w$.

4.1.3 Results

Figure 4.3 shows the results for the entire sample of 644 points. This produces changes consistent with those expected from Figure 4.2. The correlation between E_p change and rainfall change is –0.65, giving an r^2 value of 0.42, which is highly significant. This shows that the hypothesis of P change being inversely correlated with E_p change is confirmed. The practical outcome is that if rainfall increases, E_p increases are likely to be small or slightly negative, whereas if rainfall decreases, E_p is likely to undergo larger increases. The correlation between δT and δP is –0.33 and δT and δE_p is 0.48, which is lower than that between δE_p and δP. On a seasonal basis, correlations between δP and δE_p are –0.71 for JJA, –0.62 for SON, –0.61 for DJF and –0.56 for MAM, which are also very significant.
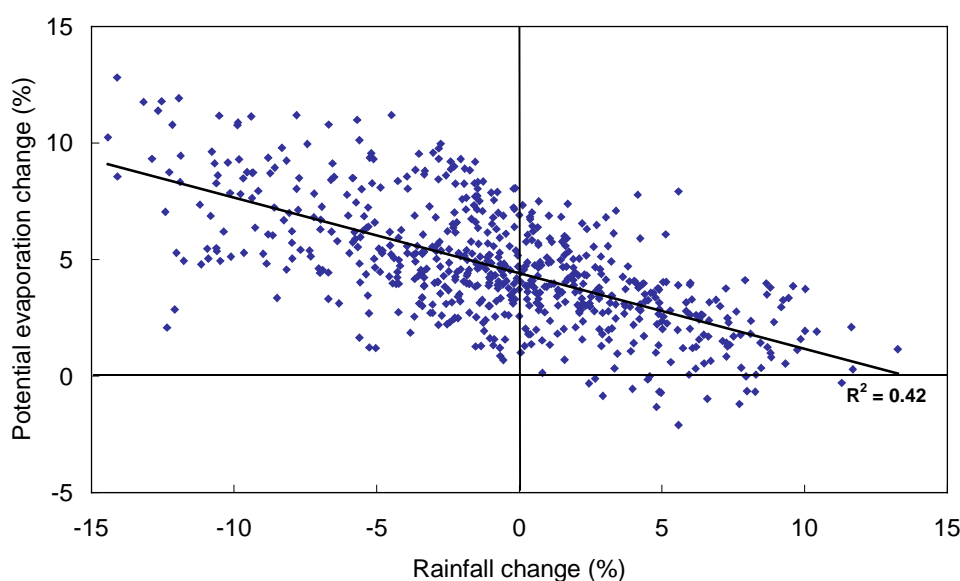
Figure 4.3. Scatterplot showing samples of P and E_p change for seven climate models over Queensland with line of best fit.

In Figure 4.3, about 45% of the samples imply a rainfall increase, and 97.5% represent an increase in E_p. How does this translate into impacts? One of the simplest ways is to view Figure 4.3 in terms of $P - E$ deficit and to use this information to estimate the likelihood of the climate becoming wetter or drier, as indicated by changes in E_p, which is more relevant for impacts on agriculture than just considering changes in P. In Figure 4.4, this is shown by the samples in Fig. 4.3 overlain by several lines that mark the degree of change where δP and δE_p cancel each other out. In other words, these lines show the amount of rainfall increase needed to balance an increase in E_p if one wanted to maintain the same moisture level. They show that in semi-arid climates where P is half E_p, comparatively large increases in rainfall (2:1 P: E_p as percentages) are needed to balance increases in E_p. Even in moist climates where P is twice E_p, some increases in P are required to balance an increase in E_p. The majority of the data points in Fig. 4.4 lie to the left of the three climate lines shown, towards drier conditions. This implies that for most climates in Queensland, the trend from the climate model results is towards drier soil conditions rather than wetter.

In summary, it has been shown that potential evaporation and precipitation changes simulated by climate models are not independent, but rather are related to each other. This reduces the possible number of future climate states. Analysis of the change in precipitation minus evaporation suggests most climate models are predicting generally drier conditions for Queensland in a warmer world.
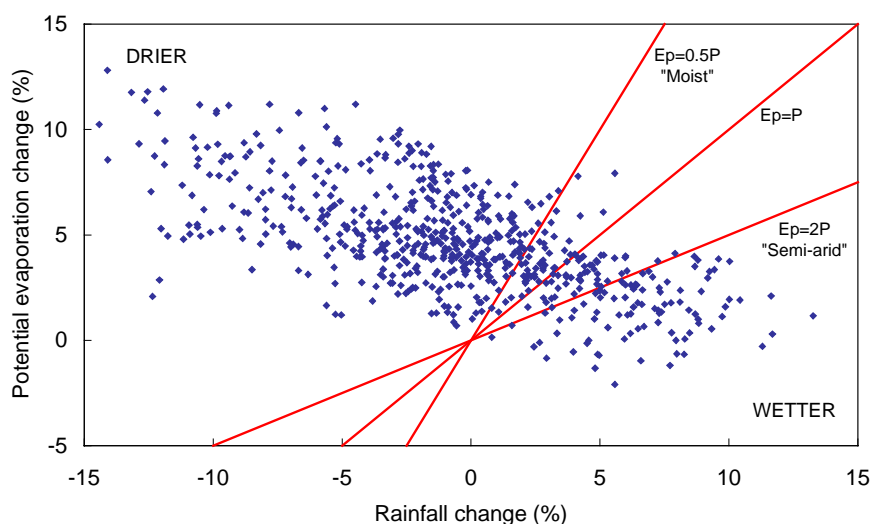
Figure 4.4. Scatterplot showing samples of P and E_p change for seven climate models over Queensland with line of best fit with lines showing neutral changes in P/E ratio for moist, balanced and semi-arid climates.

4.2   Implementation of new variables in OZCLIM

OZCLIM is an interactive climate change scenario generator running under MS Windows. It is able to generate many different patterns of climate change based upon user specifications.

Previous versions of OZCLIM were able to construct climate change scenarios for four variables: mean temperature, maximum and minimum temperature, and precipitation. Two different patterns of change from two models could be generated. In the new version of OZCLIM, three new variables important for climate impact studies are included: evaporation, vapour pressure and radiation. In addition, patterns of change for eight more models have been included (see Table 4.1). This has been done to more fully represent the possible range of model predictions. In addition, observed values of point potential evaporation, vapour pressure and radiation have been added (obtained from the Climate Research Unit, University of East Anglia), for comparison with simulated results.

Table 4.1. *List of models and variables incorporated into Version 2.0.1 Beta of OZCLIM*

Models	Variable
CSIRO Mk2	Mean temperature
Hadley CM2	Maximum temperature
Hadley CM3	Minimum temperature
GFDL	Precipitation
Canadian Climate Centre	Evaporation
CSIRO DARLAM 60 km	Vapour pressure
CSIRO DARLAM 125 km	Radiation
Max Planck OPYC3	
Max Planck LSG	
NCAR CGCM	

Climate change scenarios can be generated for two regions. The first has a horizontal resolution of 0.25 degrees over all of Australia, from 44°S to 10°S and 110°E to 154°E. The second region encompasses the Murray-Darling Basin at a resolution of 0.05 degree, from 38°S to 24°S and 138°E to 153°E.

In addition to more models and variables, the new version of OZCLIM has enhanced functionality, as illustrated in the sample screen shown in Fig. 4.5. Using the regridding function (icon to far right in row just above the image), any image can be regridded to the user's specification, based upon latitude, longitude and resolution. Basic statistics calculated for an image can also be calculated: for example, area averages. Images can be exported in jpeg format for inclusion in other documents. Finally, basic online help pages have been added. More detailed help pages are under development.

Figure 4.5. Sample screen from Version 2 of OZCLIM.

5. Impacts

5.1 Introduction

The previous sections have described the results of climate modelling and data analysis. This work provides the indispensable foundation for quantifying specific impacts of climate change on agriculture, coastal infrastructure, and so on. Although estimates of impacts are often bounded by large uncertainties, consi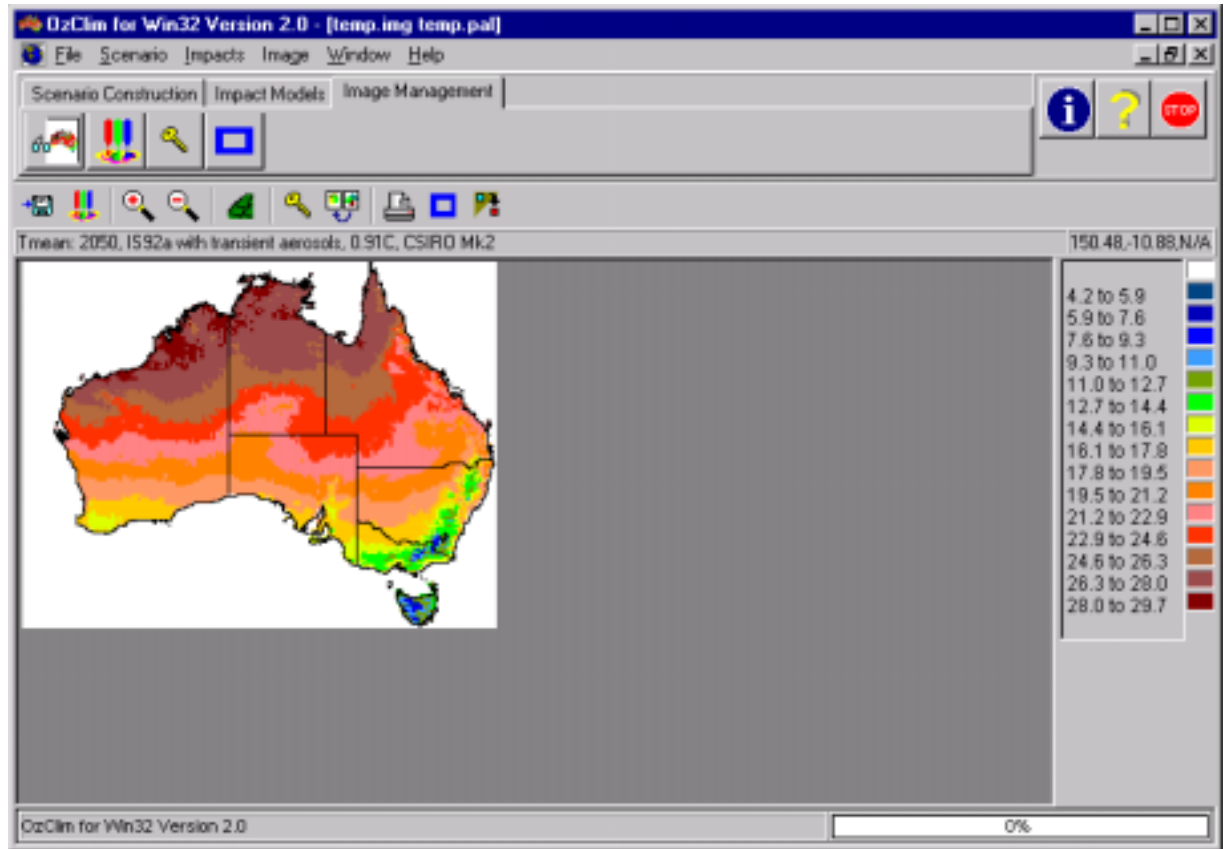derable work has been performed on the effects of climate change on various sectors. This section describes recent impact studies that have been performed for Queensland or that have been performed elsewhere but may have particular relevance for Queensland.

A very important issue in determining the likelihood of particular impacts of climate change is the level of certainty of the climate change predictions used to determine the impact. The main scientific issue that limits better assessments of the impacts of climate change in Queensland remains the uncertainty regarding the effect of global warming on ENSO. This uncertainty substantially affects predictions of rainfall and tropical cyclone frequency in Queensland in a warmer world, and increases the uncertainty of predictions of impacts that rely upon precipitation forecasts. Having said this, as mentioned earlier in the report, the balance of evidence suggests a change towards more El Niño-like conditions in a warmer world and generally drier conditions in most parts of Queensland.

Forecasts of temperature changes, however, have much lower uncertainty. Impacts that are more closely related to temperature changes have lower levels of uncertainty also. The low latitude and already warm conditions of Queensland, combined with its existing strong interannual variability, make it particularly vulnerable to increases in temperatures, especially if these are combined with decreases in precipitation. Nevertheless, the impacts of climate change would not be uniformly negative in all sectors in all locations: some positive impacts are anticipated.

5.2 Use of scenarios in impact studies

A number of impact studies in Queensland have used the CSIRO (1996) climate change scenarios. These scenarios suggested the possibility of both positive and negative changes in rainfall over the State. Later scenarios (Hulme and Sheard, 1999) are based on the current consensus among climate models, which mostly suggests decreases in rainfall over Queensland as climate warms. Therefore it is becoming more likely that impact studies in future will use scenarios that imply rainfall decreases rather than increases over Queensland.

5.3 Impacts on Queensland (ranked in order of confidence)

It is important to understand the use of probabilities in impact analysis, as part of a risk assessment approach. In this approach, a phenomenon that is of high risk but of low probability may still be worth considering as a potential impact. To take an extreme example, if there is a 1% risk that a certain experiment would result in the death of the experimenter, versus a 99% chance that nothing would happen, it would be foolish to ignore the 1% risk given the possible consequences. Similarly, if climate change impacts are of low probability but high effect, they could still be worth considering in terms of their policy implications (Moss and Schneider, 1999). In the

context of the following discussion, the probability of a particular impact of climate change must necessarily be related to the scientific confidence of the prediction, given the current state of scientific knowledge.

Very High Confidence (better than 9 out of 10 probability)

Effect of Sea Level Rise on Coastal Infrastructure

Queensland has substantial built infrastructure in coastal regions, and development continues to proceed rapidly. Predictions of sea-level rise are of high confidence because global sea-level rise (mostly due to the expansion of the oceans as they warm) is strongly related to global mean temperature, which to a very high degree of confidence is predicted to increase in this century. Walsh et al. (1998) give a recent summary of the science behind sea-level rise as it applies to the Gold Coast region, and Betts (1999) discussed the considerations of how this science might be used by local government in planning for sea level rise. Recent guidelines for the response to sea-level rise have been developed (May et al., 1998; RAPI, 1998; Institution of Engineers, 1998). Implications of sea-level rise are very site-specific, but in some locations could include increased beach erosion and more frequent flooding, as well as requiring changes to planning regulations.

Another impact of sea-level rise is an associated increase in the intrusion of salt water into coastal aquifers (Ghassemi et al., 1996), with implications for the quality of coastal water supply.

Potential for expansion of vector-borne diseases

Bryan et al. (1996) note that although endemic malaria was eradicated from Australia by 1981, the vectors that carry the disease are still present. Climate modelling shows that global warming will enlarge the potential range of the main vector, the *Anopheles* mosquito. By the year 2030, it could extend along the Queensland coast to Gladstone, about 800 km south of its present limit. However, Australian health services currently deal with malaria cases effectively, removing infected patients from possible contact with vectors. Thus climate change by itself is unlikely to cause the disease to return to Australia.

Higher energy costs for buildings

Higher temperatures certainly mean higher costs for air-conditioning of buildings in Queensland, in the absence of design changes (Lowe, 1988). There are likely also to be changes in cooling efficiencies associated with warmer ambient temperatures for structures such as cooling towers (IPCC, 1996), as well as changes in electricity demand patterns associated with warmer summers.

Increased heat stress on cattle

A study by Davison et al. (1996) determined how dairy cattle in Queensland and New South Wales were affected by heat stress in the current climate. Heat stress on dairy cattle was predicted to rise with increasing temperaures in a study performed for the Hunter Valley in New South Wales (Jones and Hennessy, 2000). They also investigated the cost-effectiveness of the use of shade and sprinklers to reduce heat

stress, and found that such measures would be generally cost-effective in a warmer world.

For beef cattle, Howden et al. (1999a) found 30% increases in heat stress in Queensland by 2100. They suggested possible increases in water consumption by cattle as a result, as well as effects on livestock productivity.

High confidence (about 9 out of 10)

Stresses on coral reefs

The possible effects of rises in sea surface temperature on coral reefs have been summarized in Walsh et al. (2000). The main possible impact is coral bleaching, where coral becomes pale because it loses its symbiotic algae due to high sea temperatures. Death occurs if the bleaching event is prolonged or extreme. Bleaching is projected to increase in a warmer world (Hoegh-Guldberg, 1999). The main uncertainty at the present time is whether the reef would be able to adapt to higher average temperatures. It is possible that coral reefs will adapt through the introduction of heat-adapted species or by the migration of species to higher latitudes (Done, 1999); however, the rate of adaptation is generally believed to be considerably slower than the rate of increase in episodes of high SST. Therefore it is considered likely that bleaching will become more frequent.

Other risks to the reef include those associated with changes in river outflow: episodes of low salinity, nutrient outflow, turbidity and chemical pollution, all of which can damage coral reefs. Changes in river outflow rates are less certain than changes in temperature, however.

Coral reefs are likely to suffer very little damage from sea-level rise itself (Wilkinson, 1999).

Loss of biodiversity

Some native trees survive in very narrow temperature ranges: 25% of Australian Eucalyptus trees have ranges less than 1^oC (Hughes et al., 1996). Rapid temperature changes outside of this range could cause reductions in the biodiversity of Australian native forests. In addition, species adapted to cooler climates in Queensland may suffer habitat loss.

Increase in risk of fruit-fly infestation in southern Queensland

Sutherst et al. (2000) found that the high altitude apple growing areas of south-east Queensland (e.g. the Darling Downs) were more vulnerable to fruit-fly infestation under increases of temperature.

Decreased suitability for growing fruit that requires chilling

For stone fruit and apples, a number of studies have suggested that a warmer climate would give less days that provide the cool temperatures required for these types of fruit (Hennessy and Clayton-Greene, 1995; Basher et al., 1998).

Spread of warm climate adapted weeds

Sutherst et al. (1996) showed that a warmer climate would favour the spread of weeds already adapted to warm climates.

Medium to High Confidence (2 out of 3 or better)

Increase in intensity of the heaviest rainfall events -- impacts

While average rainfall may decrease in some parts of Queensland, studies have shown that the heaviest rainfall events will likely increase in intensity. Impacts of this may include the following:

- Impact on existing or future water storage design to account for changes in extreme events (ANCOLD, 1986; Pisaniello and McKay, 1998).
- Impact on freshwater and marine ecosystems from increases in soil erosion and associated nutrient and pollutant mobilization in near-coastal regions (Larcombe et al., 1996).
- Increases in insurance costs associated with increased likelihood of storm damage to public and private infrastructure (IPCC, 1996; Leigh et al., 1998a,b).
- Implications for emergency planning and evacuation of low-lying regions (IPCC, 1996).
- Altering the design of roads and bridges to cope with enhanced runoff and flood events (CSIRO and PPK, 1999).

Increase in storm surge heights in selected locations

Storm surge, which is a dome of water pushed ahead of a storm, causes coastal inundation under extreme conditions. The risk of storm surge depends greatly on the local topography and coastline and on the shape of the ocean floor. Not all coastal locations in Queensland are vulnerable to storm surge. Nevertheless, the central business district of Cairns is vulnerable in the current climate. McInnes et al. (2000) found that, due to predicted tropical cyclone intensity increases (see Chapter 3) and sea-level rise, the 1 in 100 year storm surge event increased by 0.4-0.7 m. The planning implications of this have yet to be assessed. Current uncertainties in this prediction include the question of whether a change towards a more El Niño-like mean state would substantially reduce the total number of cyclones affecting the coast of Queensland. This has not yet been estimated quantitatively.

Effects on transport infrastructure

CSIRO and PPK (1999) identified potential effects on the transport infrastructure of Queensland. Important climate variables for transport include extreme rainfall and winds, temperatures, storm surge, flood frequency and severity, sea waves and sea level. By 2070, if no adaptation was undertaken, it was considered that significant effects on transport infrastructure would occur. The development of new design standards was recommended for roads and rail, for areas under threat of flooding; in addition, detailed risk assessments for airports in low-lying coastal locations was also recommended.

Increased risk of fire

The incidence of bush fires in Queensland is expected to increase in a warmer world (Williams et al., 2000). The main uncertainty in this prediction is the quality of the GCM simulation of relative humidity.

Little impact on heat-related mortality by 2030

Since 1800, about 50 deaths per year in Australia have been caused by climatically-related phenomena. About 40% of these have been due to heatwaves (Pittock et al., 1999). However, Guest et al. (1999) predicted little change in mortality for Brisbane by 2030.

Moderate confidence (better than 1 in 2)

Increased drought

Based upon current simulations, some increases in drought frequency in Queensland are likely in the next century for most months (Walsh et al., 2000; see also section 4 of the current report, as well as McKeon and Hall, 2000).

Reduction in stream and river flow

Dry conditions in much of Queensland are associated with El Niño conditions, and ENSO is significantly related to summer streamflow in much of the state (Chiew et al., 1998). Given the possible trend towards more El Niño-like conditions in a warmer world, this may have a negative effect on summer streamflow.

Initial increase in wheat yield

Howden et al. (1999c) investigated climate change impacts on wheat yield, using the CSIRO (1996) scenarios. Because of increases in carbon dioxide, wheat yields in Queensland were forecast to increase considerably, although this was counterbalanced somewhat by decreases in the protein content of the grain and thereby its quality. In a warmer world, yield increases in the Emerald wheat-growing region of central Queensland, at the northern margin of Australia's wheat-growing belt, may be limited by higher than optimal temperatures for wheat (Howden et al., 1999b).

Later in the 21st century, however, it was found that wheat yields begin to plateau and then fall, due to diminishing returns from high CO_2 and increasing losses from higher temperatures, combined with possible decreases in rainfall.

Increase in forest plantation productivity in fertile regions

Howden and Gorman (1999) showed that plantation forests such as *pinus radiata*, fertile sites were likely to have increased productivity for moderate warmings, while infertile sites could have decreased production.

Low confidence (possible only)

Pastures

Recent work by McKeon et al. (1998), Hall et al. (1998), and Howden et al. (1999d) found that increased carbon dioxide was likely to have a beneficial effect on native

pastures. However, decreases in rainfall of more than 10% would counteract this effect and lead to a fall in productivity. Thus future productivity depends very much on assumptions regarding changes in rainfall.

Unknown

Hail

Hailstorms are the second most costly weather phenomenon in terms of insured damage (tropical cyclones are the most costly; Insurance Council of Australia, 1997). McMaster (1997) used predictions from several GCMs to make estimates of the possible effect of climate change on hail frequency in New South Wales, finding little impact. Further work needs to be performed in Queensland to address this issue.

Land Salinity

Land salinity is a major problem in many parts of Queensland, but a comprehensive assessment of the impact of climate change on salinity has yet to be carried out. Changes in land use independent of climate change would naturally have large impacts.

5.4   Adaptation to Climate Change

The potential to adapt to these impacts varies considerably. For instance, adaptation of buildings to be more energy-efficient in a warmer world may be considerably less costly than protecting those same buildings against sea-level rise. The cost of adaptation is an important factor in considering whether the impact of climate change on a particular section would be a matter for concern. A number of the studies mentioned above have made suggestions regarding possible adaptations that would ameliorate the impact of climate change on the sector in question.

Specific adaptations are not discussed here. In general, though, a risk assessment approach, combined with a cost-benefit analysis of the effectiveness of the adaptation in question, has potential to inform the development of policy on climate change impacts. An example of this approach is provided in the study by Jones and Hennessy (2000). It was shown that cost-effective adaptations, such as shade and sprinklers, could be introduced to deal with the problem of increased heat stress on dairy cattle, given knowledge of the probability of various increases in temperature in future decades. Cost-benefit analysis of this kind could serve as a guide to the identification of potential adaptation strategies.

These approaches require knowledge of the likely impacts of climate change, which can only come from detailed studies. This particularly applies to impacts that are related to changes in extreme events, which are predicted to change faster than changes in average climate.

6. Future Work

To resolve some of the outstanding climate change issues important to Queensland, there needs to be further work both on the improvement of climate models and on more specific climate impact studies. Most important for the future of this work is continued development of the CSIRO Mark 3 climate model, which has already demonstrated the potential to clarify the issue of the effect of climate change on ENSO. A clearer result on this issue would greatly improve the reliability of predictions of the effects of climate change on Queensland rainfall.

A more precise description of the relationship between climate change and ENSO would also help to resolve an outstanding issue regarding the effect of climate change on tropical cyclones, namely whether climate change would necessarily cause fewer tropical cyclones to affect the coast of Queensland, even though those that form are likely to be more intense.

Despite some remaining uncertainties regarding the effects of global warming, some predictions are of sufficient confidence to warrant more specific impacts studies to determine their relevance to policy, particularly those impacts that are closely related to temperature changes. These studies should be performed in a collaboration between climate scientists, impact researchers and policy specialists. The risks of climate change for selected sectors or activities should be examined, and appropriate management or adaptation strategies formulated. Close interaction between climate scientists and policy makers on specific projects is required to enable this process to occur.

7. References

Allan, R. J., Lindesay, J.A. and Parker, D.E. 1996*. El Niño Southern Oscillation and Climatic Variability.* CSIRO publications, Melbourne Australia, 416 pp.

ANCOLD 1986. *Guidelines on Design Floods for Dams.* Australian National Committee on Large Dams. Available from Mr Len McDonald, Assistant Secretary of ANCOLD, 6 Kiama Street, Greystanes, NSW, 2145, Australia.

Basher, R.E., Pittock, A.B., Bates, B., Done, T., Gifford, R.M., Howden, S.M., Sutherst, R., Warrick, R., Whetton, P., Whitehead, D., Williams, J.E. and Woodward, A. 1998**.** Australasia. In: Watson, R.T., Zinyowera, M.C. and Moss, R.H. (eds.), *The Regional Impacts of Climate Change: An Assessment of Vulnerability*. Cambridge University Press, Cambridge New York, 878 pp.

Beer, T. and Williams, A. 1995. Estimating Australian forest fire danger under conditions of doubled carbon dioxide concentrations. *Clim. Change*, **29**, 169-188.

Betts, H. 1999. The implication of future climate change on floodplain planning at Gold Coast City. NSW Floodplain Managers' Conference, May 1999.

Black, P.G. 1992. Evolution of maximum wind estimates in typhoons. ICSU/WMO Symposium on tropical cyclone disasters, October 12-18, Beijing, China.

Bouchet, R.J. 1963. Evapotranspiration reelle et potentielle signification climatique. *Int. Assoc. Hydro. Sci. Pub*., **62**, 134-142.

Bureau of Meteorology, Special Services Unit Report 1997. *Characteristics of Severe Thunderstorms in Australia in Relation to Transmission Line Failures.* Available from Bureau of Meteorology, Special Services Unit, GPO Box 1289K, Melbourne 3001.

Bryan, J.H., Foley, D.H. and Sutherst, R.W. 1996. Malaria transmission and climate change in Australia. *Med. J. Australia*, **164**, 345-347.

Chiew, F.H.S., Piechota, T.C., Dracup, J.A., McMahon, T.A. 1998. El Niño/Southern Oscillation and Australian rainfall, streamflow and drought: Links and potential for forecasting. *J. Hydrology,* **204**, 138-149.

Clark, K.M. 1997. Current and potential impact of hurricane variability on the insurance industry. *Hurricanes: Climate and Socioeconomic Impacts*, Diaz, H.F. and Pulwarty, R.S. (eds.), Springer, 273-284.

Collins, M. 2000. The El Niño–Southern Oscillation in the second Hadley Centre coupled model and its response to greenhouse warming. *J. Climate*, **13**, 1299-1312.

CSIRO and PPK 1999. *The Effects of Climate Change on Transport Infrastructure in Regional Queensland.* Report to Queensland Transport, Brisbane, by CSIRO Atmospheric Research and PPK Environment and Infrastructure Pty. Ltd.

CSIRO 1996. *Climate Change Scenarios for the Australian Region*. Climate Impact Group, CSIRO Division of Atmospheric Research, Melbourne, 8 pp.

Cullen, M.J.P. 1993. The unified forecast/climate model. *Meteor. Mag.*, **122**, 81-94.

Davison, T., McGowan, M., Mayer, D., Young, B., Jonsson, N., Hall, A., Matschoss, A., Goodwin, P., Goughan, J. and Lake, M. 1996. *Managing Hot Cows in Australia*. Queensland Department of Primary Industries, 58 pp.

Deacon, E.L. 1965: Wind gust speed: averaging time relationship*. Aust. Meteorol. Mag.,* **51**, 11-14.

DKRZ-Model User Support Group (eds.) 1992. *ECHAM3 - Atmospheric General Circulation Model*. Report No. 6, Deutsches Klimarechenzentrum, Hamburg. http://www.dkrz.de/forschung/reports/ReportNo.6.ps

Done, T.J. 1999. Coral community adaptability to environmental change at the scale of regions, reefs and reef zones. *Amer. Zoolog.*, **39,** 66-79.

Emori, S., Nozawa, T., Abe-Ouchi, A., Numaguti, A., Kimoto, M., and Nakajima, T. 1999. Coupled ocean-atmosphere model experiments of future climate change with an explicit representation of sulfate aerosol scattering. *J. Meteorol. Soc. Japan*, **77**, 1299 – 1307.

Flato, G.M., Boer, G.J., Lee, W.G., McFarlane, N.A., Ramsden, D., Reader, M.C. and Weaver, A.J. 2000. The Canadian Centre for Climate Modelling and Analysis global coupled model and its climate. *Clim. Dyn.,* **16**, 451-467.

Ghassemi, F., Howard, K.W.F., and Jakeman, A.J. 1996. Seawater intrusion in coastal aquifers and its numerical modelling. In: Zannetti, P. (ed.) *Env. Modelling*, **3**, 299-328.

Gordon, C, Cooper, C., Senior, C.A., Banks, H., Gregory, J.M. Johns, T.C., Mitchell, J.F.B. and Wood, R.A. 2000. The simulation of SST, sea ice extents and ocean heat transports in a version of the Hadley Centre coupled model without flux adjustments. *Clim. Dyn.*, **16**, 147-168.

Gordon, H.B. and O'Farrell, S.P. 1997. Transient climate change in the CSIRO coupled model with dynamic sea ice. *Mon. Wea. Rev.*, **125**, 875-907.

Guest, C.S., Willson, K., Woodward, A., Hennessy, K., Kalstein, L.S., Skinner, C., and McMichael, A.J. 1999. Climate and mortality in Australia; retrospective study, 1979-1990, and predicted impacts in five major cities in 2030. *Clim. Res.,* **13**, 1-15.

Hall, W.B., McKeon, G.M., Carter, J.O., Day, K.A., Howden, S.M., Scanlan, J.C., Johnston, P.W., and Burrows, W.H. 1998. Climate change and Queensland's grazing lands: II. An assessment of impact on animal production from native pastures. *Rangeland J.,* **20**, 177-205.

Hennessy, K.J. and Clayton-Greene, K. 1995. Greenhouse warming and vernalisation of high-chill fruit in Southern Australia. *Clim. Change,* **30**, 327-348.

Hoegh-Guldberg, O. 1999. Climate change, coral bleaching and the future of the world's coral reefs. *J. Marine Fresh. Res.*, **50**, 839-866.

Holland, G.J. 1997. The maximum potential intensity of tropical cyclones. *J. Atmos. Sci.*, **54**, 2519-2541.

Holland, G.J. 1980. An analytical model of the wind and pressure profiles in hurricanes. *Mon. Wea. Rev.*, **108**, 1212-1218.

Holmes, J.D. and Moriarty, W.W. 1999. Application of the Generalised Pareto Distribution to wind engineering. *J. Wind Eng. and Ind. Aerodyn.*. **83**, 1-10.

Howden, S.M. and Gorman, J.T. (eds.). 1999. *Impacts of Global Change on Australian Temperate Forests*. Working Paper Series 99/08, CSIRO Wildlife and Ecology, Canberra, 146 pp.

Howden, S.M., Hall, W.B. and Bruget, D. 1999a. Heat stress and beef cattle in Australian rangelands: recent trends and climate change. In: Eldridge, D. and Freudenberger, D (eds.) *People and Rangelands: Building the Future.* Proc. VI International Rangelands Congress, Townsville, July 1999, pp. 43-45.

Howden, S.M., McKeon, G.M., Reyenga, P.J., Entel, M. Meinke, H. and Flood, N. 1999b. Past and future competitiveness of wheat and beef cattle production in Emerald, NE Queensland. In: *Modsim'99 International Congress on Modelling and Simulation Proceedings*, December 6-9th, Hamilton, New Zealand. pp 817-822.

Howden, S.M., Reyanga, P.J., and Meinke, H. 1999c. *Global Change Impacts on Australian Wheat Cropping*. Working Paper Series 99/04. CSIRO Wildlife and Ecology, Canberra, 121 pp.

Howden, S.M., Reyanga, P.J., Meinke, H. and McKeon, G.M. 1999d. *Integrated Global Change Impact Assessment on Australian Terrestrial Ecoystems: Overview Report.* Working Paper Series 99/14. CSIRO Wildlife and Ecology, Canberra, 51 pp.

Hughen, K.A., Schrag, D.P., Jacobsen, S.B. and Hantoro, W. 1999. El Niño during the last interglacial period recorded by a fossil coral from Indonesia. *Geophys. Res. Letters*, **26**, 3129-3132.

Hughes, L., Cawsey, E.M. and Westoby, M. 1996. Climatic range sizes of Eucalyptus species in relation to future climate change. *Glob. Ecol. and Biogeogr. Letters*, **5**, 23-29.

Hulme, M. and Sheard, N. 1999. Climate Change Scenarios for Australia. Climatic Research Unit, Norwich, UK, 6 pp. Available at http://www.cru.uea.ac.uk

Institution of Engineers 1998. *Coastal Engineering Guidelines for Working with the Australian Coast in an Ecologically Sustainable Way.* National Committee on Coastal and Ocean Engineering, Institution of Engineers, Australia, Barton, ACT, 82 pp.

Insurance Council of Australia 1997. *Major Disasters since June 1967 Revised to June 1995.* Melbourne: Insurance Council of Australia.

IPCC 1996. *Climate Change 1995: The Science of Climate Change*. Contribution of Working Group I to the Second Assessment Report of the Intergovernmental Panel on Climate Change [Houghton, J.T., L.G. Meira Filho, B.A. Callander, N. Harris, A. Kattenberg, and K. Maskell (eds)]. Cambridge University Press, Cambridge and New York, 572 pp.

Ishizaki, H. 1983. Wind profiles, turbulence intensities and gust factors for design in typhoon-prone regions. *J. Wind Eng. and Ind. Aerodyn.*, **13**, 55-66.

Jeffrey, S.J., Carter, J.O., Beswick, A.R. and Moodie, K.M. 2001. Using spatial interpolation to construct a comprehensive archive of Australian climate data, *Environmental Modelling and Software*, in press.

Jones, D.A. and Trewin, B. 2000. The spatial structure of monthly temperature anomalies over Australia. *Aust. Met. Mag*., **49**, 261-276.

Jones, R.N. 2000. Analysing the risk of climate change using an irrigation demand model. *Clim. Res*, **14**, 89-100.

Jones, R.N. and Hennessy, K.J. 2000. *Climate change impacts in the Hunter Valley: a risk assessment of heat stress affecting dairy cattle*. CSIRO Atmospheric Research, 22 pp.

Knutson, T.R. and Tuleya, R.E. 1999. Increased hurricane intensities with CO_2-induced warming as simulated using the GFDL hurricane prediction system. *Clim. Dyn*., **15**, 503-519.

Knutson, T.R., Tuleya, R.E., Shen W. and Ginis, I. 2000. Impact of CO_2-induced warming on hurricane intensities as simulated in a hurricane model with ocean coupling. *Proceedings of the 24th Conference on Hurricanes and Tropical Meteorology*, Ft. Lauderdale, May 29-June 2, 2000, American Meteorological Society, 478-479.

Kowalczyk, E. A., Garratt, J.R. and Krummel, P.B. 1991. *A soil-canopy scheme for use in a numerical model of the atmosphere -1D stand-alone model*. Tech. Paper No. 23, CSIRO Atmospheric Research, Aspendale, Australia, 56pp.

Kowalczyk, E. A., Garratt, J.R. and Krummel, P.B. 1994. *Implementation of a soil-canopy scheme into the CSIRO GCM: Regional aspects of the model response.* Tech. Pap. 32, CSIRO Atmospheric Research, Aspendale, Australia, 59 pp.

Krayer, W.R. and Marshall, R.D. 1992. Gust factors applied to hurricane winds. *Bull. Amer. Meteorol. Soc.*, **73**, 613-617.

Larcombe, P., Woolfe, K. and Purdon, R. 1996. *Great Barrier Reef: Terrigenous Sediment Flux and Human Impacts*, 2nd Edition, CRC Reef Research, Townsville, 174 pp.

Lau, K.-M. and Wang, H. 1999. Interannual, decadal-interdecadal, and global warming signals in sea surface temperature during 1955-97. *J. Climate*, **12**, 1257-1267.

Leigh, R., Cripps, E., Taplin, R. and Walker, G. 1998a. Insurance and climatic change: the implications for Australia with respect to natural hazards. *Aust. J. of Env. Manag.*, **5**, 81-96.

Leigh, R., Cripps, E., Taplin, R. and Walker, G. 1998b. *Adaptation of the Insurance Industry to Climate Change and Consequent Implications*. Final Report for the Department of Environment, Sport and Territories, Canberra. Climate Impacts, Macquarie University, Sydney.

Lowe, I. 1988. The energy policy implications of climate change. In: *Greenhouse: Planning for Climate Change.* Pearman, G.I. (ed.), CSIRO Publications (East Melbourne) and E.J. Brill (Leiden), pp. 602-612.

Maier-Reimer, E. and Mikolajewicz, U. 1991. The Hamburg Large Scale Geostrophic Ocean General Circulation Model (Cycle 1).
http://www.dkrz.de/forschung/reports/ReportNo.2.ps

May, P., Waterman, P. and Eliot, I. 1998: *Responding to Rising Seas and Climate Change: A Guide for Coastal Areas.* Environment Australia, Canberra, 42 pp.

McInnes, K.L., Walsh, K.J.E. and Pittock, A.B. 2000. *Impact of sea level rise and storm surges on coastal resorts: Final Report.* A project for CSIRO Tourism Research. Available from CSIRO Atmospheric Research, Aspendale, 24 pp.

McKeon, G.M., Hall, W.B., Crimp, S.J., Howden, S.M., Stone, R.C. and Jones, D.A. 1998. Climate change in Queensland's grazing lands. I. Approaches and climatic trends. *Rangeland J.*, **20**, 147-173.

McKeon, G.N. and Hall, W.B. 2000. *Learning from history: preventing land and pasture degradation under climate change.* Final report to the Australian Greenhouse Office, 362 pp.

McMaster, H. J. 1997. Climate and hail damage to winter cereal crops in New South Wales. Ph.D. Thesis, Macquarie University, Sydney.

Meehl, G.A., Collins, W.D., Boville, B.A., Kiehl, J.T., Wigley, T.M.L. and Arblaster, J.M. 2000. Response of the NCAR Climate System Model to increased CO_2 and the role of physical processes. *J. Climate*, **13**, 1879-1898.

Morton, F.I. 1983. Operational estimates of areal evapotranspiration and their significance to the science and practice of hydrology. *J. Hydrol.*, **66**, 1-76.

Moss, R.H. and Schneider, S.H. 1999. *Toward Consistent Assessment and Reporting of Uncertainties in the IPCC TAR: Initial Recommendations for Discussion by Authors.* IPCC Guidance Paper distributed to Lead Authors.

Münnich, M., Cane, M.A. and Zebiak, S.E., 1991. A study of self-excited oscillations of the tropical ocean-atmosphere system. Part II: non-linear cases. *J. Atmos. Sci.,* **48**, 1238-1248.

Nguyen, K.C. and Walsh, K.J.E. 2001. Interannual, decadal and transient greenhouse simulations of tropical cyclone-like vortices in a regional climate model of the South Pacific. *J. Climate*, in press.

Oberhuber, J. 1992. The OPYC Ocean General Circulation Model. http://www.dkrz.de/forschung/reports/ReportNo.7.ps

Pisaniello, J.D.and McKay, J. 1998. The need for private dam safety assurance policy – a demonstrative case study. *Aust. J. Emerg. Manag.,* **12**, 46-48.

Pittock, A.B., Allan, R.J., Hennessy, K.J., McInnes, K.L., Suppiah, R., Walsh, K.J., Whetton, P.H., McMaster, H. and Taplin, R. 1999. Climate change, climatic hazards and policy responses in Australia. In: *Climate Change and Extreme Events*, T.E. Downing, A.A. Olsthoorn and R.S.J. Tol (eds.), Routledge, pp. 19-59.

RAPI 1998. *Good Practice Guidelines for Integrated Coastal Planning.* Royal Australian Planning Institute, Hawthorn, Vic. 105 pp.

Rotstayn, L. D. 1997. A physically based scheme for the treatment of stratiform clouds and precipitation in large-scale models. I: Description and evaluation of the microphysical processes. *Quart. J. Roy. Meteor. Soc.*, **123**, 1227-1282.

Rotstayn, L. D., Ryan, B.F. and Katzfey, J.J. 2000. A scheme for calculation of the liquid fraction in mixed-phase stratiform clouds in large-scale models. *Mon. Wea. Rev.*, **128**, 1070-1088.

Standards Australia. 1989. *S.A.A. Loading code, Part 2, Wind loads*. AS1170.2-1989.

Sutherst, R.W., Collyer, B.S., and Yonow, T. 2000. The vulnerability of Australian horticulture to the Queensland fruit fly, Bactrocera (Dacus) tryoni, under climate change. *Aus. J. Agric. Res.*, **51**, 467-480.

Sutherst, R.W., Yonow, T., Chakraborty, S., O'Donnell, C. and White, N. 1996. A generic approach to defining impacts of climate change on pests, weeds and diseases in Australasia. In: Bouma, W.J., Pearman, G.I. and Manning, M.R. (eds.) *Greenhouse: coping with climate change*. CSIRO Publishing, Victoria, Australia, 190-204.

Timmermann, A., Oberhuber, J., Bacher, A., Esch, M., Latif, M. and Roeckner, E. 1999. Increased El Niño frequency in a climate model forced by future greenhouse warming. *Nature*, **398**, 694-696.

Troup, A.J. 1967. Opposition of anomalies of upper tropospheric winds at Singapore and Canton Island. *Aust. Met. Mag.*, **15**, 32-37.

Tsutsui, J., Kasahara, A. and Hirakuchi, H. 1999. The impacts of global warming on tropical cyclones – a numerical experiment with the T42 version of NCAR CCM2. *Proceedings of the 23rd Conference on Hurricanes and Tropical Meteorology,* 10-15 January 1999, Dallas, American Meteorological Society, 1077-1080.

Walsh, K., Hennessy, K., Jones, R., Pittock, A.B., Rotstayn, L., Suppiah R. and Whetton, P. 2000. *Climate change in Queensland under enhanced greenhouse conditions: Second Annual Report.* CSIRO Atmospheric Research, 129 pp.

Walsh, K. J. E. and Katzfey, J.J. 2000. The impact of climate change on the poleward movement of tropical cyclone-like vortices in a regional climate model. *J. Climate*, **13**, 1116-1132.

Walsh, K.J.E. and Ryan, B.F. 2000. Tropical cyclone intensity increase near Australia as a result of climate change. *J. Climate*, **13**, 3029-3036.

Walsh, K.J.E., Jackett, D.R., McDougall, T.J. and Pittock, A.B. 1998. *Global warming and sea level rise on the Gold Coast.* Consultancy report prepared

for the Gold Coast City Council, April 1998. CSIRO Atmospheric Research, 34 pp.

Whetton, P.H., Rayner, P.J., Pittock, A.B. and Haylock, M.R. 1994. An assessment of possible climate change in the Australian region based on an intercomparison of general circulation modeling results. *J. Climate*, **7**, 441-463.

Wilkinson, C.R. 1999. Global and local threats to coral reef functioning and existence: review and predictions. *J. Marine Fresh. Res.,* **50**, 867-878.

Williams, A.J., Karoly, D.J., and Tapper, N. 2000. The sensitivity of Australian fire danger to climatic change. *Climatic Change*, in press.

Wilson, S.G. 2000. How ocean vertical mixing and accumulation of warm surface water influence the "sharpness" of the equatorial thermocline. *J. Climate,* **13,** 3638-3656.

Xie, P. and Arkin, P.A. 1997. Global precipitation: a 17-year monthly analysis based on gauge observation, satellite estimates, and numerical model outputs. *Bull. Amer. Meteorol. Soc*., **78**, 2539-2558.

Yoshimura, J., Sugi M. and Noda, A. 1999. Influence of greenhouse warming on tropical cyclone frequency simulated by a high-resolution AGCM. *Proceedings of the 23rd Conference on Hurricanes and Tropical Meteorology*, 10-15 January 1999, Dallas, American Meteorological Society, 1081-1084.

Yu, B., Rose, C.W., Coughlan, K.J. and Fentie, B. 1997. Plot-scale rainfall-runoff characteristics and modelling at six sites in Australia and South-East Asia." *Trans. Amer. Soc. Agricult. Eng.*, **40**, 1295-1303.